Physiological and Molecular Characterization of Zinc Uptake in Rice

2020.9

Sheng HUANG

Graduate School of Environmental and Life Science

Okayama University

Table of contents

Chapter 1 Introduction

Zinc (Zn) is an essential micronutrient for plant growth and development (Marschner, 2012). It plays structural and catalytic roles in large number of proteins. However, Zn deficiency is the most widely occurring micronutrient deficiency in crops worldwide, which has been a limiting factor of crop production on millions of hectares of arable land, especially in alkaline soil (Barker and Pilbeam, 2015). Furthermore, this deficiency also results in Zn deficiency in humans because Zn in edible parts of crops is our primary source of Zn intake. Therefore, it is important to understand the molecular mechanisms of Zn transport and regulation in crops for preserving Zn accumulation in edible parts.

1. Overview of Zn in plants

Zn is the second most abundant transition metal in living organisms after Fe (Marschner, 2012). Zn is involved in a wide variety of physiological processes (Broadley et al., 2007). Zn is taken up predominantly as a divalent cation (Zn^{2+}). When the pH increases in the soil, it is also taken up as a monovalent cation ($ZnOH^{+}$) (Marschner, 2012). It is reported that the average total Zn concentration in cultivated soils is around 65 mg/kg (Alloway, 2009), while the Zn concentration in most agricultural soil ranges from 10 to 300 mg/kg (Alloway, 1995; Barber, 1995; Broadley et al., 2007). The phytoavailability of Zn in soil depends on rhizosphere microbial community composition, pH value,

redox potential, bioavailability and concentration in soil (Alloway, 2008, 2009; Hafeez et al., 2013).

Zn can be transported from soil solution to the root stele through the apoplastic pathway in the regions where the Casparian band is not fully formed (White, 2001; White et al., 2002). However, most Zn is taken up from the soil to the stele though symplastic pathway (Lasat and Kochian, 2000), which is mediated by various transporters. When Zn enters into the xylem, it will be translocated to the shoots in the form of complex with organic compounds or free divalent cation. Finally, Zn will be delivered to different leaves and grains through phloem, in which Zn is present in the form of Zn-organic compound complex. All these processes require various different transporters.

2. Function of Zn in plants

Zn plays very important roles in many physiological and biochemical process. Firstly, Zn is an essential component of many enzymes which participates in the synthesis and degradation of carbohydrates, lipids, proteins, and nucleic acids. Secondly, Zn can stabilize the molecular structure of cellular components and membranes. Thirdly, Zn plays an essential role in polynucleotide transcription and thus in the process of genetic expression (Cakmak, 2000; Marschner, 2012; Hafeez et al., 2013). Therefore, when the plants suffer from Zn deficiency, it will cause chlorosis and stunting, and finally results in low yields and death (Broadley et al., 2011). On the other hand, when Zn

concentration is present in excess, it will show toxicity to plants although the tolerance to high Zn differs with plant species (Van Assche and Clijsters, 1986; Clemens and Peršoh, 2009; Tennstedt et al., 2009). Zn toxicity can result in the inhibition of root elongation in non-tolerant plants and also lead to chlorosis and inhibition of photosynthesis (Godbold et al., 1983; Van Assche and Clijsters, 1986; Ruano et al., 1988; Sagardoy et al., 2009).

2.1 Role of Zn in enzyme component

In higher plants, Zn is required for mediating the activity of various enzymes. Zn is an important cofactor for the activity of six enzyme classes including oxidoreductases, hydrolases, lyases, ligases, transferases, and isomerases (Sousa et al., 2009). In these enzyme classes, Zn-binding sites have identified as four types, including catalytic, co-catalytic, structural, and protein interface sites. These Zn-binding sites determine the biological activity of these enzymes. For example, carbonic anhydrase is a kind of enzymes with catalytic type Zn sites. It contains a single Zn atom that can catalyze the hydration of CO_2. Zn ion in carbonic anhydrase is coordinated to three protein ligands and one water molecule (Fig. 1.1A, Sandmann and Böger, 1983; Badger and Price, 1994). Co-catalytic type Zn sites are usually present in enzymes including two or more Zn atoms. Aspartic acid and histidine are the most common ligands in these co-catalytic sites. On the other hand, structural Zn sites contribute to maintenance of the structure of enzymes such as alcohol dehydrogenase and proteins involved in DNA replication

and gene expression. In these proteins, Zn ions are mostly bound to four cysteine residues. As for alcohol dehydrogenase, different from most of other enzyme, it contains two Zn atoms for each molecule; one of them with catalytic and the other with structural functions. The catalytic one usually binds to histidine and water molecule, and the structural one usually binds to four cysteine (Fig. 1.1B, Coleman, 1992; Auld and Bergman, 2008). Furthermore, Zn which bridges subunits at the protein interface is able to affect the protein-protein interaction (Auld and Bergman, 2008; Auld, 2009).

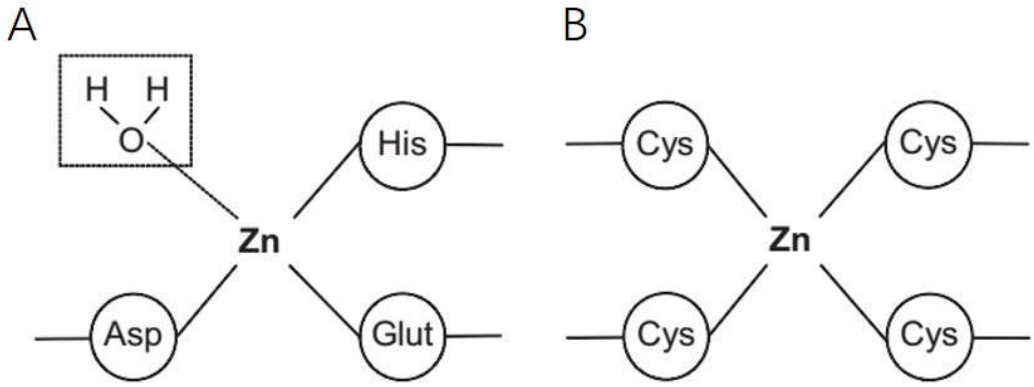

Fig 1.1 Diagram of binding of zinc and amino acid ligands in protein (Marschner, 2012).

2.2 Role of Zn in stabilizing the molecular structure

Zn plays an important role in stabilizing the molecular structure of cellular components and membranes. It is required for maintaining the integrity of bio-membranes. Zn is able to bind to phospholipid and sulphur-containing substance of membrane components, and form tetrahedral complexes with cysteine residues of polypeptide chains to protect membrane lipids and proteins from oxidative damage (Cakmak and

Marschner, 1988a; Cakmak, 2000; Maschner, 2012). It was reported that under Zn deficiency condition, the phospholipid concentration and the degree of unsaturation of fatty acids in membrane lipids were significantly decreased in root cells, resulting in increase of plasma membrane permeability (Cakmak and Marschner, 1988c). In addition, upon resupply Zn to the roots, the restoration of membrane lipids was detected, indicating the importance of Zn in stabilizing of membranes (Welch et al., 1982).

2.3 Role of Zn in the process of genetic expression

It has been reported that Zn plays an important role in DNA and RNA metabolism in humans, animals and plants. A lot of studies have revealed the function of Zn-dependent proteins or Zn containing proteins in DNA replication, transcription and the regulation of gene expression (Coleman, 1992; Vallee and Falchuk, 1993; Andreini et al., 2009). In the transcriptional regulation, Zn is an indispensable factor in these proteins to recognize and bind downstream nucleic acid sequences. Various Zn dependent proteins are involved in the regulation of DNA transcription process (Andreini et al., 2009). The Zn finger transcription factor family such as Cys2His2 (C2H2) is the most known transcription factor. Fig. 1.2 shows a schematic diagram of the role of Zn in the structure of a C2H2 zinc finger in protein (Marschner, 2012). In eukaryotic cell, a lot of proteins contain zinc finger domains, which play an important role in the recognition and binding to DNA, protein and RNA. Many Zn finger proteins contain DNA-binding domains and function as transcriptional factors to regulate the target gene transcription

(Fig. 1.3). Some Zn finger proteins function as protein adaptors to mediate the protein-protein interaction. Additionally, some of Zn finger proteins can interact with RNAs and regulate gene expression at the post-transcriptional levels (Miller et al., 1985; Choo et al., 1994; Dai et al., 1998).

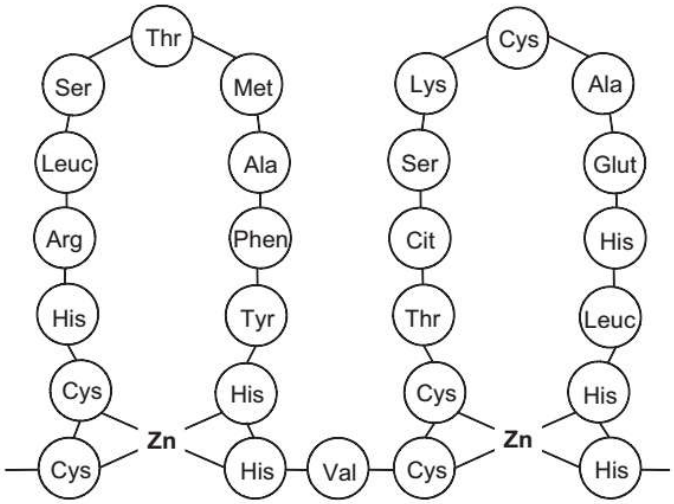

Figure 1.2 Schematic diagram of the role of Zn in the structure of a C2H2 zinc finger in protein (Marschner, 2012).

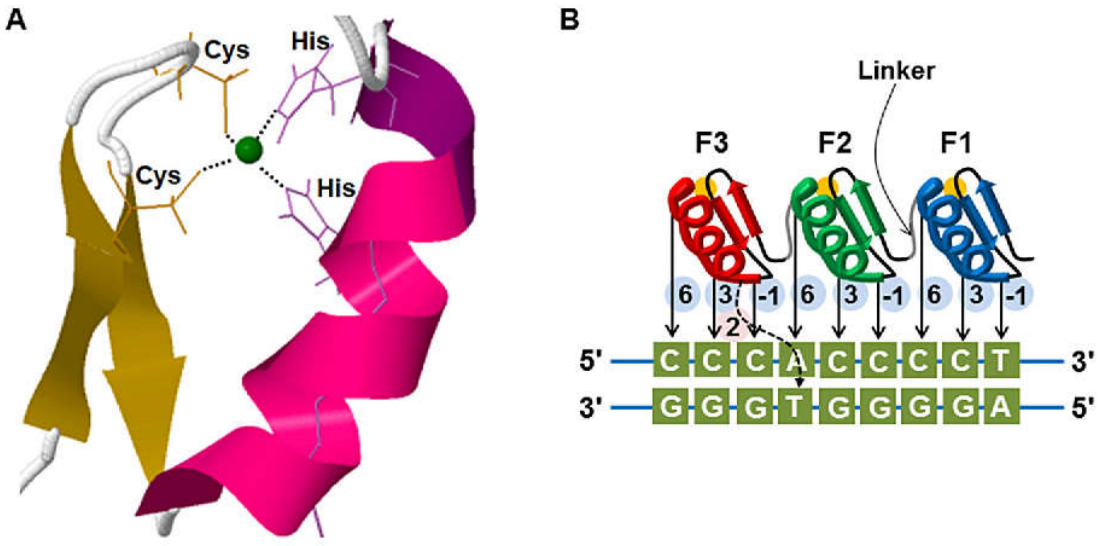

Figure 1.3 Structure of C2H2 zinc finger and DNA banding pattern. (A) Structure

of Zinc finger, (B) Interaction of zinc finger protein with a DNA sequence (Hossain et al., 2015).

3 Zn deficiency and toxicity

Zinc deficiency of crops is widespread all over the world (Welch et al., 2002). According to the Food and Agriculture Organization (FAO), about 30% of the cultivable soils of the world contain low levels of plant available Zn (Sillanpaa, 1990). In normal soils, the microelements such as Zn inherit primarily from the rocks through geochemical and pedochemical weathering processes. The total amount of Zn present in the soil is also dependent on the rock type, intensity of weathering, climate and numerous other predominating factors during the process of soil formation (Saeed et al., 1997). At the same time, high pH and high contents of $CaCO_3$, organic matter, clay and phosphate can fix Zn and result in the reduction of available Zn in the soil (Trehan and Sekhon, 1977). Generally, Zn deficiency occurs in calcareous soils, sandy soils, peat soils and soil with high P and Si (Alloway, 2004; 2008). Flooding also results in low Zn availability to plants, because of the changes in pH in the soil and the formation of insoluble Zn compounds such as reaction of Zn with sulfide (Mikkelsen et al., 1977).

When plants suffer from Zn deficiency, it will cause their abnormal growth and development. Visible symptoms of Zn-deficiency appear as stunted growth, chlorosis and smaller leaves, spikelet sterility (Fig. 1.4). For example, in cereals such as wheat, typical symptoms are reduction of shoot elongation and development of whitish-brown

necrotic patches on middle-aged leaves, but young leaves remain yellowish green in color that show no necrotic lesions (Cakmak et al., 1996).

Fig 1.4 Zn deficiency symptoms in crops (Photo credits: South Dakota State University; IPNI; Howard F. Schwartz, Colorado State University, Bugwood.org; IRRI).

On the other hand, Zn deficiency can also affect the quality of harvested products. Furthermore, it will increase the susceptibility of plants to be injured by high light or high temperature and increase the risk by fungal diseases (Marschner, 1995; Cakmak et al., 2000). Different plant species show different sensitivity to Zn deficiency. For example, maize and rice are more sensitive to Zn-deficiency than rye, oats and pea (Cakmak et al., 1997). In cereal, rye shows the highest tolerance to Zn deficiency, followed by triticale, barley and bread wheat (Cakmak et al., 1997).

Zn shows toxicity to plants when it is present in excess (Clemens, 2001; Haydon et., al 2007). An excess supply of Zn affects the growth of both roots and shoots. The root elongation, which is a sensitive parameter for heavy metal toxicity, is rapidly inhibited

by high Zn and the shoots become stunted and chlorotic. Furthermore, the root epidermis may be lignified by Zn toxicity (Påhlsson et al., 1989). The precise cause of Zn toxicity is unknown, but excess Zn may bind to inappropriate intracellular ligands or compete with other metal ions for enzyme active sites or transporters (Ishimaru et al., 2011). The symptoms of Zn toxicity in plants are usually similar to those of Zn deficiency. On the other hand, high concentration of Zn supply will cause the deficiency of other mineral elements such as Fe because they show similar ion features (Woolhouse, 1983; Sagardoy et al., 2009). The photosynthesis is strongly inhibited in plants exposed to excess Zn (Garty et al. 1992)). This inhibition is attributed to high Zn-induced deficiency of Mg and Mn, which play important roles in the photosynthesis systems (Ruano et al., 1987; Boardman and McGuire, 1990; Sagardoy et al., 2009).

On the other hand, Zn is also an essential element for humans. However, dietary deficiency of Zn in humans has been estimated as the 40th leading risk factor underlying global burden of disease (GBD, 2016). Over 30% of the world's population is Zn deficient (WHO, 2002; White and Broadly, 2005). Zn deficiency causes various diseases, such as dyspepsia. Zn in edible parts is the primary sources of Zn intake for humans, therefore, boosting Zn density in edible part is very important for human health. This is especially important for rice because rice is a staple food for half of the world's population, which provides an important source of our dietary intake of Zn.

4. ZIP family

The transport of metals including Zn from soil to different organs and tissues have been proposed to be mediated by different transporters such as members of the Zn-regulated transporter, iron-regulated transporter-like proteins (ZIP; ZRT-IRT-related protein), yellow stripe1-like (YSL) family, heavy metal ATPases (HMA), cation diffusion facilitator (CDF) (Grotz et al., 1998; Guerinot, 2000; Sinclair and Krämer, 2012). ZIP family transporters were first identified in yeast (ZRT1) and Arabidopsis (IRT) (Zhao and Eide, 1996; Eide et al., 1996). Homologous ZIP proteins are present in many plant species. For example, there are 15 members in Arabidopsis (Milner et al., 2013), 17 in rice (*Oryza sativa*) (Chen et al., 2008), 14 in wheat (*Triticum aestivum*) (Evens et al., 2017), 12 in barley (*Hordeum vulgare*) (Tiong et al., 2014), and 23 in common bean (*Phaseolus vulgaris* L.) (Astudillo et al., 2013). A phylogenetic tree of ZIP family members from different plant species is shown in Fig. 1.5. Most ZIP proteins have 309–470 amino acids and are predicted to have eight trans-membrane domains and a similar membrane topology in which the amino- and carboxyl-terminal ends of the proteins are located on the outside surface of the plasma membrane (Guerinot, 2000). The overall length of ZIP proteins varies considerably because of the variation between the transmembrane domains (TM) TM3 and TM4, which is predicted to contain a potential metal binding domain rich in histidine residues and on the cytoplasmic side (Guerinot, 2000). Based on the affinity, there are both low-affinity and high-affinity ZIP transporters. Many of the ZIP family members have been characterized to be involved in uptake and transport of metals including Zn in plants (Eide et al., 1996; Korshunova

et al., 1999; Guerinot, 2000; Vert et al., 2001, 2002; Connolly et al., 2002), however, their exact role in plants is still poorly understood.

Based on transport assays mainly in yeast mutants, ZIP transporters show broad substrate transport activity; they transport Fe, Zn, Mn, Cd, and Co (Korshunova et al., 1999; Waters and Sankaran, 2011; Milner et al., 2013). The ZIP genes also show different expression patterns; some are only expressed in the roots (Bughio et al., 2002; Ishimaru et al., 2006), whereas others are expressed in different tissues (Fig. 1.6, Ishimaru, et al., 2005; Yang et al. 2009; Lee et al., 2010a; Lee et al., 2010b; Kavitha et al., 2015; Sasaki et al., 2015).

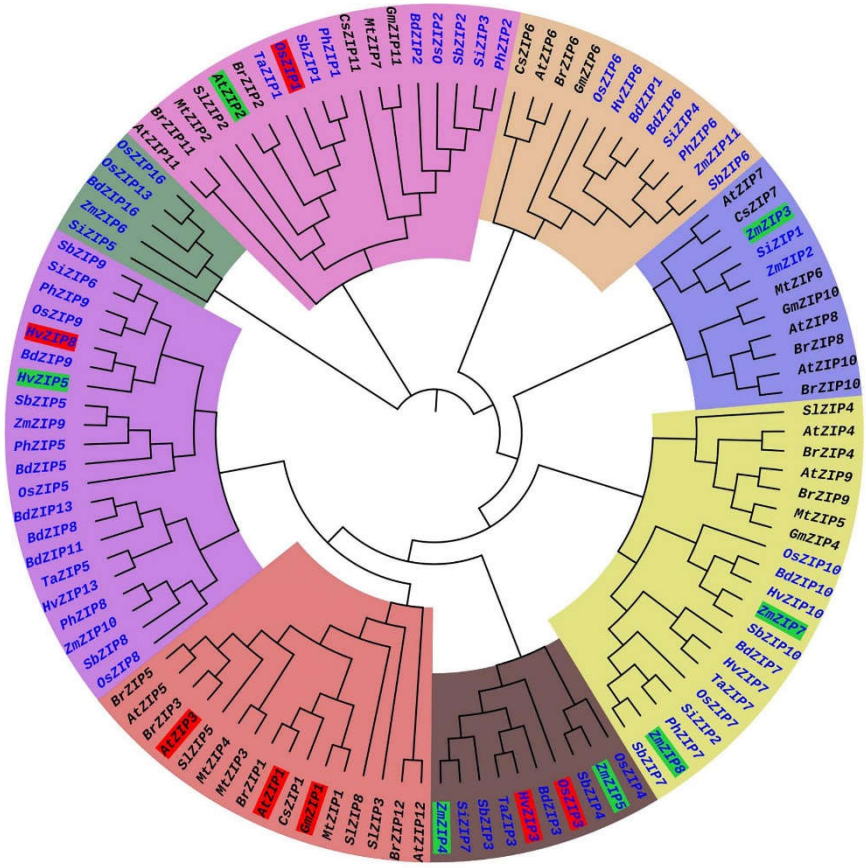

Figure 1.5 Phylogenetic tree of ZIP transporter family proteins of plants. The phylogenetic tree was constructed from 113 ZIP transporter protein sequences collected

from 14 plant species including 8 monocot (Blue) and 6 dicot plants (Black). Each major cluster is highlighted with different color. The low-affinity and high-affinity ZIP transporters are highlighted in red and green, respectively (Krishna et al., 2020).

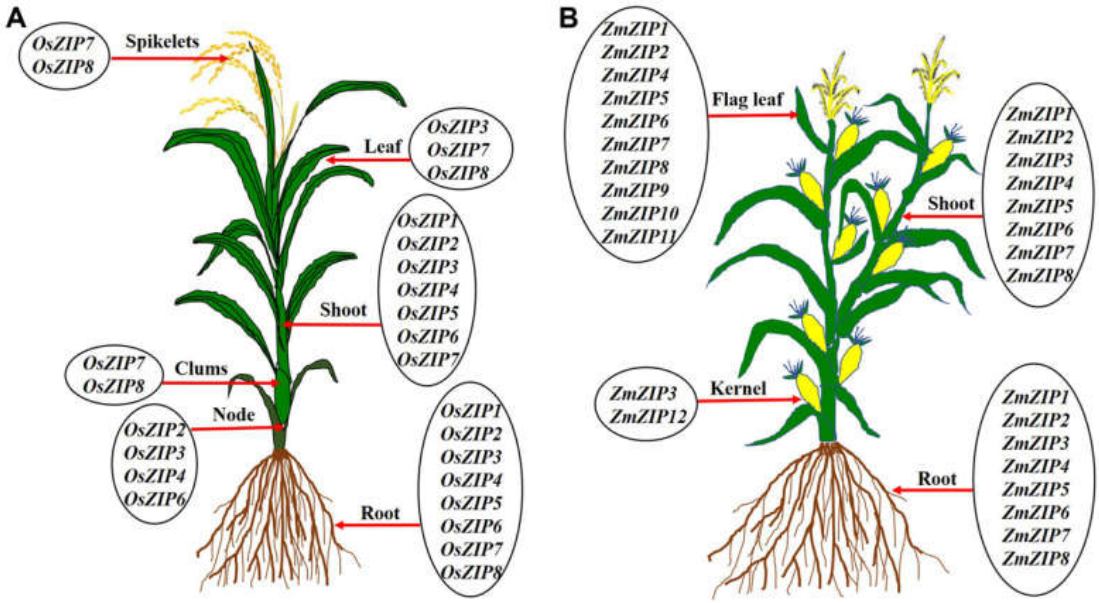

Fig. 1.6 Expression of ZIP transporter genes in different organs of rice (A), and maize (B) (Krishna et al., 2020).

5. Factors affecting Zn uptake

The uptake of Zn has been reported to be affected by many factors. For example, it was reported that Zn uptake is affected by presence of high Fe concentration. In a study with wheat seedlings, low Fe^{2+} concentration (10 µM) did not affect the Zn uptake from solutions containing 1 or 10 µM Zn (Adriano et al., 1971). However, at a higher Fe^{2+} concentration (100 µM), Fe completely suppressed the Zn uptake by rice seedlings from a solution of 0.05 µM $ZnCl_2$ (Giordano et al., 1974).

On the other hand, Zn uptake is also affected by phosphorus (P). High concentrations

of P have been detected in Zn-deficient plants (Cakmak and Marschner, 1986). Akhtar et al. (2010) reported that an increase in P supply resulted in a significant reduction of Zn uptake per unit of root dry weight and tissue Zn concentration in oilseed rape (*Brassica napus* L.). Zn concentrations and uptake by a P-efficient cultivar were significantly lower and more sensitive to P uptake than P-inefficient cultivar, indicating that high P-use efficiency may inhibit Zn uptake in plant. Similar results were found in wheat. An increase in P availability also caused a significant suppression of Zn uptake and tissue Zn concentration in wheat (Zhu et al., 2001). High P uptake efficiency may depress Zn uptake and limit the concentration of Zn in grains of wheat grown in low-P or low-Zn soils. With increasing P concentration in the shoot, Zn deficiency symptoms become more severe, which was associated with physiological availability of Zn in plants, but not the total Zn concentration (Cakmak and Marschner, 1987; Broadley et al., 2011).

Other elements have also been reported to affect Zn uptake. Grewal et al. (1998) reported that Zn uptake in a Zn efficient cultivar was enhanced with the increased rate of B supply under high Zn condition but not in a Zn inefficient cultivar. However, Hosseini et al., (2007) reported that high concentration application of boron (B, 20-80 mg/kg) depressed Zn accumulation, whereas low concentration application of B (2.5-10 mg/kg) did not affect Zn accumulation. Furthermore, copper (Cu) treatment in leaves was found to decrease the Zn content in soybean, whereas Cu treatment though roots enhanced Zn accumulation (Bernal et al., 2007).

Silicon (Si), the most abundant mineral element in soil, was also reported to affect

Zn accumulation in plants. In maize, Si supply increased the growth, but decreased Zn concentration in leaves under high Zn condition (Kaya et al., 2009). In rice, which is a typical Si accumulating species, Si supply increased shoot biomass and increased Zn concentration under Zn limited condition. However, the mechanisms underlying Si-affected Zn accumulation are unknown.

6. Root structure and uptake system of mineral elements in rice

In this study, rice (*Oryza sativa*) was used as an experimental material. Rice roots have a distinct anatomy, which is characterized by two Casparian strips at both the exodermis and endodermis (Enstone et al., 2002) and a highly developed aerenchyma in mature roots in which almost all of the cortex cells between the exodermis and endodermis are destroyed. Therefore, movement of an element from the soil solution to the stele requires two steps; from the soil solution to the aerenchyma across the exodermal cells, and from apoplastic solution in aerenchyma to stele across the endodermal cells (Ma and Yamaji, 2015; Che et al., 2018). Both influx and efflux transporters are required for this movement at the exodermis and endodermis of the roots (Ma and Yamaji, 2008; Sasaki et al., 2016); Recently, great progress has been made in understanding the uptake system of some mineral elements in rice. For example, Si uptake is mediated by OsLsi1 (influx) and OsLsi2 (efflux) (Ma et al., 2006; Ma et al., 2007), while Mn uptake is mediated by OsNramp5 (influx) and OsMTP9 (efflux) (Sasaki et al., 2012; Ueno et al., 2015). OsLsi1 and OsNramp5 are polarly localized at the distal side of the exodermis

and endodermis of mature root zones of rice, while OsLsi2 and OsMTP9 are localized at the proximal side of the same cells (Fig. 1.7, Ma et al., 2006; Ma et al., 2007; Sasaki et al., 2012; Ueno et al., 2015). Knockout either of them results in significant decrease of root Si or Mn uptake. However, most transporters involved in uptake of mineral elements including Zn have not been identified.

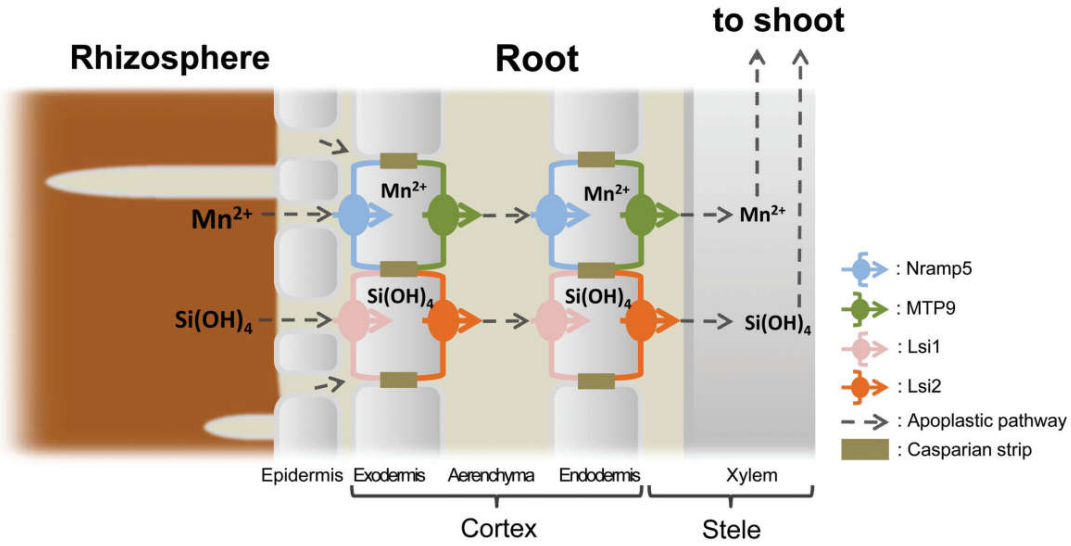

Figure 1.7 Schematic presentation for efficient uptake systems for manganese (Mn) and silicon (Si) in rice roots (Sasaki et al., 2016).

Chapter 2 Identification of transporter genes involved in Zn uptake in rice

1. Introduction

Transport of Zn has been proposed to be mediated by ZIP family transporters in different plant species. In Arabidopsis, AtZIP1, AtZIP3 and AtZIP4 showed Zn transport activity in yeast (*Saccharomyces cerevisiae*) mutant, Δ*zrt1*Δ*zrt2* and have been proposed to be involved in Zn transport. AtZIP1 and AtZIP3 are mainly expressed in the roots, but AtZIP4 is expressed in both roots and shoots (Grotz et al. 1998; Guerinot 2000). Over-expression of AtZIP1 increases the Zn accumulation in Arabidopsis (Gaitán-Solís et al., 2015). In barley, HvZIP7 has been reported to be induced by Zn deficiency and localized at the vascular tissues of roots and leaves. Over-expression of *HvZIP7* increased Zn uptake (Tiong et al., 2014). Besides *HvZIP7*, several other ZIP family genes including *HvZIP3*, *HvZIP5*, *HvZIP8*, *HvZIP10*, *HvZIP13* were also reported to be induced by Zn deficiency and the increased expression of these six genes is associated with enhanced uptake and root-to-shoot translocation of Zn in barley (Tiong et al., 2015).

In maize, ZmIRT1 showed transport activity in yeast. Expressing of *ZmIRT1*, *ZmZIP3* and *ZmZIP7* altered Zn homeostasis and increased the Zn accumulation, revealed that these ZIP transporters may be involved in Zn transport in maize (Li et al.,

2013; Mondal et al., 2013). On the other hand, in rice, several ZIP members have been functionally characterized in terms of transport activity, expression patterns, and ectopic expression analysis. OsZIP1, OsZIP3, OsZIP4, OsZIP5, OsZIP7a, and OsZIP8 showed influx transport activity for Zn in yeast (Ramesh et al., 2003, Ishimaru et al., 2005; Yang et al., 2009; Lee et al., 2010a; Lee et al., 2010b; Tan et al., 2019). However, OsZIP2 in yeast and OsZIP6 in *Xenopus* oocytes did not show transport activity for Zn (Ramesh et al. 2003; Kavita et al., 2015). Rice ZIP genes also show different expression patterns; *OsZIP1*, *OsZIP4*, *OsZIP5*, *OsZIP6*, *OsZIP7a*, and *OsZIP8* are expressed in both the roots and shoots (Ramesh et al., 2003; Ishimaru et al., 2005; Kavitha et al., 2015; Yang et al., 2009; Lee et al., 2010a; Lee et al., 2010b; Krishna et al., 2020), whereas *OsZIP3* is mainly expressed in the nodes (Sasaki et al., 2015). Furthermore, the expression of *OsZIP4*, *OsZIP5*, *OsZIP6*, *OsZIP7a*, and *OsZIP8* is up-regulated by Zn-deficiency, whereas *OsZIP1* and *OsZIP3* are constitutively expressed (Suzuki et al., 2012; Sasaki et al., 2015). On the other hand, overexpression of *OsZIP4* and *OsZIP5* causes decreased Zn accumulation in the shoots, but increased Zn accumulation in the roots (Ishimaru et al., 2007; Lee et al., 2010a). Based on these findings, OsZIP1 has been proposed to function in Zn uptake from soil (Ramesh et al. 2003, Bashir et al. 2012), whereas OsZIP4, OsZIP5, OsZIP7, and OsZIP8 are involved in Zn translocation/distribution in the shoots (Ishimaru et al., 2005; Lee et al., 2010a; Lee et al., 2010b; Sasaki et al., 2015; Tan et al., 2019). However, except for *OsZIP3*, which is responsible for the preferential distribution of Zn to developing tissues in the nodes (Sasaki et al. 2015), the exact physiological roles of most ZIP genes *in planta* remain

poorly understood.

In the present chapter, in order to identify transporter genes involved in Zn uptake in rice, I performed RNA-seq using the roots treated with or without Zn for three days. I selected two genes for further functional characterization, *OsZIP1* and *OsZIP9*. *OsZIP1* showed the highest expression in the roots among *ZIP* genes, while *OsZIP9* showed the strongest induction by Zn-deficiency.

2. Materials and methods

2.1 Plant materials and growth conditions

Seeds of the wild-type rice (cv. Nipponbare), two independent CRISPR/Cas9 *OsZIP9* knockout lines (T2), one RNAi line, and transgenic lines (T2) carrying the promoter of *ZIP9* fused with *GFP* were soaked in water in dark at 30°C. After 2 days, the germinated seeds were placed on a plastic net floating on a 0.5 mM $CaCl_2$ solution in a 1.2-L plastic pot. The seedlings (7-d-old) were transferred to a 3.5-L plastic pot containing 1/2 Kimura B solution (0.4 μM Zn, pH 5.6) (Ma et al., 2002). The nutrient solution was exchanged every 2 days. All plants were grown in a controlled greenhouse at 25–30°C, under natural light.

2.2 RNA sequence analysis

To perform the RNA-seq analysis, 20-day-old seedlings (cv. Nipponbare) were treated with or without 0.4 μM Zn for 1 day and then the roots were sampled for RNA

extraction with three replicates as described below. The RNA extracted was subjected to RNA-sequencing using Illumina HiSeq4000. A total of 16~21 M stranded paired-end (2×100 bp) sequences was obtained for each sample. All data analysis was performed on the Galaxy/NAAC server (https://galaxy.dna.affrc.go.jp/nias/static/register_en.html). After quality control by Trimmomatic (Bolger et al., 2014), sequences were mapped to *Oryza sativa* cv. Nipponbare reference genome (IRGSP-1.0) by TopHat2 (Kim et al., 2013). Transcript assembly, calculation of normalized transcript abundance (RPKM), and statistics of differential expression (Q-value of False Discovery Rate > 0.05) was performed using Cufflinks (Trapnell et al., 2010).

2.3 Cloning of full-length cDNA of *OsZIP1* and *OsZIP9*

The full-length ORF of *OsZIP1* and *OsZIP9* was amplified by PCR using primers 5′-ATGGCCAGGACGATGACGAT-3′ (forward), 5′-TCAGTCCCAGATCATGACGACAG-3′ (reverse) for *OsZIP1* and 5′-ATGGCTTTCGATCTCAAGCTAAC -3′ (forward) and 5′-TCAAGCCCAAATACCAAGCAAG-3′ (reverse) for *OsZIP9,* which were designed based on a putative cDNA clone (Os01g0972200 for OsZIP1 and Os05g0472400 for OsZIP9, respectively) in the Rice Annotation Project Database (http://rapdb.dna.affrc.go.jp/) with a putative translational start and stop site. Total RNA was extracted from rice roots (cv. Nipponbare) using a RNeasy Plant Mini Kit (Qiagen, http://www.qiagen.com) and then converted to cDNA using the protocol

supplied by the manufacturer of ReverTra Ace qPCR RT Master Mix with gDNA remover (TOYOBO). The amplified cDNA was cloned into pGEM®-T vector (Promega, https://www.promega.com/) and the sequence was confirmed by a sequence analyzer (ABI Prism 3130; Applied Biosystems, http://www.appliedbiosystems.com/).

2.4 Phylogenetic analysis

The alignment was performed with ClustalW using default settings (http://clustalw.ddbj.nig.ac.jp/), and the phylogenetic tree was constructed using the neighbor-joining algorithm with MEGA version 6.0 (Tamura et al., 2013). Bootstrap support was calculated (1000 replications).

2.5 Transport activity assay of OsZIP1 and OsZIP9

To investigated the transport activity, the full-length ORF of *OsZIP1* and *OsZIP9* was amplified by PCR using primers 5′-ATCGAGCTCAAAAAAATGGCCAGGACGATGACGAT-3′ (forward) and 5′-GTCAGATCTGTCCCAGATCATGACGACAGCC-3′ (reverse) for *OsZIP1*, 5′-AGGATCCAAGATGGCTTTCGATCTCAAGCTAAC-3′ (forward) and 5′-TCTCGAGTCAAGCCCAAATACCAAGCAAG-3′ (reverse) for *OsZIP9*. The resultant constructs were introduced into pYES2 vector (Invitrogen) through restriction sites of *Sac*I and *Bgl*II for *OsZIP1*, *Bam*HI and *Xho*I for *OsZIP9* under the control of galactose-inducible promoter, followed by introducing into a wild-type yeast strain (BY4741; MATa his2Δ0 met15Δ0 ura3Δ0) or the Zn uptake defective double mutant

(ZHY3; MATa ade6 can1 his3 leu2 trp1 ura3 zrt1::LEU2 zrt2::HIS3).

Growth of yeast strain ZHY3 expressing empty vector, *OsZIP1* or *OsHMA2* (positive control) were tested on a synthetic medium containing 2% (w/v) Glu or Gal, 0.67% (w/v) yeast nitrogen base without metals (BIO 101 Systems), 0.2% (w/v) appropriate amino acids, and 2% (w/v) agar buffered at pH 6 with 50 mM MES and supplemented with 0, 5, 10, 50 or 100 μM $ZnSO_4$. After spotting at five yeast cell dilutions (optical densities at 600 nm of 0.2, 0.02, 0.002, 0.0002 and 0.00002), plates were incubated at 30°C. After 3 days, the plates were photographed.

For OsZIP9 transport activity assay, ZHY3 expressing *OsZIP9* or empty vector were grown in the Sc(-Uracil) medium containing 0.67% (w/v) yeast nitrogen base without amino acids (Difco), 2% (w/v) glucose, 0.2% (w/v) appropriate amino acid, and 2% (w/v) agar at pH 6.0 for selection. The yeast cells were first incubated in Sc(-Uracil) liquid medium with 50 mM MES containing 2% (w/v) galactose or 2% (w/v) glucose (as a negative control) for two hours, followed by washing three times with the sterilized milli-Q water. The yeast cells were then exposed to a solution containing 5 μM of stable isotope $^{67}ZnCl_2$ (97% enrichment, Taiyo Nippon Sanso, Tokyo, Japan). At 0, 20, 40, 60, and 120 minutes of incubation with shaking at 30°C, the yeast cells were harvested by centrifugation (2300 g, 5 min). Yeast pellet was washed three times with 5 mM $CaCl_2$ solution and then digested by 2 N HCl for the determination of metals as described below.

To examine the transport activity for Zn, Fe, and Cu, the wild-type yeast cells (BY4741) expressing *OsZIP9* or empty vector were prepared as above and then

cultured for 4 hours in the presence of 2% (w/v) galactose for gene induction, followed by exposure to a solution containing 5 μM of each stable isotope including $^{67}ZnCl_2$ (97% enrichment), $^{65}CuCl_2$ (99.7% enrichment), or $^{57}FeCl_2$ (96.1% ^{57}Fe). $^{57}FeCl_2$ was prepared from $^{57}FeCl_3$ by reduction with ascorbic acid. These stable isotopes were purchased from Taiyo Nippon Sanso (Tokyo, Japan). After incubation with shaking for 2 hours at 30°C, the yeast cells were harvested by centrifugation (2300 g, 5 min) and subjected to determination of metals as described below.

2.6 Expression analysis of *OsZIP1* and *OsZIP9*

To investigate the expression pattern of *OsZIP1* and *OsZIP9* in different organs at different growth stages, we used the same cDNA samples collected in the field as described in Sasaki et al. (2015).

To investigate the response of *OsZIP1* and *OsZIP9* expression in roots to metal deficiency, 20-d-old seedlings (cv. Nipponbare) were grown in the 1/2 Kimura B solution with or without Mn, Fe, Cu, or Zn for three days. To further examine the time-dependent response, seedlings (20-d-old) were exposed to -Fe or -Zn for 1 and 3 days and root samples were taken for expression analysis as described below.

For spatial expression analysis, different root segments (0–0.5, 0.5–1.0, 1.0–1.5, 1.5–2.0, 2.0–2.5, and 2.5–3.0 cm from the root tip) were excised from the roots of 5-d-old seedlings.

Samples taken were immediately frozen in liquid nitrogen and then subjected to total RNA extraction using a RNeasy Plant Mini Kit (Qiagen). cDNA was synthesized by

ReverTra Ace qPCR RT Kit (TOYOBO) or SuperScript II (Invitrogen) according to the manufacturer's instruction. The expression analysis of *OsZIP1* and *OsZIP9* was determined with SsoFast EvaGreen Supermix (Bio Rad) or KOD SYBR qPCR Mix (TOYOBO) on a real-time PCR machine (CFX384 or CFX96 (Bio-Rad)). *Histone* H3 and *Actin* were used as internal controls. Relative gene expression was calculated by the ΔΔCt method. The primer sequences used were 5′-CGTCATGGCTGTCGTCATGATCTG-3′ (forward), 5′-AATGGGGTGATAGAAATCGAACATG-3′ (reverse) for *OsZIP1*, 5′-ATCTTCTTCTCGCTAACCACAC-3′ (forward), 5′-GCAGCCGCTGCGTCGAGAAT-3′ (reverse) and 5′-GTTCTTCGAAGGGATAGGGCT-3′ (forward), 5′-ATACCGATCATAATCCCAACCG-3′ (reverse) for *OsZIP9*; 5′-GGTCAACTTGTTGATTCCCCTCT-3′ (forward), 5′-AACCGCAAAATCCAAAGAACG-3′ (reverse) for *HistoneH3*; 5′-GACTCTGGTGATGGTGTCAGC-3′ (forward), 5′-GGCTGGAAGAGGACCTCAGG-3′ (reverse) for *Actin*.

2.7 Generation of transgenic rice lines

For generation of the transgenic lines carrying the promoter of *ZIP1* or *ZIP9* fused with *GFP*, the promoter regions of *OsZIP1* (2117 bp) and *OsZIP9* (3001 bp) were first amplified with PCR using the primers 5′-CGGGGTACCTTTAGATGGTATGCAAACAACGAGG-3′ (forward) and 5′-

CGCGGATCCGGTCGTGGCTCGCGCC-3′ (reverse) for *pOsZIP1* 5′-TGGTACCCATAAGTTGGGCTGATATTTCAG-3′ (forward) and 5′-TGGATCCCTTTTTAGCCTGTGGCCAAAGAT-3′ (reverse) for *pOsZIP9*. The amplified region was introduced into the pGEM®-T easy vector. After confirmation of the sequence, the plasmid was introduced into pPZP2H-lac vector including GFP by *Kpn*I and *Bam*HI, followed by vector transfer to calluses (cv Nipponbare) via *A. tumefaciens*-mediated transformation (Hiei et al., 1994).

OsZIP9 knockout lines were generated by using CRISPR/Cas9 using the plant expression vector of Cas9 (pU6gRNA) and single guide RNA expression vector (pZDgRNA_Cas9ver.2_HPT) as described before (Che et al., 2019). Twenty bases upstream of the PAM motif were selected as candidate target sequences (Fig. 2.6A). Two targets of *OsZIP9* were selected. The primers for target sequences in the ORF region of *OsZIP9* are 5′-GTTGACCCCGCTGAGCTGCCCACG-3′ (forward) and 5′-AAACCGTGGGCAGCTCAGCGGGGT-3′ (reverse) for *oszip9-1*; 5′-GTTGCGAGCGGTCTGATCGTGCTT-3′ (forward) and 5′-AAACAAGCACGATCAGACCGCTCG-3′ (reverse) for *oszip9-2*. The derived constructs were transformed into calluses as described above.

To genotype the resultant mutants, genomic DNA was extracted from leaves of transgenic rice plants. PCR amplifications were carried out using primer pairs flanking the designed target sites. The PCR products (about 500 bp) were sequenced directly using internal specific primers, of which the binding positions are desirably at about

200 bp upstream of the target sites. Two homologous knockout lines without Cas9 were selected and the T2 generation was used in the following phenotypic analysis.

An RNAi line was generated according to Miki and Shimamoto (2004). The expression level of *OsZIP9* in the RNAi line was investigated as described above.

2.8 Immunostaining analysis for transgenic lines carrying *OsZIP1* or *OsZIP9* promoter-*GFP*

To investigate the tissue-specificity of *OsZIP1* and *OsZIP9* expression, immunostaining was performed in the transgenic lines carrying *OsZIP1* promoter-*GFP* (T0) and *OsZIP9* promoter-*GFP* (T2) by using an antibody against GFP (Thermo Fisher Scientific). For *pZIP1-GFP*, 3-week-old plants grown in 1/2 Kimura B were used. Cross sections from the root tip (0-1 cm from the tip) and mature region (1-2 cm and 2-3 cm from the root tip) were prepared. For *pZIP9-GFP*, two-week-old plants grown in 1/2 Kimura B solution were exposed to a solution containing 0.4 μM Zn or not for 5 days. Cross sections from the root tip (0.2 cm from the tip) and mature region (1.5 cm from the root tip) were prepared and the method for immunostaining was the same as described previously (Yamaji et al., 2007). The signal of fluorescence was observed with a confocal laser scanning microscopy (TCS SP8x, Leica Microsystems).

2.9 Subcellular localization of OsZIP9

Subcellular localization of OsZIP9 was investigated by transiently expressing GFP-OsZIP9 fusion into rice protoplasts and onion epidermal cells. The ORF of *OsZIP9* was

amplified by PCR from rice (cv Nipponbare) root cDNA using primers with the *Bsr*GI and *Not*I site 5′-ATGTACAAGTTCAGGTTCAGGTGGAATGGCTTTCGATCTCAAGCTAAC-3′ (forward) and 5′-TGCGGCCGCTCAAGCCCAAATACCAAGCAAGG-3′ (reverse). The ORF was fused with a linker (SSGSGG) and then inserted into the cauliflower mosaic virus 35S GFP vector at the N terminus according to Sasaki et al. (2012). Rice protoplast transformation was performed by the polyethylene glycol method as described previously (Chen et al., 2006). The same plasmid with DsRed was transformed into onion epidermal cells as per the method described previously (Yokosho et al., 2016). The GFP signal was observed with a confocal laser scanning microscope (TCS SP8x, Leica Microsystems).

The subcellular localization of OsZIP9 was also investigated using double staining with 4',6-diamidino-2-phenylindole (DAPI) as a nuclei marker and an OsZIP9 antibody. The synthetic peptide (DASSSHDHERGN) was used to immunize rabbits to obtain antibodies against OsZIP9. The antiserum was purified through a peptide affinity column. The roots of WT and the knockout line exposed to -Zn for 4 days were used for the immunostaining. The method for immunostaining and secondary antibody incubation were the same as described previously (Yamaji and Ma, 2007). The fluorescence signal was observed through confocal laser scanning microscopy (TCS SP8x, Leica Microsystems).

2.10 Phenotypic analysis of *OsZIP9* knockout lines

The wild-type rice and two independent *OsZIP9* knockout lines (T2, *oszip9-1*, *oszip9-2*) generated by CRISPR/Cas9 were used for phenotypic analysis. In a hydroponic solution, seedlings (19-d-old) grown in a 3.5-L plastic pot were transferred to a 1.2-L plastic pot (one plant for each line) with a nutrient solution containing different Zn concentrations; 0.02, 0.2, and 2 μM. The treatment solution was renewed every two days. After 17 days, the plants were photographed. The roots were washed with 5 mM $CaCl_2$ three times and separated from the shoots. The fresh weight of the roots and shoots were recorded. The concentrations of mineral elements in the roots and shoots were determined as described below.

For soil culture, both wild-type rice and two independent knockout lines were grown in a pot containing 3.5 kg soil collected from a field of the Institute of Plant Science and Resources, Okayama University, under flooded conditions. Tap water was supplied daily and a 2-cm water layer was maintained on the top soil. Plants were grown in a temperature-controlled glasshouse (around 22–30°C) under natural light. At the ripening stage, the plant was harvested and separated into straw and brown rice. The concentrations of mineral elements were determined as described below.

2.11 Short-term uptake experiment with stable isotope ^{67}Zn

Seedlings (WT, knockout lines, RNAi line) grown in 0.02 μM Zn for 17 days were exposed to a solution containing 0.4 μM ^{67}Zn. After 24 hours, the roots were washed and separated from the shoots as described above.

A kinetic study of Zn uptake was performed by exposing the seedlings (WT, knockout

lines, RNAi line) grown in -Zn solution for 7 days to different ^{67}Zn concentrations in the range of 0–2 μM at 25°C and 4°C. After 30 min, the roots were washed three times with 5 mM $CaCl_2$ and harvested for element determination as described below.

2.12 Determination of metals in plant and yeast samples

The roots and shoots were dried at 70°C for at least three days before being digested by HNO_3 (60%[w/v]) as described previously (Sasaki et al., 2012). The concentrations of mineral elements in digestion solutions derived from plants and yeast were determined by Inductively Coupled Plasma-Mass Spectrometry (ICP-MS, 7700X; Agilent Technologies). The concentrations of ^{67}Zn, ^{65}Cu, and ^{57}Fe were determined with isotope mode. ΔZn, ΔFe, and ΔCu (net Zn, Fe, or Cu increase) were calculated according to Yamaji et al. (2013).

3. Results

3.1 Expression profiles of ZIP family genes in rice roots

Since ZIP family members have been proposed to be involved in Zn transport, in order to identify exact transporter genes involved in Zn uptake, I investigated the expression profile of ZIP family transporter genes in rice roots by using RNA-seq. As a result, among 12 ZIP genes expressed in the roots, *OsZIP1* showed the highest expression (Table 2.1). On the other hand, *OsZIP9* showed the highest induction by Zn-deficiency, although its expression was very low under normal Zn condition. Therefore, I selected *OsZIP1* and *OsZIP9* for further functional characterizations.

Gene ID		-Zn signal intensity	+Zn signal intensity	-Zn/+Zn fold change
Os01g0972200	**OsZIP1**	**55.53**	**49.57**	1.12
Os05g0164800	**OsZIP6**	44.84	42.85	1.05
Os05g0198400	**OsZIP7**	26.07	16.58	1.57
Os03g0411800	**OsZIP2**	16.34	16.04	1.02
Os08g0207500	**OsZIP4**	33.00	13.58	2.43
Os05g0472700	**OsZIP5**	27.26	8.86	3.08
Os06g0566300	**OsZIP10**	16.65	3.82	4.36
Os07g0232800	**OsZIP8**	6.83	2.84	2.41
Os05g0472400	**OsZIP9**	**20.98**	**2.63**	**7.97**
Os03g0667500	**OsIRT1**	2.00	2.04	0.98
Os03g0667300	**OsIRT2**	0.78	0.58	1.34
Os04g0613000	**OsZIP3**	0.04	0.09	0.45

Table 2.1 Transcription abundance of ZIP transporter family genes in rice roots form RNA-seq results. (FPKM values were shown).

3.2 Results of *OsZIP1*

3.2.1 Cloning of *OsZIP1*

We amplified the full-length coding region of *OsZIP1* (Os01g0972200) by PCR from complementary DNA (cDNA) of rice roots (cv Nipponbare). *OsZIP1* is composed of 2 exons and 1 intron and encodes a protein of 353 amino acids (Fig. 2.1A). OsZIP1 shares 25% identity with OsZIP9 and 10-55% identity with other ZIP members (Fig. 2.2B). Similar to other rice ZIP members, OsZIP1 protein was predicted to have eight transmembrane domains (TMHMM Server v. 2.0; http://www.cbs.dtu.dk/services/TMHMM/) (Fig. 2.1B).

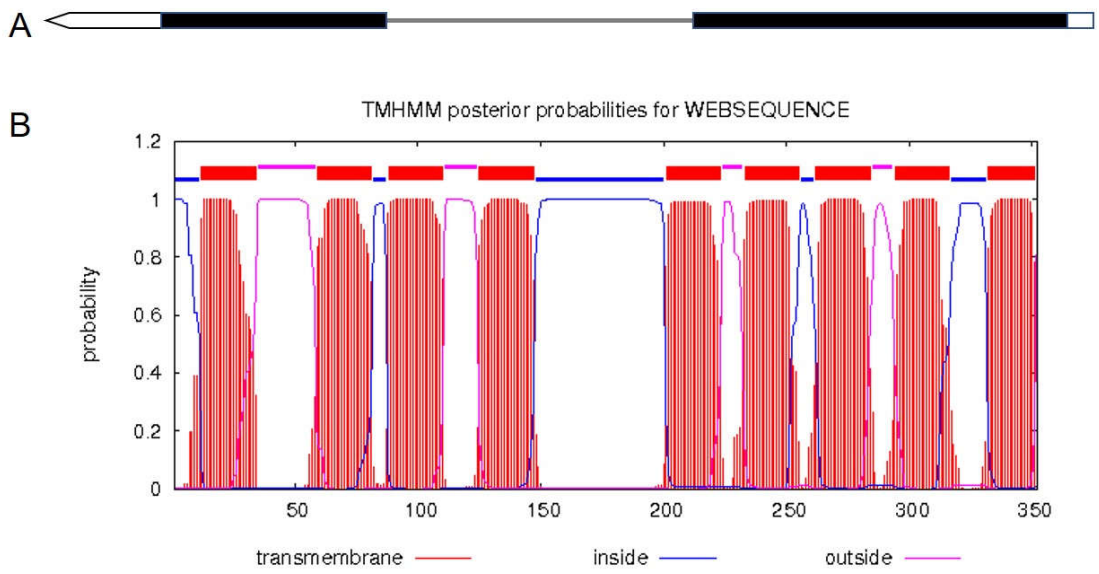

Figure 2.1 Structure diagram of *OsZIP1* (A) and trans-membrane domains predicted by TMHMM (B).

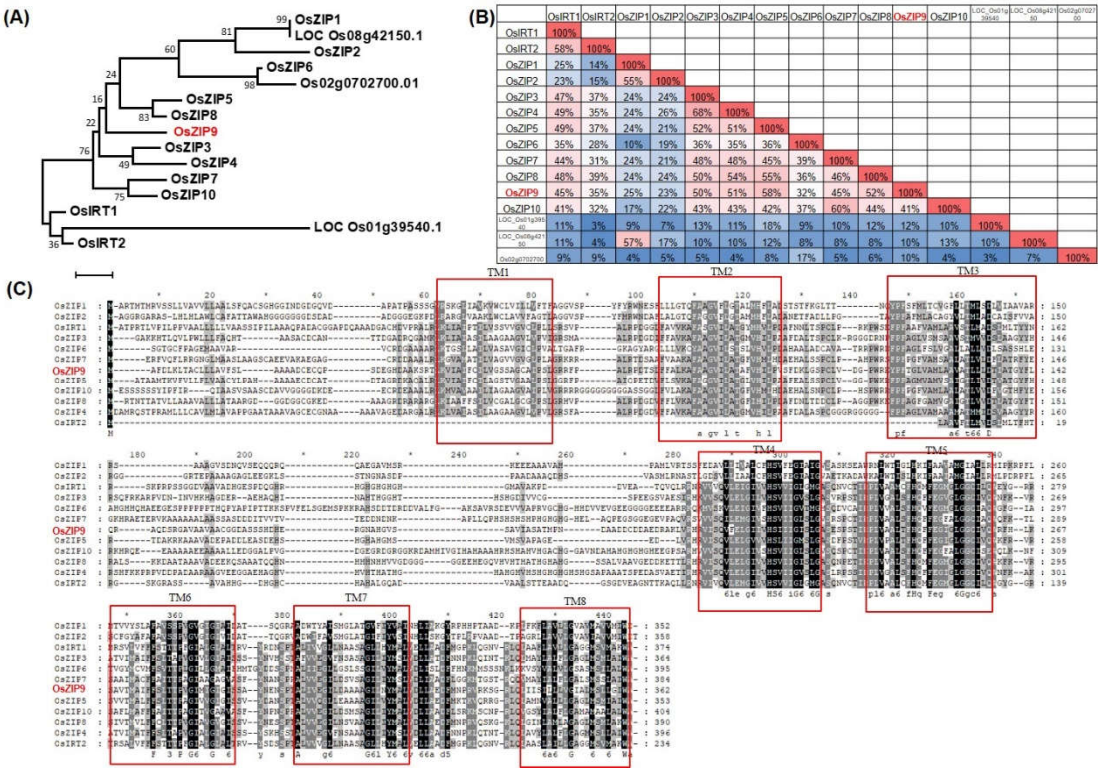

Figure 2.2 Sequence analysis of OsZIPs. (A) Phylogenetic analysis of OsZIP9 homologues in rice. OsIRT1, LOC_Os03g46470; OsIRT2, LOC_Os03g46454; OsZIP1, LOC_Os01g74110; OsZIP2, LOC_Os03g29850; OsZIP3, LOC_Os04g52310; OsZIP4,

LOC_Os08g10630; OsZIP5, LOC_Os05g39560; OsZIP6, LOC_Os05g07210; OsZIP7, LOC_Os05g10940; OsZIP8, LOC_Os07g12890; OsZIP9, LOC_Os05g39540; OsZIP10, LOC_Os06g37010; LOC_Os01g39540; LOC_Os08g42150; Os02g0702700. (B) Identity matrix for ZIP proteins in rice. Values show identity of each protein. (C) Alignment of amino acid sequences of OsZIP proteins. Boxes with red line show transmembrane domains.

3.2.2 Transport activity test of OsZIP1

To examine whether OsZIP1 is able to transport Zn, we expressed it in Zn uptake-defective yeast cells (ZHY3) under control of the galactose-inducible promoter. In the presence of galactose (gene induction), similar to OsHMA2 as a positive control (Yamaji et al., 2013), the yeast expressing full-length of *OsZIP1* was able to complement the growth at low Zn concentration (0, 5, 10 μM). However, at higher Zn concentrations (50 and 100 μM), the growth did not differ between yeast expressing *OsZIP1* and vector control (Fig. 2.3). By contrast, in the presence of glucose (no gene induction), the growth was similar between yeast carrying *OsZIP1* or an empty vector (Fig. 2.3). These results indicate that OsZIP1 functions as an influx transporter for Zn in yeast.

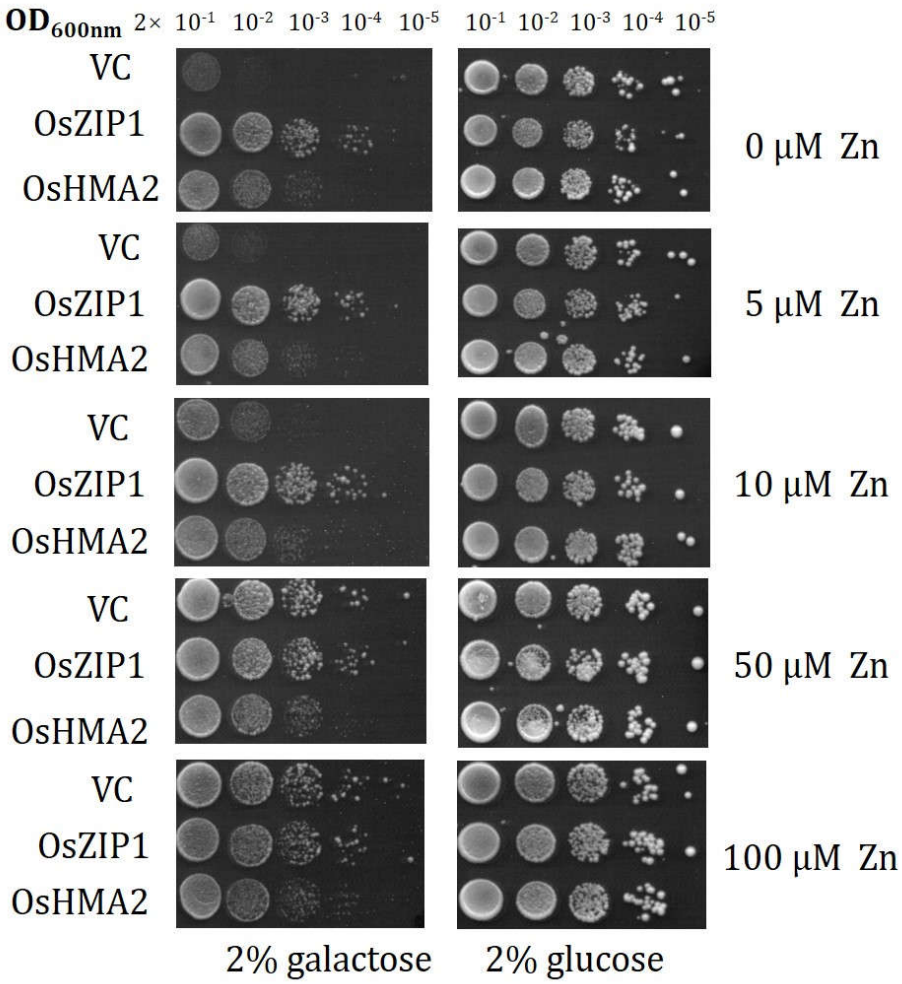

Figure 2.3 Transport activity of OsZIP1 for Zn. Growth of ZHY3 (zinc uptake defective yeast strain) expressing empty vector (VC), *OsZIP1* or *OsHMA2* (positive control). The yeast was incubated on a plate containing 0, 5, 10, 50 and 100 μM Zn in the presence of 2% glucose or galactose for 3 d.

3.2.3 Expression pattern of *OsZIP1*

The expression pattern of *OsZIP1* was investigated in rice plants grown in either soil or nutrient solution by quantitative reverse transcription PCR (RT-qPCR). In samples derived from rice grown in the field, *OsZIP1* was found to be mainly expressed in the roots at all growth stages (Fig. 2.4A). In samples from hydroponically cultivated rice,

the expression of *OsZIP1* in the roots was slightly induced by Cu-deficiency, but not by Zn-, Fe- or Mn-deficiency (Fig. 2.4B).

I also investigated the spatial expression pattern of *OsZIP1* in different root regions. The expression of *OsZIP1* was very low in the root tip region (0–0.5 cm from the root tip) (Figs. 2.4C). However, higher expression was detected in root mature regions (>1.0 cm, Figs. 2.4C).

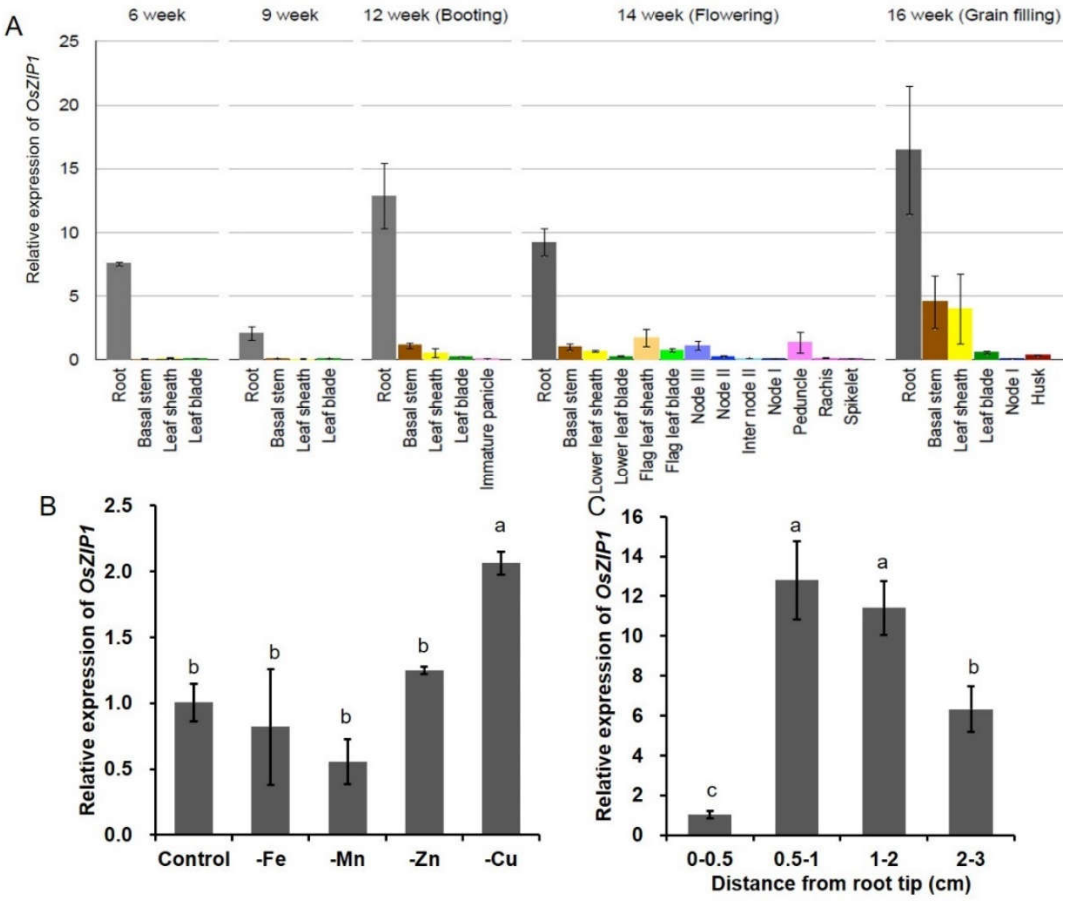

Figure 2.4 Expression pattern of *OsZIP1*. (A) Growth stage- and organ-dependent expression of *OsZIP1*. Samples of various organs were taken from rice grown in the field at different growth stages. (B) Response of *OsZIP1* expression to metal deficiency. Rice seedlings were grown in the 1/2 Kimura B solution with or without Cu, Zn, Fe, or Mn for three days. (C) Spatial expression pattern of *OsZIP1* in roots. Different root

segments (0–0.5, 0.5–1.0, 1.0–2.0, and 2.0–3.0 cm from the root tip) were collected from roots of 5-d-old seedlings. The expression level of *OsZIP1* was determined by RT-qPCR. *Histone* H3 was used as internal control. The expression relative to root at 6 weeks (A), control condition (B), and the root segment of 0–0.5 cm (C) are shown. Data are means ±SD of three biological replicates. Statistical comparison was performed by ANOVA followed by Tukey-Kramer's test. Different letters indicate significant difference (p<0.01).

3.2.4 Tissue specificity of *OsZIP1* expression

To investigate the tissue specificity of *OsZIP1* expression, we generated transgenic lines carrying the promoter of *OsZIP1* fused with *GFP*. Immunostaining using GFP antibody in *pOsZIP1-GFP* plants showed that the signal was detected in both root tip (0-1 cm from the tip) and mature regions (1-2 and 2-3 cm from root tip). Furthermore, the GFP signal was detected at exodermis, cortex, endodermis, pericycle and stele in both root tip and mature regions (Fig. 2.5), but not in the epidermis.

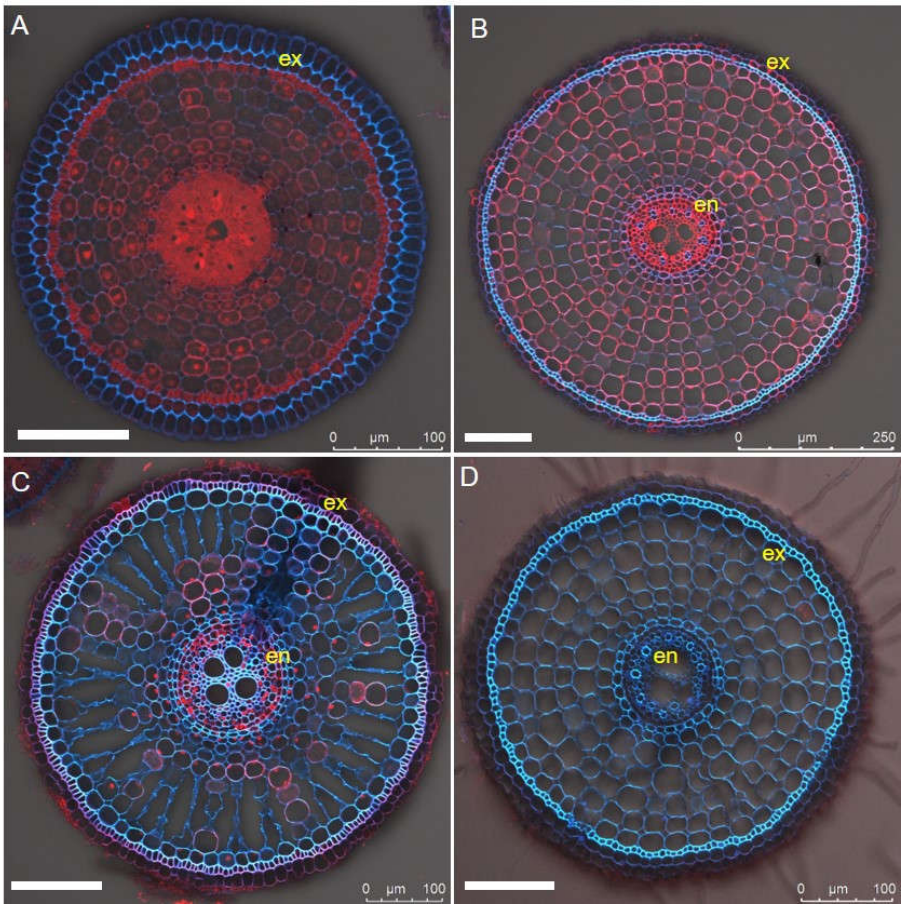

Figure 2.5 Tissue specificity of *OsZIP1* expression. Immunostaining with a GFP antibody was performed in transgenic rice carrying the *OsZIP1* promoter fused with *GFP* in the root tips (A, 0-1 cm from root tip), mature root regions (B, 1-2 cm) and (C, 2-3 cm from root tip). Wild-type rice was used as a negative control (D). Red color indicates the GFP antibody-specific signal. Blue color indicates cell wall autofluorescence. ex, exodermis; en, endodermis, Scale bars, 100 µm.

3.3 Results of *OsZIP9*

3.3.1 Cloning of *OsZIP9*

The full-length coding region of *OsZIP9* (LOC_Os05g39540/Os05g0472400) was amplified by PCR from complementary DNA (cDNA) of rice roots (cv Nipponbare).

OsZIP9 is composed of three exons and two introns (Fig. 2.6) and encodes a protein of 363 amino acids. OsZIP9 shares 23–52% identify with other ZIP members (Fig. 2.2B) and forms a separate clade from other ZIP members (Fig. 2.2A). Similar to other rice ZIP members, OsZIP9 protein was predicted to have eight trans-membrane domains (TMHMM Server v. 2.0; http://www.cbs.dtu.dk/services/TMHMM/) (Figs. 2.2C and 2.6C).

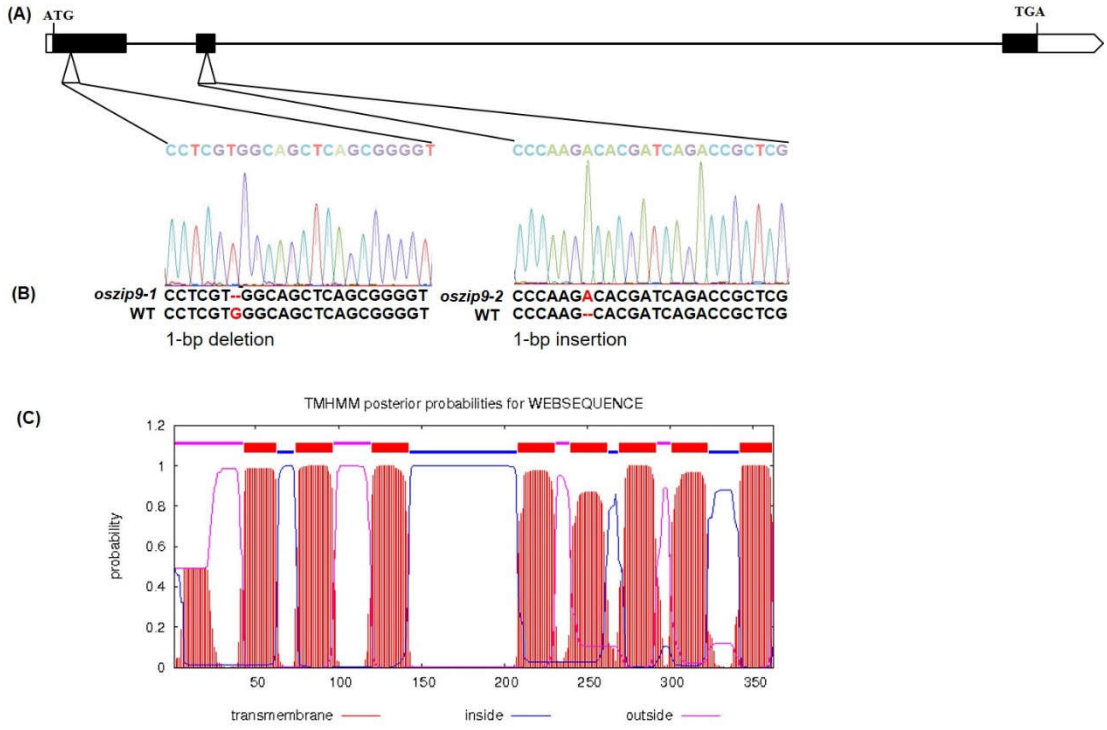

Figure 2.6 Mutated sequences of *OsZIP9* gene in CRISPR/Cas9 mutants. (A) Two target sites of *OsZIP9* by using CRISPR/Cas9 system. White boxes represent UTR regions, black boxes represent exons, the lines between boxes represent introns. The triangles represent the target sites in CRISPR/Cas9 system. (B) Comparison of sequence between wild-type rice (WT) and two CRISPR/Cas9 lines. *Oszip9-1* with a 1-bp deletion, *oszip9-2* with a 1-bp insertion. (C) Trans-membrane domains predicted by TMHMM.

3.2 Transport activity test of OsZIP9.

To examine whether OsZIP9 is able to transport Zn, we expressed it in Zn uptake–defective yeast cells (ZHY3) under control of the galactose-inducible promoter. A time-course experiment with stable isotope ^{67}Zn showed that in the presence of glucose (no *OsZIP9* expression) there was no difference in Zn accumulation ($\Delta^{67}Zn$) between vector control and yeast expressing *OsZIP9* (Fig. 2.7A). However, when the expression of *OsZIP9* was induced by the presence of galactose, yeast expressing *OsZIP9* showed much higher $\Delta^{67}Zn$ compared with the empty vector control (Fig. 2.7B).

To examine the transport specificity of OsZIP9 for metals, the transport activity for Fe, Cu, and Zn was compared by using respective stable isotopes, specifically ^{67}Zn, ^{65}Cu, or ^{57}Fe, in wild-type yeast cells (BY4741). In the presence of galactose, OsZIP9 transported only Zn and not Fe or Cu (Fig. 2.7C).

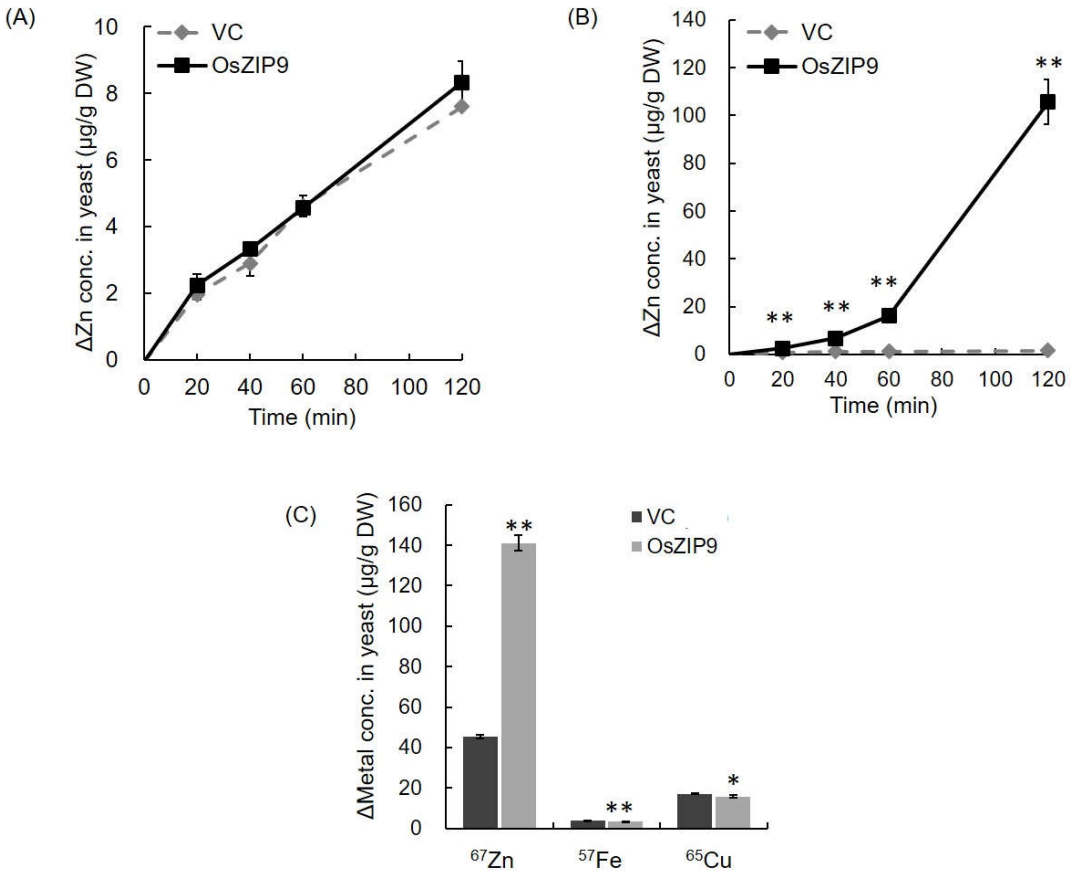

Figure 2.7 Transport activity of OsZIP9 for metals in yeast cells. (A-B) Time-dependent uptake of OsZIP9 for ^{67}Zn in the presence of glucose (A) and galactose (B). Zn uptake defective yeast cells (ZHY3) expressing *OsZIP9* or empty vector (VC) were exposed to a solution containing 5 μM ^{67}Zn for different time periods. (C) Transport activity for different metals. Wild-type yeast cells (BY4741) expressing *OsZIP9* or empty vector (VC) were exposed to a solution containing 5 μM of ^{67}Zn, ^{57}Fe, or ^{65}Cu for two hours in the presence of galactose. The concentration of stable metal isotopes was determined by isotope mode of ICP-MS. ΔMetal was calculated by subtracting the natural abundance of each metal isotope. Data are means ±SD of three biological replicates. The asterisks indicate significant differences (*p<0.05 or**p<0.01 by T-test). All data were compared with VC in each part.

3.3 Expression pattern analysis of *OsZIP9*.

The expression pattern of *OsZIP9* was also investigated in plants grown in either soil or nutrient solution by RT-qPCR. In the field samples, *OsZIP9* was found to be mainly expressed in the roots at all growth stages (Fig. 2.8A). In samples from hydroponically cultivated rice, the expression of *OsZIP9* in the roots was strongly induced by Zn-deficiency, but not by Cu- or Mn-deficiency (Fig. 2.8B). *OsZIP9* expression was also induced by Fe-deficiency, but to a lesser extent. Time-dependent expression analysis showed that *OsZIP9* expression was significantly up-regulated following 1 day and further increased following 3 days of Zn deficiency (Fig. 2.9A). However, 1 day of Fe deficiency did not induce *OsZIP9* expression, although expression induction was observed following 3 days of Fe deficiency (Fig. 2.9B).

The spatial expression pattern of *OsZIP9* was also investigated in different root regions. The expression of *OsZIP9* was very low in the root tip region (0–0.5 cm from the root tip) (Fig. 2.8C). However, higher expression was detected in root mature regions (>1.0 cm).

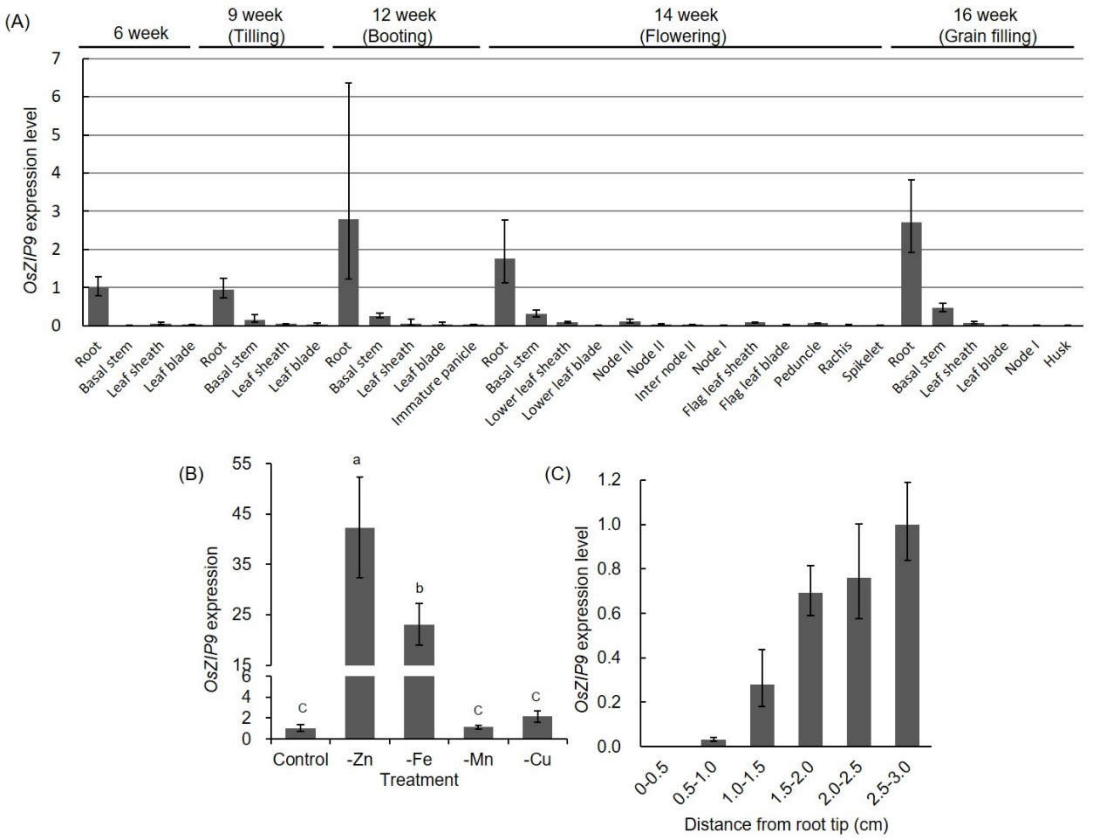

Figure 2.8 Expression pattern of *OsZIP9*. (A) Growth stage- and organ-dependent expression of *OsZIP9*. Samples of various organs were taken from rice grown in the field at different growth stages. (B) Response of *OsZIP9* expression to metal deficiency. Rice seedlings were grown in the 1/2 Kimura B solution with or without Cu, Zn, Fe, or Mn for three days. (C) Spatial expression pattern of *OsZIP9* in roots. Different root segments (0–0.5, 0.5–1.0, 1.0–1.5, 1.5–2.0, 2.0–2.5, and 2.5–3.0 cm from the root tip) were collected from roots of 5-d-old seedlings. The expression level of *OsZIP9* was determined by RT-qPCR. *Histone* H3 (A, B) and *Actin* (C) were used as internal controls. The expression relative to root at 6 weeks (A), control condition (B), and the root segment of 2.5–3.0 cm (C) are shown. Data are means ±SD of three biological replicates. Statistical comparison was performed by ANOVA followed by Tukey-Kramer's test. Different letters indicate significant difference (p<0.01).

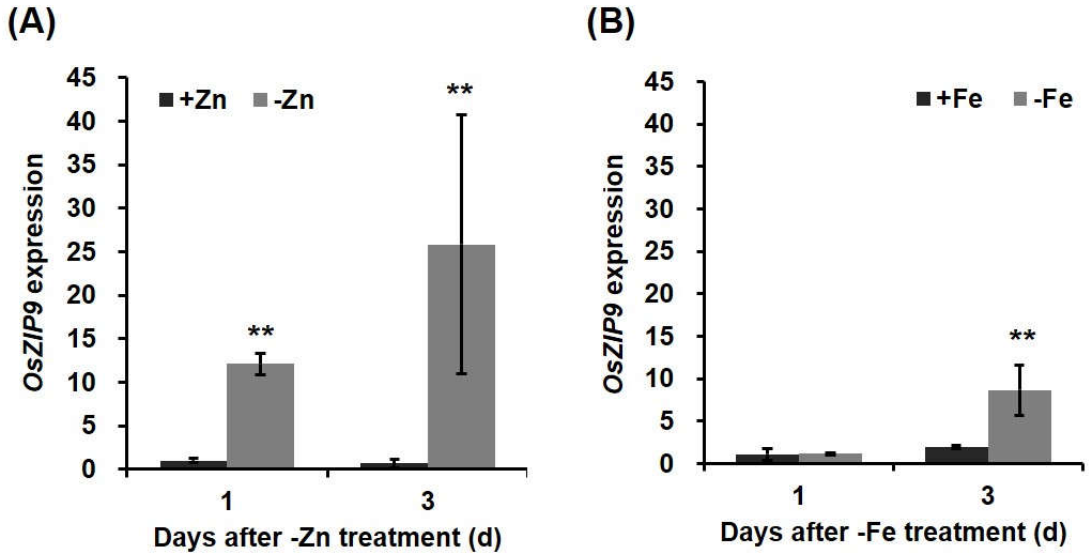

Figure 2.9 Time-dependent response of *OsZIP9* to Zn-deficiency and Fe-deficiency in the roots. (A) Time-dependent expression of *OsZIP9* in response to Zn-deficiency. (B) Time-dependent expression of *OsZIP9* in response to Fe-deficiency. Rice seedlings were grown in a solution with or without Fe or Zn for different time. The expression level of *OsZIP9* in the roots was determined by quantitative real-time RT-qPCR. *Histone H3* was used as an internal control. Data are means ±SD of three biological replicates. Statistical comparison was performed by ANOVA followed by Tukey-Kramer's test (**P<0.01).

3.4 Tissue specificity of *OsZIP9* expression

To investigate the tissue specificity of *OsZIP9* expression, transgenic lines carrying the promoter of *OsZIP9* fused with *GFP* were generated. Immunostaining using GFP antibody showed that the signal was very weak in both the root tip (0.2 cm from the root tip) and mature region (1.5 cm from the root tip) of plants supplied with Zn (Fig.

2.10, A and D). However, in Zn-deficient roots, *ZIP9* was strongly expressed at the exodermis and endodermis of the root mature region (Fig. 2.10, E, G and H). The signal in the root tip of Zn-deficient plants was also weak, which is consistent with the spatial expression pattern of *OsZIP9* (Fig. 2.8C). No signal was detected in wild-type plants (Fig. 2.10, C and F), indicating the specificity of the antibody.

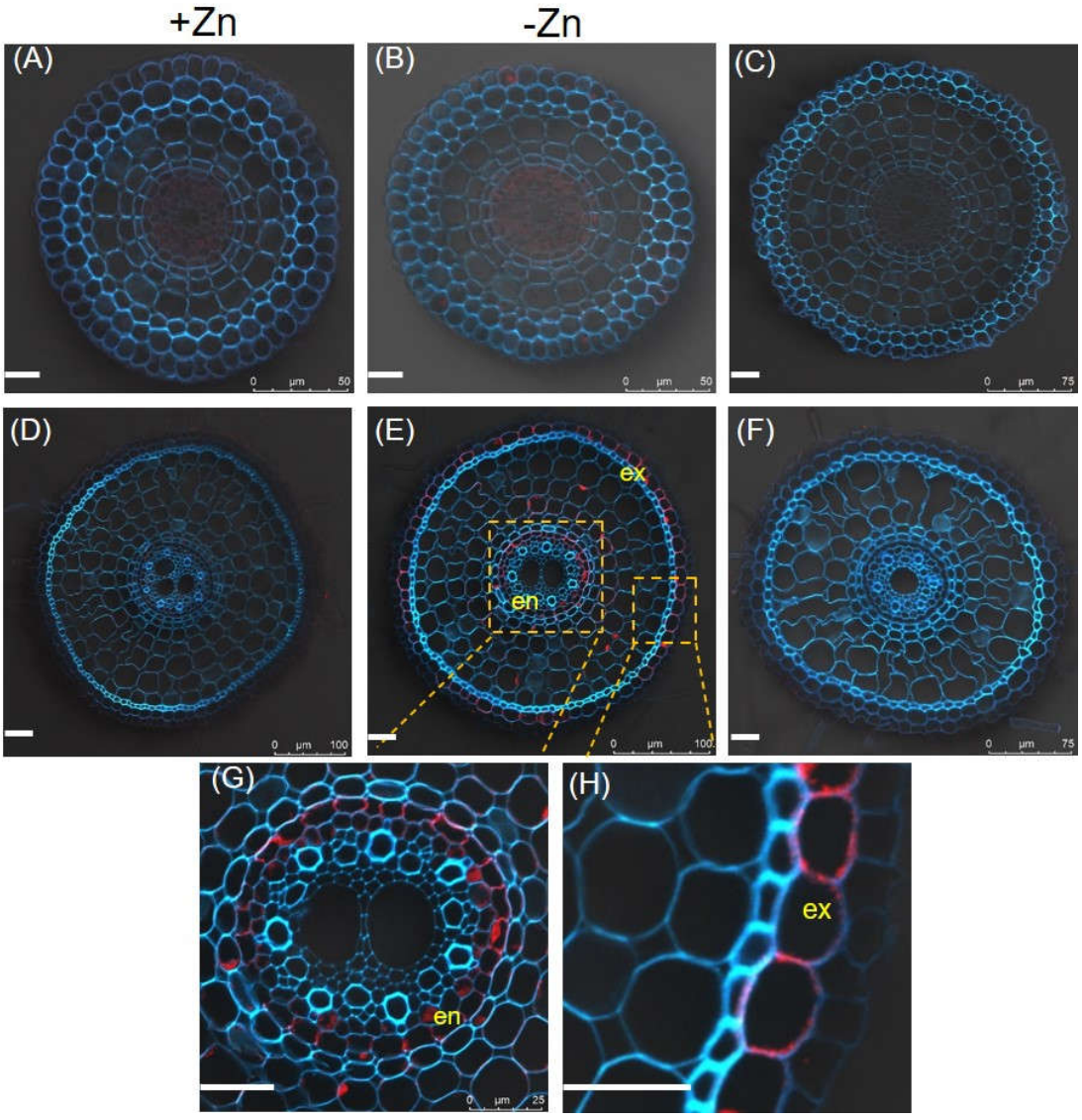

Figure 2.10 Tissue specificity of *OsZIP9* expression. Two-week-old plants of transgenic lines carrying the *OsZIP9* promoter fused with *GFP* were exposed to a solution containing Zn (A, D) or not (B, E) for 5 days. The root cross sections from the

root tip (0.2 cm from the tip) (A-C) and mature region (1.5 cm from the tip) (D-F) were prepared and used for immunostaining with an anti-GFP antibody. (G, H) Magnified image of orange box area in (E). (C, F) Wild-type rice roots as a negative control. Red color shows signal from the anti-GFP antibody and blue color from auto fluorescence of cell wall. ex, exodermis; en, endodermis. Scale bar, 25 μm.

3.5 Subcellular localization of OsZIP9

Subcellular localization of OsZIP9 was investigated by transiently expressing a GFP-OsZIP9 fusion in rice protoplasts and onion epidermal cells. In rice protoplasts expressing GFP alone, the GFP signal was detected in the cytoplasm and nuclei (Fig. 2.11, A-D). However, in protoplasts expressing GFP-OsZIP9, the GFP signal was mainly localized to the peripheral membrane of the cells, although some signal was also detected in the endomembrane (Fig. 2.11, E-H). Similar results were obtained in onion epidermal cells (Fig. 2.11, I-L).

To further confirm OsZIP9 subcellular localization, we performed double staining using DAPI and an OsZIP9 antibody. In the roots of plants exposed to -Zn conditions for 4 days, OsZIP9 was localized to the periphery of the cells, outside of the nuclei stained by DAPI (Fig. 2.11, M-P). No signal was detected in the knockout line (Fig. 2.11Q). Taken together, these results indicate that OsZIP9 is most likely localized to the plasma membrane.

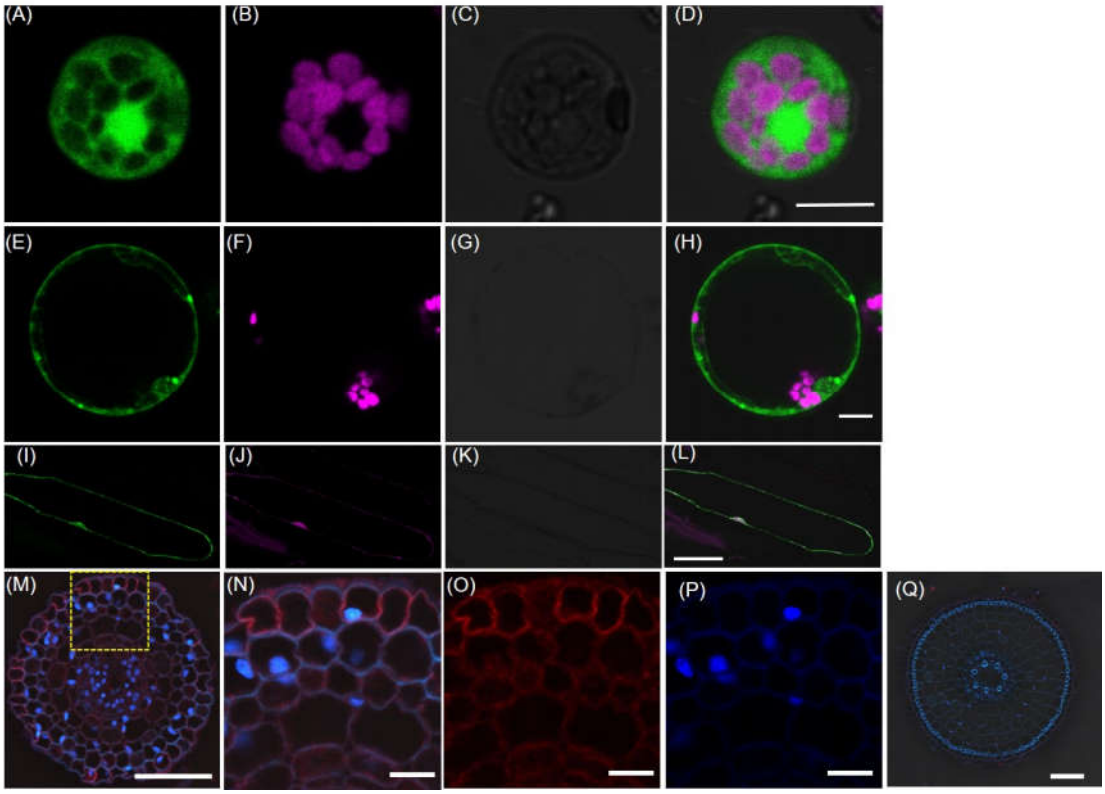

Figure 2.11 Subcellular localization of OsZIP9. (A-L) Subcellular localization of OsZIP9 in rice protoplasts and onion epidermal cells. GFP alone (A-D) or OsZIP9 fused with GFP at N-terminal (E-L) was transiently transformed into rice protoplasts (A-H) or onion epidermal cells (I-L). GFP signal (A, E and I), chlorophyll image (B, F), Ds-Red signal (J), bright field (C, G and K) and merged image (D, H and L) are shown. (M-O) Subcellular localization of OsZIP9 in rice roots. Double staining with DAPI (nuclei marker) and OsZIP9 antibody was performed in the roots of wild-type rice (M-P) and *oszip9* mutant (Q) exposed to Zn-free solution for 4 days. (N-P) Enlarged image from yellow dotted box in M. The red color shows the signal from the antibody (O) and cyan blue from autofluorescence of cell wall and nuclei stained by DAPI (P). (M-N), Merged image. Scale bar=10 μm (D, H), 100 μm (L), 50 μm (M, Q), 10 μm (N, O, P).

3.6 Phenotypic analysis of *OsZIP9* knockout lines in hydroponic and soil culture

To investigate the role of OsZIP9 in Zn transport, *OsZIP9* knockout lines were generated by the CRISPR/Cas9 technique. Two independent knockout lines with different target positions (*oszip9-1* and *oszip9-2*): one (*oszip9-1*) with a 1-bp deletion at the first exon, and the other (*oszip9-2*) with a 1-bp insertion at the second exon, were ued for phenotypic analysis (Fig. 2.6B).

When the wild-type rice and two independent knockout lines were grown in a nutrient solution containing different Zn concentrations (0.02, 0.2, or 2 μM), they showed different phenotypes. At 0.02 μM Zn, growth of the two knockout lines was obviously inhibited compared with wild-type rice (Fig. 2.12A). New leaves showed typical Zn-deficiency symptoms in the knockout lines, but not in the wild-type rice (Fig. 2.12D). The shoot fresh weight of the knockout lines was 65% of the wild-type rice (Fig. 2.12E), although the root fresh weight did not differ between different lines (Fig. 2.13F). However, at 0.2 and 2 μM Zn, growth was similar between wild-type rice and the knockout lines (Fig. 2.12, B, C, E and F).

Mineral element profiles were then compared in the roots and shoots of wild-type rice and the knockout lines exposed to different Zn concentrations. At 0.02 μM Zn, both the concentration and content of Zn in the roots and shoots were significantly lower in the knockout lines than in wild-type rice (Fig. 2.13, A-D). At 0.2 μM Zn, shoot Zn concentration and content were lower in the knockout lines than in wild-type rice, but root Zn concentration and content were similar between different lines. However, Zn concentration and content in both the roots and shoots of the different lines were

comparable at 2 µM Zn (Fig. 2.13, A-D).

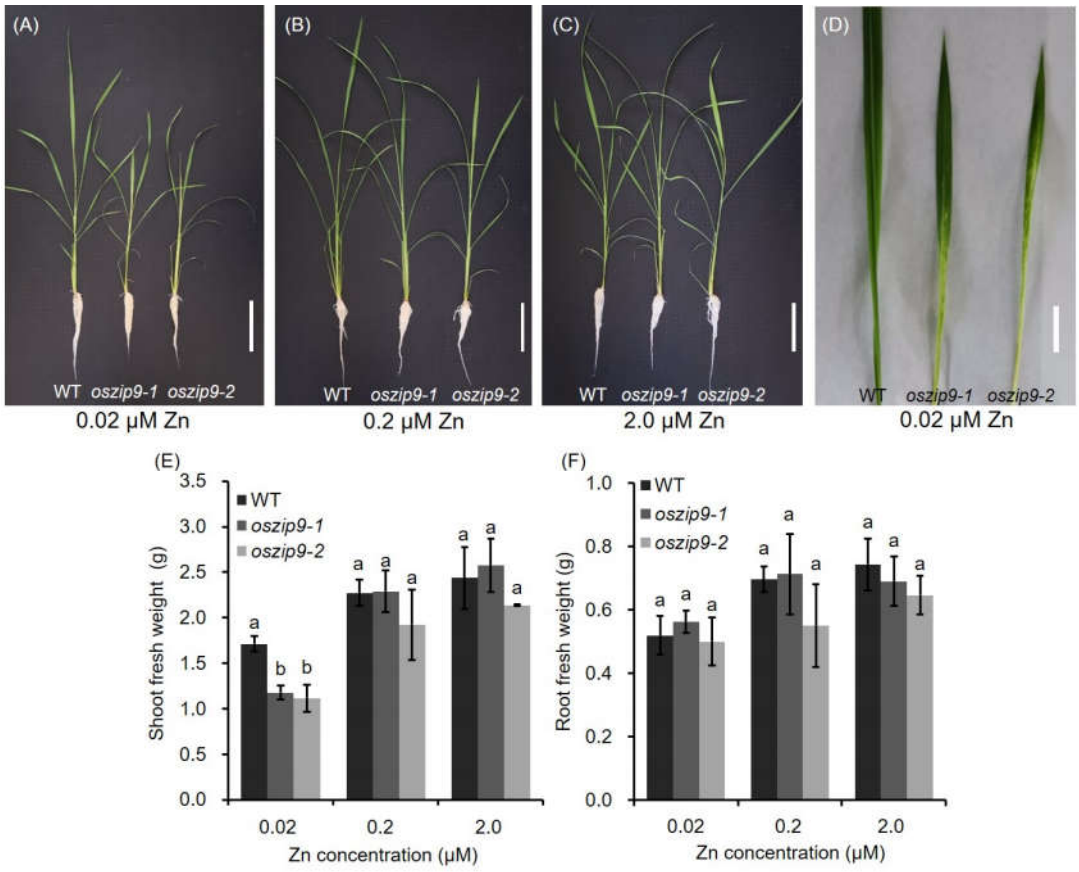

Figure 2.12 Phenotypic analysis of *OsZIP9* knockout lines in hydroponic solution. (A-C) Phenotype of the wild-type rice and two *OsZIP9* knockout lines (*oszip9-1* and *oszip9-2*). Scale bar, 10 cm. (D) Zn-deficiency symptom of new leaf. Scale bar, 2.5 cm. (E-F) Fresh weight of shoots (E) and roots (F). The plants were grown in a nutrient solution containing 0.02 (A, D), 0.2 µM (B) and 2 µM (C) Zn for 17 days. Data in E and F are means ±SD of three biological replicates. Statistical comparison was performed by ANOVA followed by Tukey-Kramer's test. Different letters indicate significant difference (p<0.01).

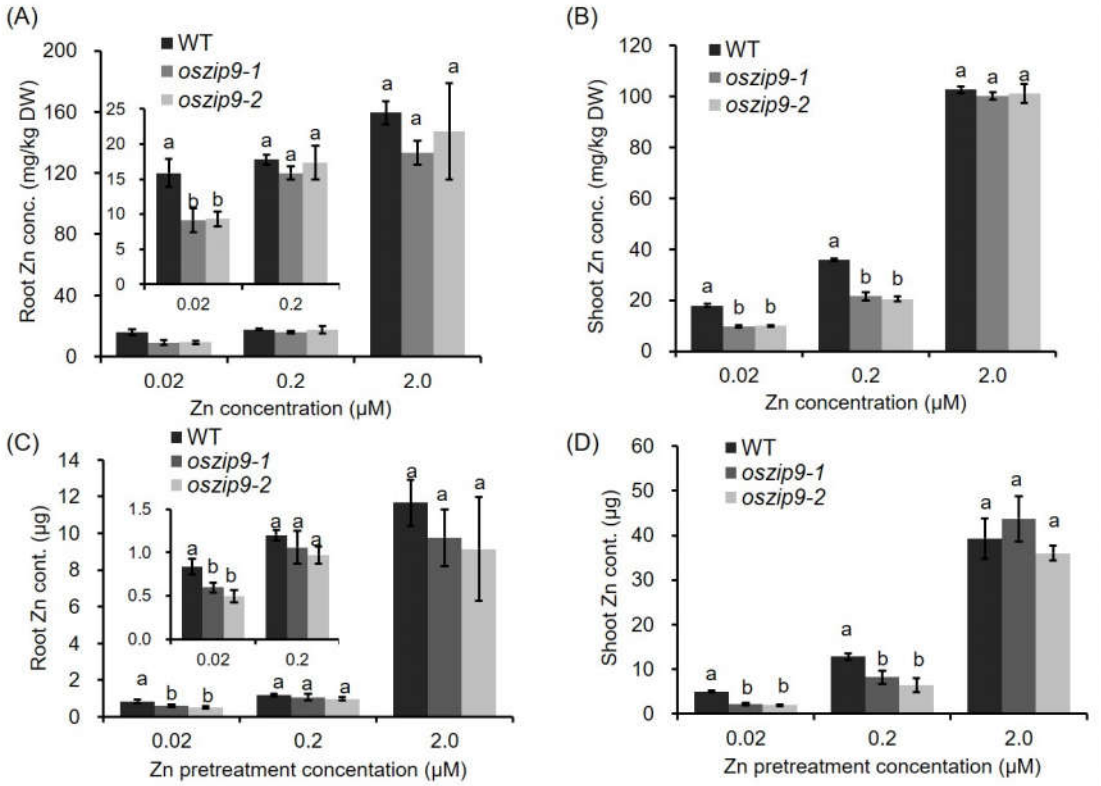

Figure 2.13 Zn concentrations and contents in wild-type rice and *OsZIP9* knockout lines. (A-B) Zn concentrations in root (A) and shoot (B) of wild-type rice and knockout lines. (C-D) Zn contents in the roots and shoots. The plants were grown in a nutrient solution containing 0.02, 0.2, or 2 μM Zn for 17 days. Data are means ±SD of three biological replicates. Statistical comparison was performed by ANOVA followed by Tukey-Kramer's test. Different letters indicate significant difference (p<0.01). All data were compared with the wild-type rice in each treatment.

There was no difference in the concentrations of Ca, Mg, K, P, Fe, Cu, and Mn in the roots of wild-type rice and the knockout lines (Figs. 2.14, A-D and 2.15, A-C); however, the knockout mutants showed higher concentrations of Ca, Mg, Fe, Cu, and Mn in the shoots at 0.02 μM Zn, but not at 0.2 and 2.0 μM Zn (Figs. 2.14, E-F and 2.15, D-F).

Moreover, the contents of these elements except Fe were similar between the different lines at all Zn concentrations tested (Figs. 2.16, E-F and 2.17, D-F), indicating that the higher concentrations observed at 0.02 μM Zn were caused by decreased growth. The shoot concentration and content of K were slightly decreased in the knockout lines, whereas those of P were not altered compared with wild-type rice (Figs. 2.14, G-H and 2.16, G-H).

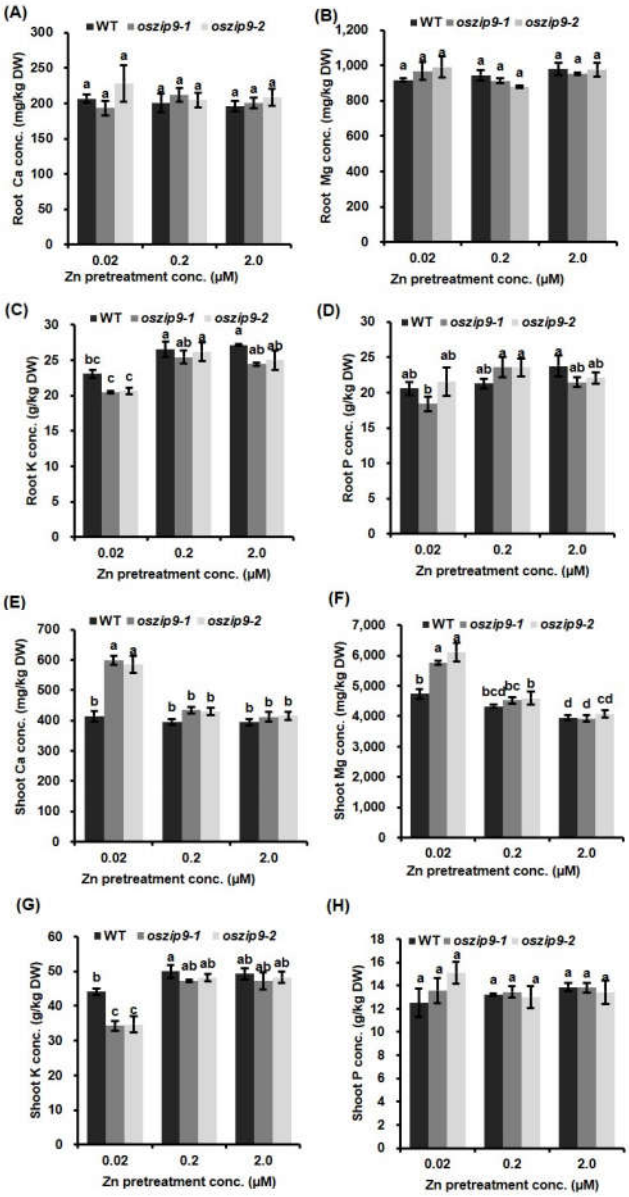

Figure 2.14 The concentration of macro-elements in the roots and shoots.

Concentration of Ca (A, E), Mg (B, F), K (C, G) and P（D, H）in the root (A-D) and shoots (E-H). Both the wild-type rice and two independent *OsZIP9* knockout lines were grown in a nutrient solution containing 0.02, 0.2 μM and 2 μM Zn for 17 days. Data are means ±SD of three biological replicates. Statistical comparison was performed by ANOVA followed by Tukey-Kramer's test. Different letters mean significant difference (p<0.01).

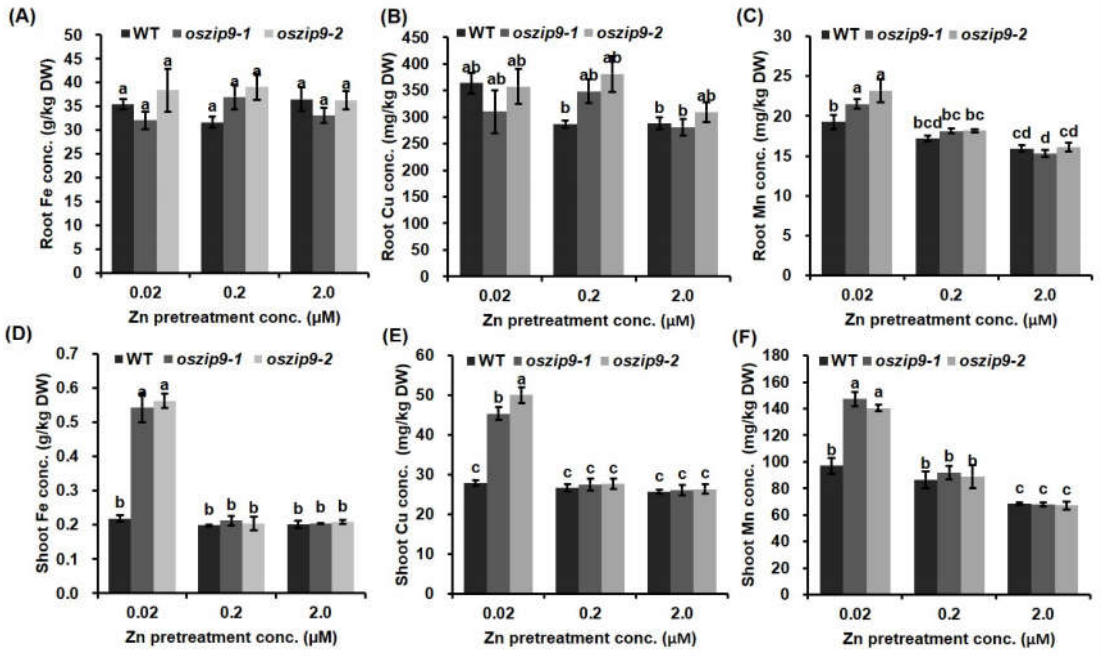

Figure 2.15 Concentration of Fe, Mn and Cu in the roots and shoots. Concentration of Fe (A, D), Cu (B, E) and Mn (C, F) in the roots (A-C) and shoots (D-F). Both the wild-type rice and two independent *OsZIP9* knockout lines were grown in a nutrient solution containing 0.02, 0.2 μM and 2 μM Zn for 17 days. Data are means ±SD of three biological replicates. Statistical comparison was performed by ANOVA followed by Tukey-Kramer's test. Different letters mean significant difference (p<0.01).

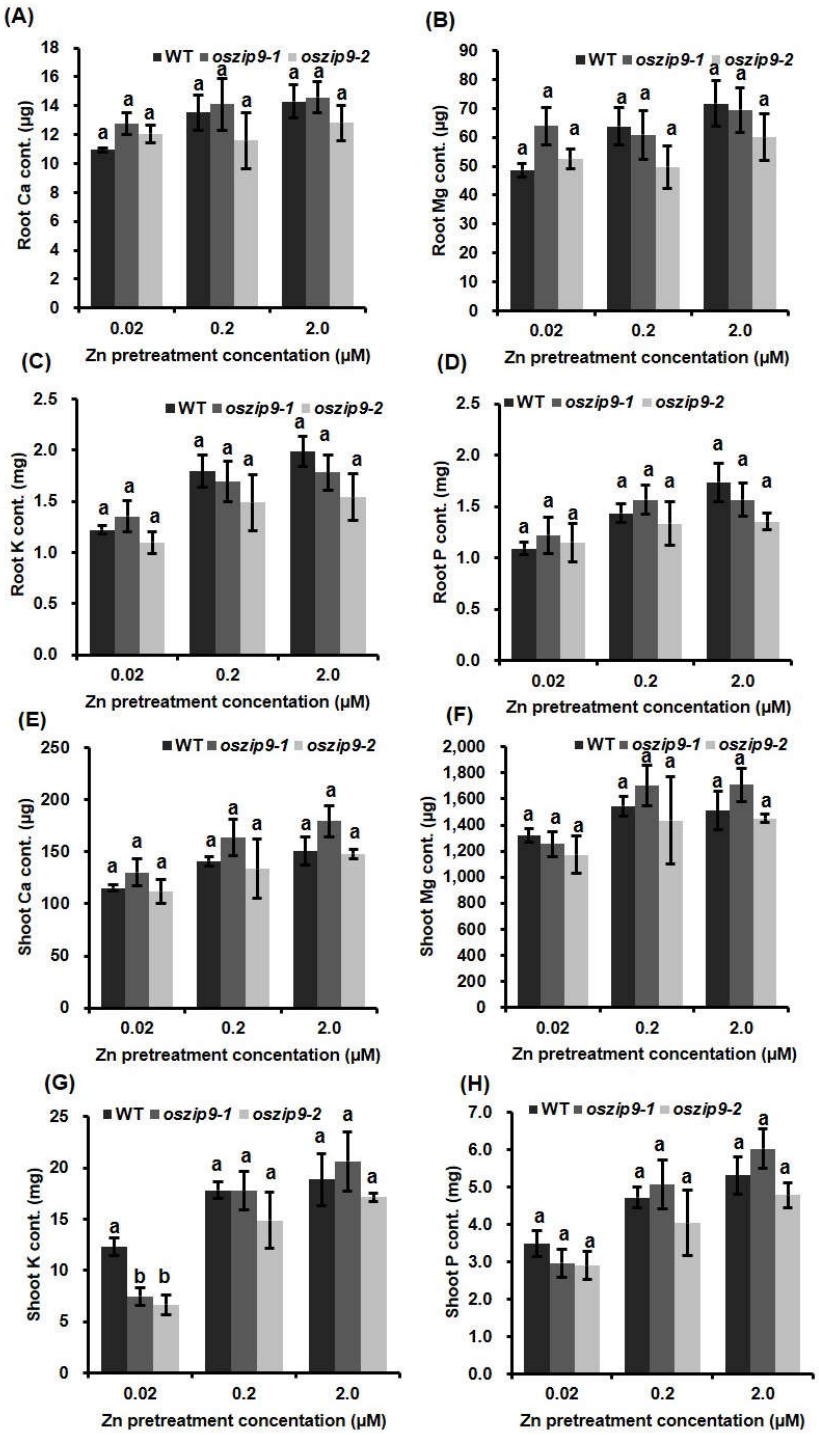

Figure 2.16 Content of macro-elements in the roots and shoots. Content of Ca (A, E), Mg (B, F), K (C, G) and P (D, H) in the roots (A-D) and shoots (E-H). Both the wild-type rice and two independent *OsZIP9* knock-out lines were grown in a nutrient solution containing 0.02, 0.2 μM and 2 μM Zn for 17 days. Data are means ±SD of three biological replicates. Statistical comparison was performed by ANOVA followed

by Tukey-Kramer's test. Different letters mean significant difference (p<0.01). All data were compared with the wild-type rice in each treatment.

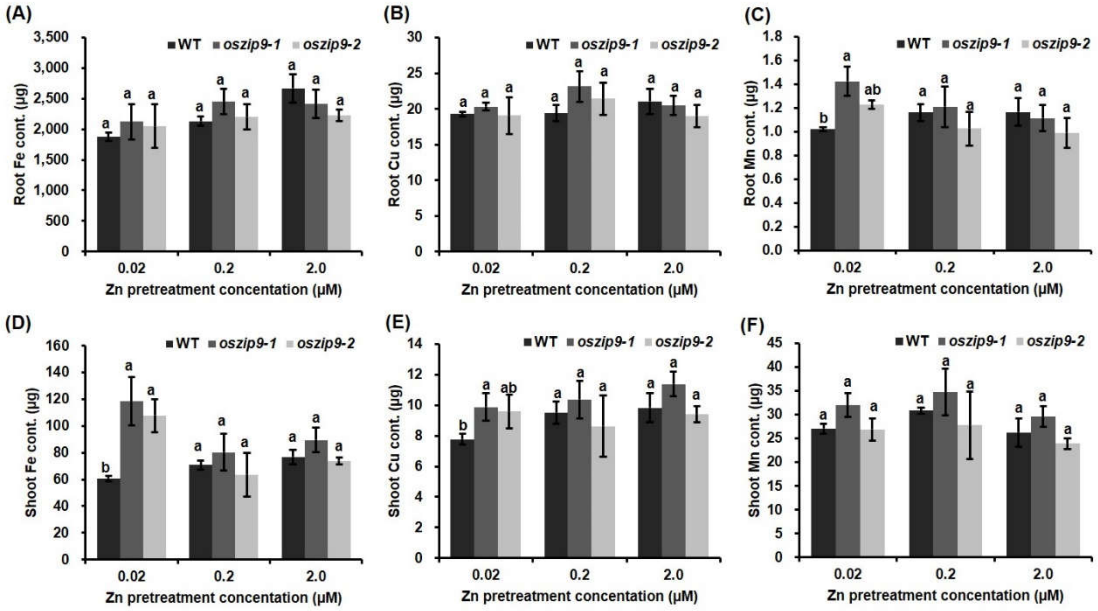

Figure 2.17 Content of Fe, Mn and Cu in the roots and shoots. Content of Fe (A, D), Cu (B, E) and Mn (C, F) in the roots (A-C) and shoots (D-F). Both the wild-type rice and two independent *OsZIP9* knockout lines were grown in a nutrient solution containing 0.02, 0.2 μM and 2 μM Zn for 17 days. Data are means ±SD of three biological replicates. Statistical comparison was performed by ANOVA followed by Tukey-Kramer's test. Different letters mean significant difference (p<0.01). All data were compared with the wild-type rice in each treatment.

When grown in soil until maturity, the knockout lines accumulated less than half the amount of Zn in wild-type rice in straw and brown rice (Fig. 2.18). However, the concentrations of other elements, including Cu, Fe, and Mn, in straw and brown rice were comparable between wild-type rice and the knockout lines, except that the

concentration of Mn in straw was slightly increased in the knockout lines compared with wild-type rice (Fig. 2.18). Accumulation of Cd and As in straw and brown rice was also compare, but no difference in the accumulation of these two toxic elements was found in either straw or brown rice between wild-type rice and the *OsZIP9* knockout lines (Fig. 2.19). Combined together, these results indicate that OsZIP9 is a specific transporter for Zn uptake in rice roots.

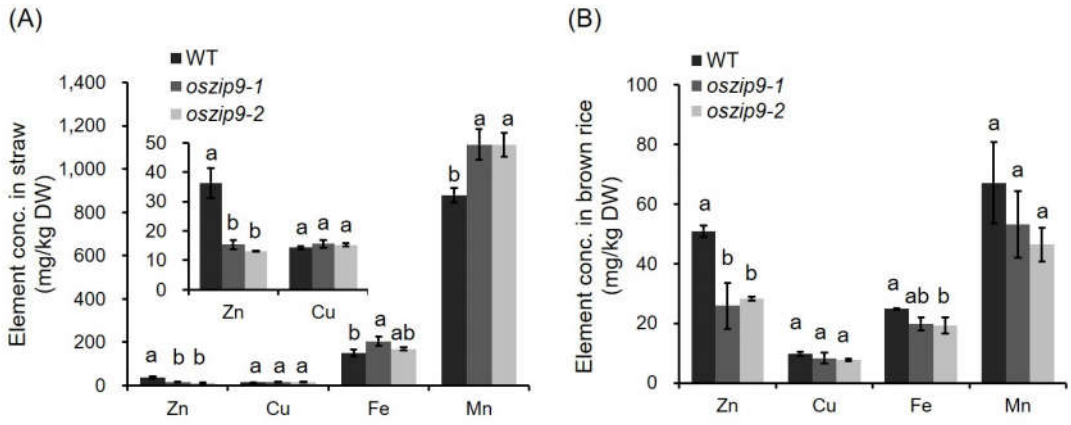

Figure 2.18 Comparison of metal accumulation between wild-type rice and two independent *OsZIP9* knockout lines grown in soil. (A, B) Metal concentrations in the straw (A) and brown rice (B). Both the wild-type rice and two independent *OsZIP9* knockout lines were grown in soil under flooded conditions until maturity. The concentration of different metals was determined by ICP-MS. Data are means ±SD of three biological replicates. Statistical comparison was performed by ANOVA followed by Tukey-Kramer's test. Different letters indicate significant difference (p<0.01). All data for each element were compared with the wild-type rice.

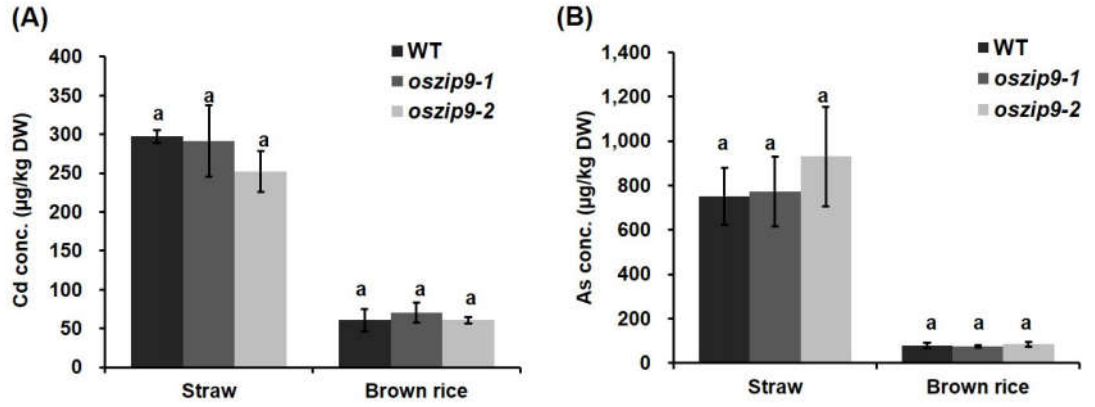

Figure 2.19 Concertation of Cd and As in straw and brown rice. Both wild-type rice and two independent *OsZIP9* knockout lines were grown in soil until maturity. The concentration of Cd (A) and As (B) in the straw and brown rice was determined by ICP-MS. Data are means ±SD of three biological replicates. Statistical comparison was performed by ANOVA followed by Tukey-Kramer's test. Different letters mean significant difference (p<0.01). All data were compared with the wild-type rice in each treatment.

3.7 Short-term uptake experiments with stable isotope ^{67}Zn

To confirm whether Zn uptake was altered in the knockout lines, a short term (24 h) labeling experiment with stable isotope ^{67}Zn was performed. Following the exposure of Zn-deficient plants to 0.4 μM ^{67}Zn for 24 h, the *OsZIP9* knockout lines accumulated much less ^{67}Zn (as Δ^{67}Zn) in both the roots and shoots compared with wild-type rice (Fig. 2.20A). The Δ^{67}Zn uptake in the knockout lines was 41% of wild-type rice (Fig. 2.21B); however, there was no difference in the root-to-shoot translocation of Δ^{67}Zn between the different lines (Fig. 2.20C). To confirm these results, an *OsZIP9* RNAi line, which showed about 80% reduction in *OsZIP9* expression compared wild-type rice (Fig.

2.21A), was also investigated. Similar to the knockout lines, the Δ^{67}Zn concentration in both the roots and shoots was lower in the RNAi line than in wild-type rice (Fig. 2.21B). The Δ^{67}Zn uptake in the RNAi line was 66% of that in wild-type rice (Fig. 2.21C), whereas the root-to-shoot translocation was similar between the RNAi line and wild-type rice (Fig. 2.21D).

Furthermore, a kinetic uptake experiment with ^{67}Zn in Zn-deficient plants at 4°C and 25°C was performed. At 4°C, there was no difference in Δ^{67}Zn uptake (30 min) between wild-type rice and the knockout lines (Fig. 2.20D). However, at 25°C, the Δ^{67}Zn uptake was higher in wild-type rice than in the knockout lines, although the uptake increased with increasing ^{67}Zn concentrations in the nutrient solution in all lines (Fig. 2.20D). The net uptake of Δ^{67}Zn calculated was significantly higher in wild-type rice than in the knockout lines (Fig. 2.20E). Knockdown of *OsZIP9* also significantly reduced the net uptake of Δ^{67}Zn (Fig. 2.21E). Together, these results support that OsZIP9 contributes to Zn uptake in rice roots.

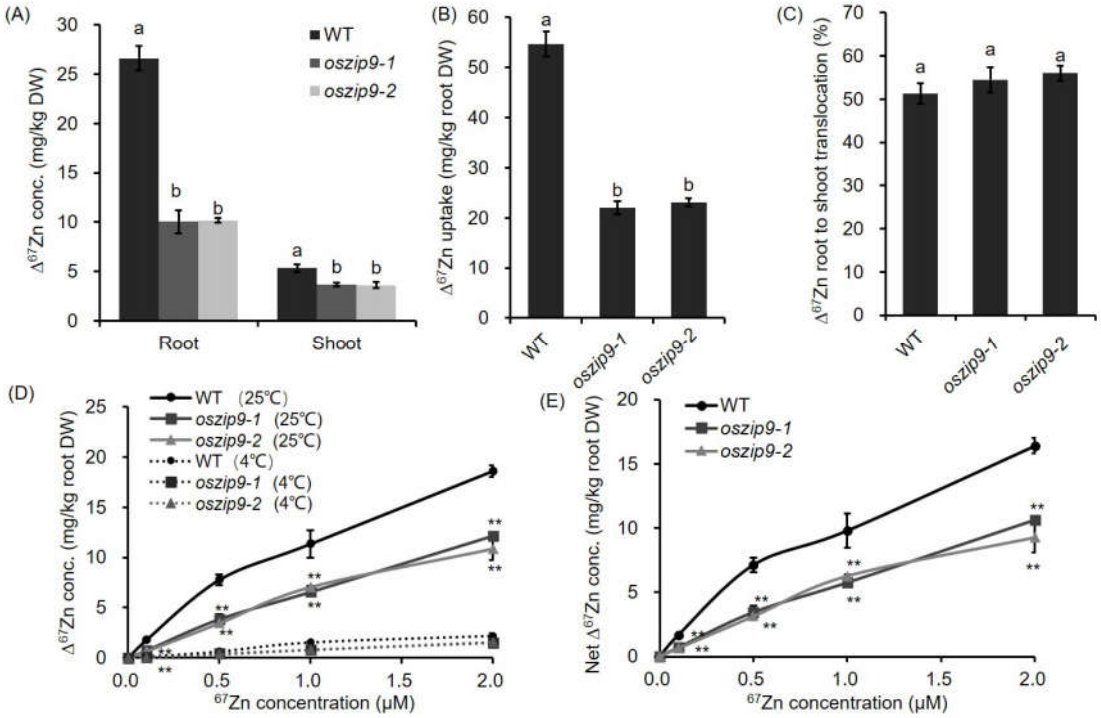

Figure 2.20 Short-term labeling experiment with ^{67}Zn. (A) Concentration of Δ^{67}Zn in the roots and shoots. (B) Uptake of Δ^{67}Zn. (C) Root to shoot translocation of Δ^{67}Zn. The wild-type rice and two independent *OsZIP9* knockout lines grown in 0.02 μM Zn conditions for 17 days were exposed to a solution containing 0.4 μM ^{67}Zn for 24 h. (D-E) Kinetic study of ^{67}Zn uptake. Seedlings grown in Zn-deficient solution for 7 days were exposed to a solution containing different concentrations of ^{67}Zn for 30 min at 25°C or 4°C. Net uptake (E) was calculated by subtracting the apparent uptake at 4°C from that at 25°C. Data are means ±SD of three biological replicates. Different letters and asterisks indicate significant difference (p<0.01) compared with wild-type. Statistical comparison was performed by ANOVA followed by Tukey-Kramer's test.

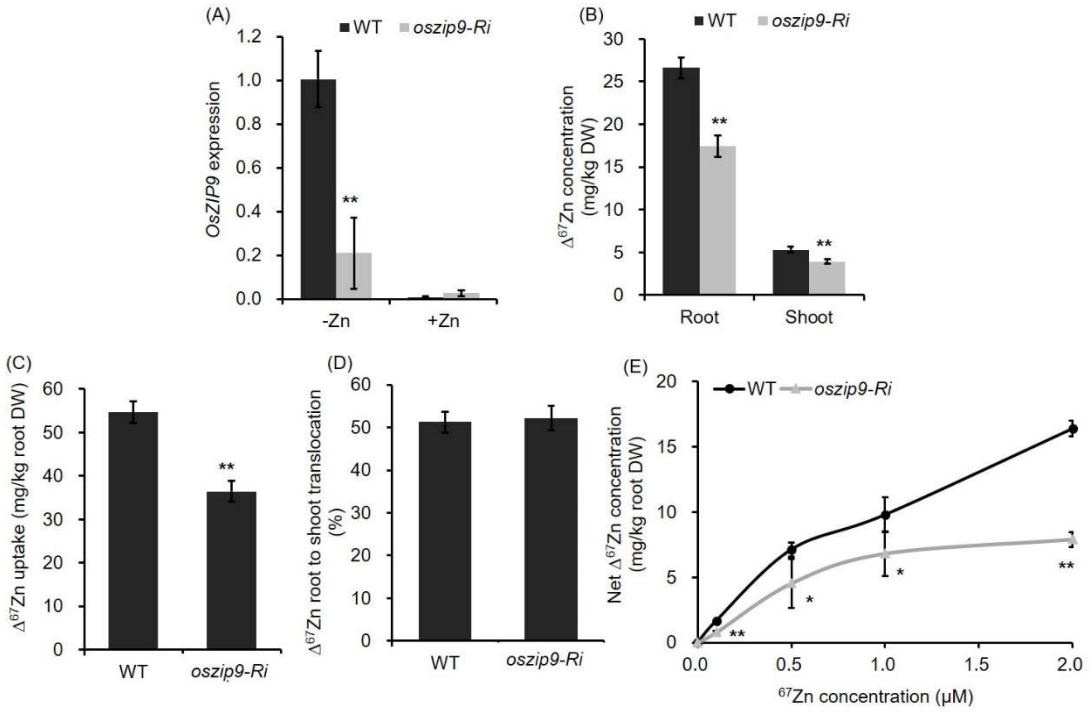

Figure 2.21 Effect of knockdown of *OsZIP9* on Zn uptake and accumulation. (A) Expression of *OsZIP9* in *oszip9* RNAi line (*oszip9-Ri*) (B) Concentration of Δ^{67}Zn in the roots and shoots. (C) Uptake of Δ^{67}Zn. (D) Root to shoot translocation of Δ^{67}Zn. The wild-type rice and the RNAi line grown in 0.02 μM Zn conditions for 17 days were exposed to a solution containing 0.4 μM ^{67}Zn for 24 h. (E) Kinetic study of ^{67}Zn uptake. Seedlings grown in Zn-deficient solution for 7 days were exposed to a solution containing different concentrations of ^{67}Zn for 30 min at 25ºC or 4ºC. Net uptake (E) was calculated by subtracting the apparent uptake at 4ºC from that at 25ºC. Data are means ±SD of three biological replicates. Statistical comparison was performed by ANOVA followed by Tukey-Kramer's test (*$p<0.05$, **$p<0.01$).

4. Discussion

Based on analyses of expression pattern, transport activity in heterologous systems, and ectopic expression, a number of transporters have been suggested to function in root Zn uptake, such as AtZIP2, AtIRT1, and AtIRT3 in Arabidopsis (Vert et al., 2002; Lin et al., 2009; Palmer and Guerinot, 2009; Milner et al., 2013); OsZIP1 and OsZIP3 in rice (Ramesh et al., 2003); and HvZIP7 in barley (Tiong et al., 2014). However, the exact transporter for Zn uptake in roots has not been identified in plants (Olsen and Palmgren, 2014). In the present study, we functionally characterized two members of ZIP family genes, OsZIP1 and OsZIP9 in rice. We found that both of them are involved Zn uptake in rice, but function differently.

4.1 OsZIP1 and OsZIP9 are differently contributed to Zn uptake in rice roots

Although both *OsZIP1* and *OsZIP9* were mainly expressed in the roots through the whole growth period (Figs. 2.4A and 2.8A), they showed different expression patterns. In the presence of Zn, the expression level of *OsZIP1* in the roots was much higher than that of *OsZIP9* (Table 2.1). However, in contrast to constitutive expression of *OsZIP1* in the roots (Fig. 2.4B), the expression of *OsZIP9* was greatly induced by Zn-deficiency (Fig. 2.8B). Furthermore, *OsZIP1* was expressed in all root cells except epidermal cells of mature root region (Fig. 5), while *OsZIP9* was only expressed in the exodermis and endodermis of the roots (Fig. 10). Since both OsZIP1 and OsZIP9 show transport activity for Zn in yeast (Figs. 2.3 and 2.7), together with expression patterns, the results show that OsZIP1 and OsZIP9 are involved in Zn uptake in rice roots, but may function

differently. OsZIP1 may function in a wide range of Zn concentration in external solution although further characterization is required in terms of subcellular localization, phenotypic analysis of knockout lines. By contrast, OsZIP9 functions only under Zn-limited condition. This conclusion is supported by the finding that knockout or knockdown of *OsZIP9* results in remarkably decreased Zn uptake at low Zn concentration in nutrient solution, but not at high Zn concentrations (Figs. 2.13, 2.20 and 2.21) and knockout of *OsZIP9* decreased Zn uptake from soil (Fig. 2.18).

4.2 OsZIP9 acts as a high-affinity transporter specific for Zn

OsZIP9 showed transport activity for Zn in yeast, but not for Fe and Cu (Fig. 2.7). Transport activity for Mn was not tested in yeast because a stable isotope of Mn was not available. However, no difference in Mn accumulation was found between wild-type rice and knockout lines of *OsZIP9* (Fig. 2.17). Furthermore, OsNramp5 is reported to mediate Mn uptake in rice (Sasaki et al., 2012). Therefore, it is unlikely that OsZIP9 contributes to Mn uptake and that OsZIP9 is a transporter specific for Zn.

Since knockout or knockdown of *OsZIP9* resulted in decreased Zn uptake only under Zn-limited conditions, but not under Zn-sufficient conditions in nutrient solution (Figs. 2.13 and 2.21), suggesting that OsZIP9 functions as a high-affinity transporter for Zn. This is contrast to AtZIP9 and AtZIP12 in Arabidopsis, whereby knockout of *AtZIP9* and *AtZIP12* only affects Zn uptake at high Zn concentrations and not at low Zn concentrations (Inaba et a., 2015). In paddy soil, the Zn concentration in soil solution is very low (Wang et al., 2019). In fact, OsZIP9 plays an important role in Zn uptake

from soil because knockout mutants of *OsZIP9* exhibited significant decreases in Zn accumulation in both the straw and brown rice under flooded conditions (Fig. 2.18). This is also supported by higher expression of *OsZIP9* under flooded conditions compared to upland conditions (Wang et al., 2019). Since knockout of *OsZIP9* did not completely abolish Zn uptake even under Zn-limited conditions (Fig. 2.13), other unidentified transporters may also be involved in Zn uptake in rice. One candidate is OsZIP1 because it is also highly expressed in the roots as discussed above.

As described in Introduction, efficient uptake of a mineral element in rice roots requires a cooperative transport system, which is mediated by influx and efflux transporters polarly localized at the root exodermis and endodermis (Ma and Yamaji, 2008; Sasaki et al., 2016). Expression of *OsZIP9* at the exodermis and endodermis in the root mature region indicates that it is responsible for transport of Zn from soil to the exodermis and from apoplastic space in aerenchym to the endodermis. Therefore, an efflux transporter for cooperative Zn transport with OsZIP9 is required for efficient Zn uptake, which remains to be identified in the future.

4.3 OsZIP9 is not involved in Fe response directly

The expression of *OsZIP9* was also induced by Fe-deficiency to some extent, although the extent of expression induction was not as high as that caused by Zn deficiency (Fig. 2.8B). However, expression induction by Zn deficiency occurred earlier than by Fe deficiency (Fig. 2.9), suggesting that induction by Fe deficiency was caused by indirect effects, although the exact mechanism is unknown. In *OsZIP9*

knockout mutants, higher Fe accumulation in the shoots was observed at low Zn supply in nutrient solution (Fig. 2.18). Since the mutant plants suffered from Zn deficiency at low Zn concentrations (Figs. 2.12 and 2.13), some genes related to Fe uptake in the roots may have been induced. However, in soil culture, knockout of *OsZIP9* did not affect Fe accumulation in the shoots (Fig. 2.18), due to high Fe concentration in soil solution of paddy soil (Wang et al., 2019).

Chapter 3 Effect of silicon on zinc uptake in rice

1. Introduction

The uptake of Zn is affected by many factors. One of them is silicon (Si), which is the most abundant element in the earth crust. All plants rooting in soil contain significant amount of Si (Ma and Takahashi, 2002), although there is a great difference in Si accumulation in the shoots between different plant species, ranging from 0.1% to 10% of dry weight. Rice (*Oryza sativa*) is a typical Si-accumulating species, which is able to accumulate Si in the shoots to up to 10% Si of dry weight (Ma et al., 2001). This high accumulation is achieved by cooperation of two transporters for Si uptake; Lsi1 and Lsi2, which are polarly localized at the exodermis and endodermis of the roots (Ma et al., 2006, 2007; Ma and Yamaji, 2015). High Si accumulation in the leaves and husk is required for high and stable production of rice through mitigation of various biotic and abiotic stresses (Ma and Takahashi, 2002; Ma, 2004; Ma and Yamaji, 2006; Liang et al., 2007; Coskun et al., 2019). The significance of Si on rice production has been well demonstrated by a field experiment using a rice mutant defective in Si uptake. When *Lsi1* gene is knocked out, the grain yield was decreased to less than 10% of the wild-type rice (Tamai and Ma, 2008). Therefore, Si has been considered as an "agronomically essential element" for rice, although its essentiality for plant growth has not been recognized according to the criteria of Arnon and Stout (1939).

The beneficial effects of Si have been observed under both Zn-deficiency and -excess

stress conditions in rice and other plant species. In maize (*Zea mays.* L), exogenous Si supply increased plant growth and chlorophyll content and decreased the membrane permeability and proline content at high Zn concentration (Kaya et al., 2009). Furthermore, Si supply decreased Zn concentration in the leaves (Kaya et al., 2009). However, Si application did not alleviate Zn-toxicity in young seedlings of sorghum (*Sorghum bicolor.* L) grown under hydroponic condition (Masarovič et al., 2012) and maize (Bokor et al., 2013). In rice, Si supply increased shoot biomass and grain yield under low Zn condition (less than 50 μg L^{-1}) (Mehrabanjoubani et al., 2015), which was associated with increased Zn concentration in the shoots. At high Zn concentrations, Si addition alleviated Zn toxicity-induced growth (Song et al., 2011; Gu et al., 2012; Song et al., 2014). These effects have been attributed to the Si-reduced uptake and root-to-shoot translocation of Zn (Song et al., 2011, Gu et al., 2012), Si-enhanced antioxidant defense capacity and membrane integrity (Song et al., 2011), formation of Zn-Si complexes in less active tissues (Neumann and Zur Nieden, 2001), Si-enhanced Zn binding to the cell wall (Gu et al., 2012) and so on. Deposition of Zn-Si in the apoplastic space of root and/or shoot could be a Zn source, which can be remobilized when required at Zn-deficiency condition (Hernandez-Apaolaza, 2014). Although most studies reported that Si affected Zn accumulation in the shoots or/and roots, the exact mechanism for the Si-altered Zn accumulation is still poorly understood.

In this chapter, I investigated the physiological and molecular mechanisms underlying the Si-affected Zn uptake by using a rice mutant *lsi1* defective in Si uptake and its wild-type rice (WT).

2. Materials and methods

2.1 Plant materials and growth conditions

A rice (*Oryza sativa*) mutant *lsi1* (*GR1*) (Ma et al., 2002) and its wild-type rice (cv. Oochikara, WT) were used in this study. The *lsi1* is a mutant defective in Si uptake due to a point mutation in Si transporter Lsi1 (Ma et al., 2006). Seeds were soaked in water for two days at 30℃ in the dark, followed by transferring to plastic nets floating on a solution containing a 0.5 mM $CaCl_2$. After five days, the seedlings were transferred to a 3.5-L pot containing a half-Kimura B solution (pH 5.6) (Ma et al., 2002). The solution was renewed every two days. The seedlings were grown in greenhouse at 25-30℃ under natural light. All of the experiments were performed for at least three times with three to four replicates each.

2.2 Effect of Si on root elongation at different Zn concentrations

To investigate the effect of Si on Zn toxicity in rice, 2-d-old seedlings were subjected to a 0.5 mM $CaCl_2$ solution containing different Zn concentrations including 0, 0.4, 40, and 200 μM in the presence or absence of 1mM Si for 24 h. The root length was measured by a ruler before and after the Zn exposure. Relative root elongation was calculated based on (root elongation with Zn/root elongation without Zn x 100). Eight-ten replicates for each Zn concentration were made.

2.3 Effect of Si on Zn accumulation in roots and shoots

To investigate the effect of Si on Zn accumulation, 11-d-old seedlings of both WT and

lsi1 mutant were exposed to a nutrient solution containing various concentrations of Zn including 0.04, 0.4, 4, and 40 μM in the presence or absence of 1 mM Si. The solution was renewed every two days. After 14-d growth, the roots were washed with 5 mM $CaCl_2$ for three times and subsequently separated from the shoots. Concentration of Zn in the roots and shoots was determined as described below.

2.4 Effect of Si on Δ^{67}Zn accumulation

To investigate the effect of different Si accumulation in the shoots on Zn uptake, a stable isotope ^{67}Zn (Trace Sciences International, 97% enrichment) was used. Seedlings (21-d-old) of both WT and *lsi1* were pre-cultured in a solution containing 1 mM Si and 0.4 μM Zn for 0, 1, 3, 7 days, followed by exposing to a nutrient solution containing 0.4 μM ^{67}Zn without Si at the same day. After 24 h, the roots and shoots were separately harvested as described above. Concentration of ^{67}Zn was determined as described below. The net accumulation of ^{67}Zn during 24 h was calculated after subtracting natural abundance.

2.5 Effect of Si pre-treatment on Δ^{67}Zn accumulation

To determine the effect of Si in the shoot or solution on Zn accumulation, seedlings (21-d-old) of both WT and *lsi1* mutant were pre-cultured in a solution containing 0.4 μM Zn in the presence (+Si) or absence (-Si) of 1mM Si. After seven days, the plants were transferred to a nutrient solution containing 0.4 μM ^{67}Zn in the presence or absence of 1 mM Si, generating four different plants; -Si-Si, -Si+Si, +Si-Si and +Si-Si.

After labeling for 24 h, the roots and shoots of different plants were harvested as described above.

2.6 Effect of Si on Δ^{67}Zn distribution in different organs

Seedlings (21-d-old) of both WT and *lsi1* mutant were cultured in a nutrient solution containing 0.4 μM Zn in the presence or absence of 1mM Si. After seven days, the plants were subjected to a nutrient solution containing 0.4 μM ^{67}Zn for 24 h. Different organs including root, basal node, leaf 2-6 were separately sampled for Δ^{67}Zn determination as described below.

2.7 Δ^{67}Zn concentration in root cell sap and xylem sap

Seedlings (17-d-old) of both WT and *lsi1* mutant were cultured in a nutrient solution containing 0.4 μM Zn in the presence or absence of 1 mM Si. After seven days, the plants were subjected to a nutrient solution containing 0.4 μM ^{67}Zn for 24 h. For root cell sap, the roots were washed three times with cold 5 mM $CaCl_2$, and then placed on a filter in a tube and frozen at -80℃ overnight. To collect the cell sap, the roots were thawed at room temperature, followed by centrifugation at 20,600 g for 10 min. For xylem sap, the shoot (2 cm above the root) was excised with a razor, and the xylem sap was collected by using a micropipette for 30 min. The Δ^{67}Zn concentration was determined as described below.

2.8 Kinetic study of ^{67}Zn uptake

Seedlings (25-d-old) of WT and *lsi1* were pre-cultured with or without 1 mM for seven days in a nutrient solution containing 0.4 μM and used for kinetic study of Zn uptake. The roots were exposed to a nutrient solution containing different ^{67}Zn concentrations ranging from 0.1 to 40 μM at 25℃ and 4℃. After 30-min exposure, the roots were washed three times with cold 5 mM $CaCl_2$ and harvested for ^{67}Zn determination as descried below. The net uptake was calculated by subtracting the apparent uptake at 4℃ from 25℃.

2.9 Effect of Si on ^{67}Zn accumulation under different humidity condition

Seedlings (21-d-old) of WT and *lsi1* mutant were pre-cultured with/without 1 mM Si for seven days in a nutrient solution with 0.4 μM Zn. The plants were then exposed to a nutrient solution containing 0.4 μM ^{67}Zn without Si at both high (70 to 100%) and low (25 to 60%) humidity condition at the same temperature in growth chambers. After 12 h, the roots and shoots of WT and *lsi1* were harvested and subjected to ^{67}Zn determination.

2.10 Expression analysis of ZIP family genes

To examine the effect of Si on the expression of ZIP family genes, root samples were taken from plants of WT and *lsi1* mutant, which had been exposed to a nutrient solution in the presence or absence of 1.0 mM Si for seven days. Samples taken were immediately frozen in liquid nitrogen and then subjected to total RNA extraction using

a RNeasy Plant Mini Kit (Qiagen). cDNA was synthesized by ReverTra Ace qPCR RT Kit (TOYOBO) or SuperScript II (Invitrogen) according to the manufacturer's instruction. The expression analysis of *ZIP genes* was determined with SsoFast EvaGreen Supermix (Bio Rad) on a real-time PCR machine (CFX384, Bio-Rad). *Histone* H3 was used as an internal control. Relative gene expression was calculated by the ΔΔCt method. The primer sequences used were from Sasaki et al. (2015).

2.11 Determination of ^{67}Zn in plant samples

The samples harvested were dried at 70°C for at least three days before being digested by HNO_3 (60%[w/v]) as described previously (Sasaki et al., 2012). The concentration of total Zn in digestion solution, root cell sap and xylem sap was determined by Inductively Coupled Plasma-Mass Spectrometry (ICP-MS, 7700X; Agilent Technologies). For determination of ^{67}Zn concentrations, an isotope mode was used. Δ^{67}Zn concentration was calculated after subtracting natural abundance of ^{67}Zn according to Yamaji et al. (2013).

3. Results

3.1 Effect of Si on Zn-induced inhibition of root elongation

Root elongation has been widely used as a parameter of metal toxicity (Barcelo and Poschenrieder, 2002). The effect of Si on the root elongation in both WT and *lsi1* mutant at different Zn concentrations was investigated. The root elongation was inhibited with

increasing Zn concentrations in the solution in both WT and *lsi1* mutant (Fig. 3.1). At 200 uM Zn, the root elongation was decreased by 23-46% in the WT and *lsi1* mutant (Fig. 3.1). However, Si did not alleviate Zn toxicity-induced root elongation in both lines (Fig. 3.1). This result indicates that Si did not directly alleviate Zn-induced inhibition of root elongation in both WT and mutant.

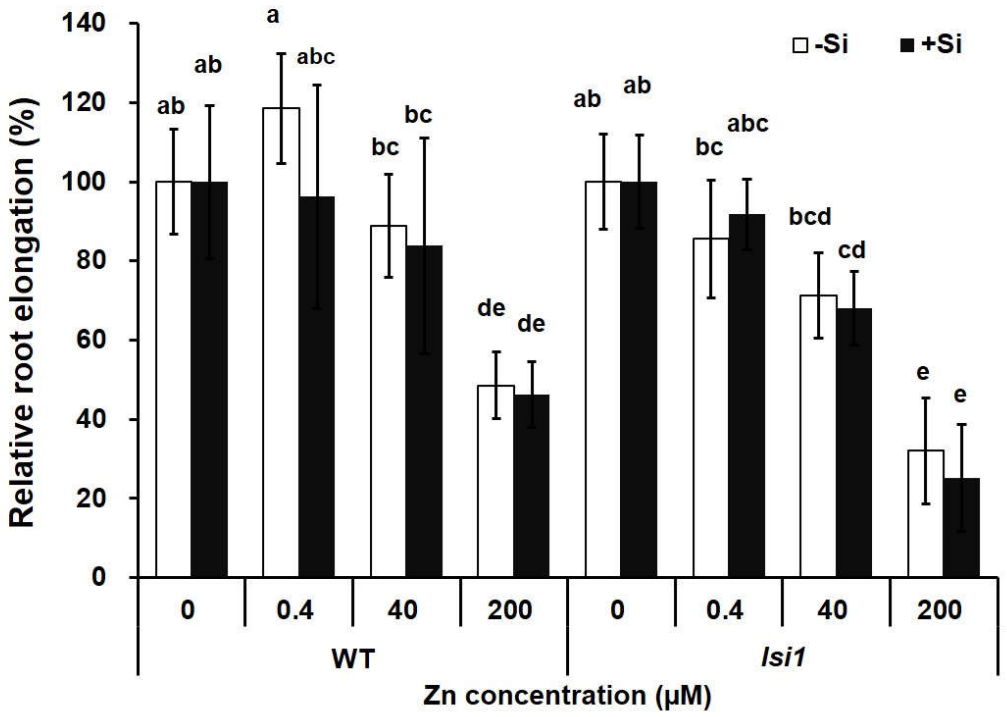

Figure 3.1 Effect of Si on root elongation of rice at different Zn concentrations. 2-d-old-seedlings of *lsi1* mutant and its wild type (WT) were exposed to a solution containing different Zn concentrations as indicated for 24 h. The root length was measured by a ruler before and after exposure to Zn. Relative root elongation was calculated based on root elongation with Zn/root elongation without Zn x 100. Data represent the mean ±SD (n=8-10). Different letters mean significant difference (p<0.01) by Tukey-Kramer's test.

3.2 Effect of Si on Zn accumulation in WT and *lsi1* mutant

When both WT and *lsi1* mutant were grown in a nutrient solution containing different Zn concentrations in the presence and absence of 1.0 mM Si for 14 days, no significant difference in the dry weight of both the shoots and roots was observed between WT and *lsi1* mutant and between plants with or without Si supply (Fig. 3.2A, B). However, Si supply decreased Zn concentration in the roots of WT at Zn concentrations from 0.4 to 10 μM, but not at 0.04 μM Zn condition (Fig. 3.3A). Si also decreased Zn concentration in the shoots of WT at all Zn concentrations tested (Fig. 3.3B). By contrast, such decrease was not observed in *lsi1* mutant at all Zn concentrations (Fig. 3.3A, B). The uptake of Zn was decreased by Si supply in WT at all Zn concentrations except 0.04 μM Zn (Fig. 3.3C), whereas it was not affected by Si in *lsi1* mutant (Fig. 3.3C). On the other hand, the root-to-shoot translocation of Zn was not altered by Si supply in both WT and mutant at all Zn concentrations (Fig. 3.3D).

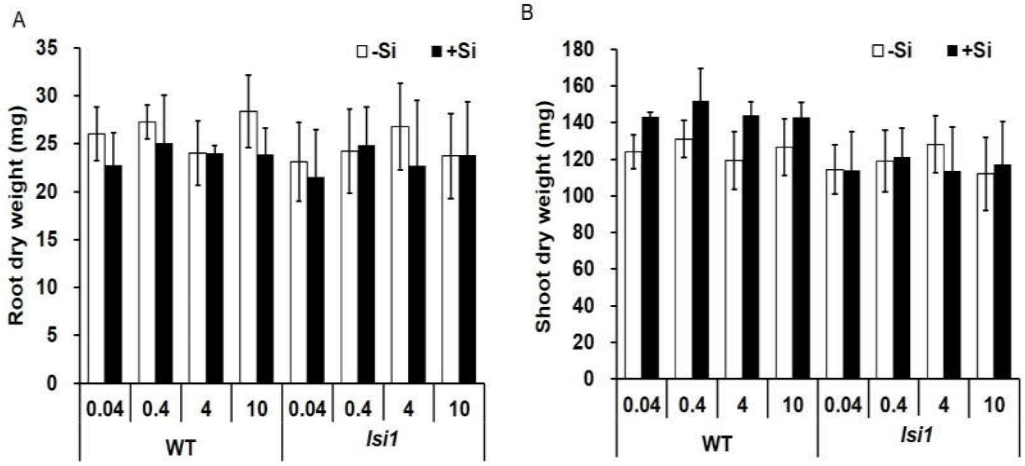

Figure 3.2 Effect of Si on growth at different Zn concentrations in wild-type rice and *lsi1* mutant. (A-B) Dry weight of root (A) and shoot (B). Seedlings (11-d-old) of

wild-type rice (WT) and *lsi1* mutant were grown in a nutrient solution containing different Zn concentrations as indicated in the presence or absence of 1 mM Si for 14 days. Data represent the mean ±SD (n=4). Different letters mean significant difference (p<0.01) by Tukey-Kramer's test.

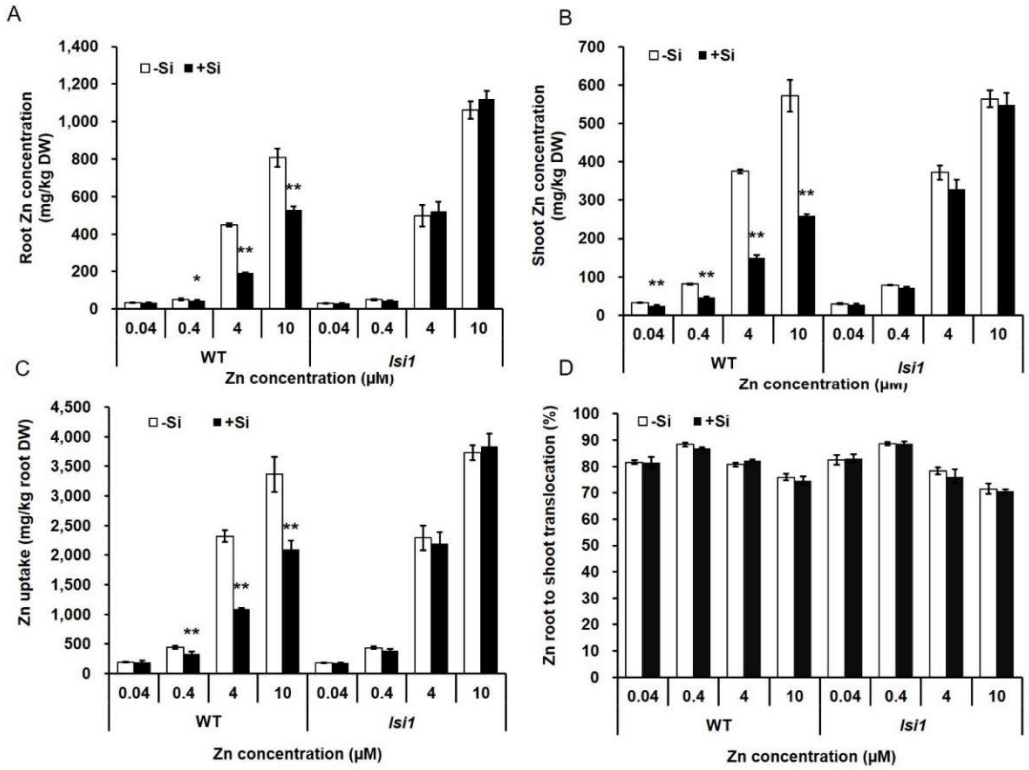

Figure 3.3 Effect of Si on Zn accumulation in wild-type rice and *lsi1* mutant. (A-D) Zn concentration in roots (A) and shoots (B), Zn uptake (C) and root-to-shoot translocation of Zn (D) in wild-type rice (WT) and *lsi1* mutant. Seedlings (11-d-old) of both WT and *lsi1* mutant were grown in a nutrient solution containing different Zn concentrations indicated in the presence and absence of 1 mM Si for 14 days. Data represent the mean ±SD (n=4). Asterisks indicate a significant difference ((*p<0.05, **p<0.01) between –Si and +Si by Tukey-Kramer's test.

3.3 Short-term labeling experiment with stable isotope ^{67}Zn

Above results indicate that Zn uptake was suppressed by Si in the WT, but not in the *lsi1* mutant (Fig. 3.3). To confirm this result, a short-term (24 h) labeling experiment with stable isotope ^{67}Zn was performed. Both WT and *lsi1* were first cultivated in a nutrient solution containing 1.0 mM Si for different days, followed by exposure to ^{67}Zn for 24 h, and the net ^{67}Zn (Δ^{67}Zn) concentration accumulated during 24 h was calculated after subtracting the natural abundance. The result showed that Si supply for one day did not affect the Δ^{67}Zn concentration in the roots and shoots of both WT and *lsi1* mutant. However, Si supply for three and seven days significantly decreased Δ^{67}Zn accumulation in the roots and shoots of WT, but not of *lsi1* mutant (Fig. 3.4A, B). The uptake of Δ^{67}Zn was significantly decreased by Si in WT exposed to Si for three and seven days, but not in *lsi1* mutant. However, the root-to-shoot translocation of Δ^{67}Zn was not altered by Si in both WT and mutant at all days (Fig. 3.4C, D).

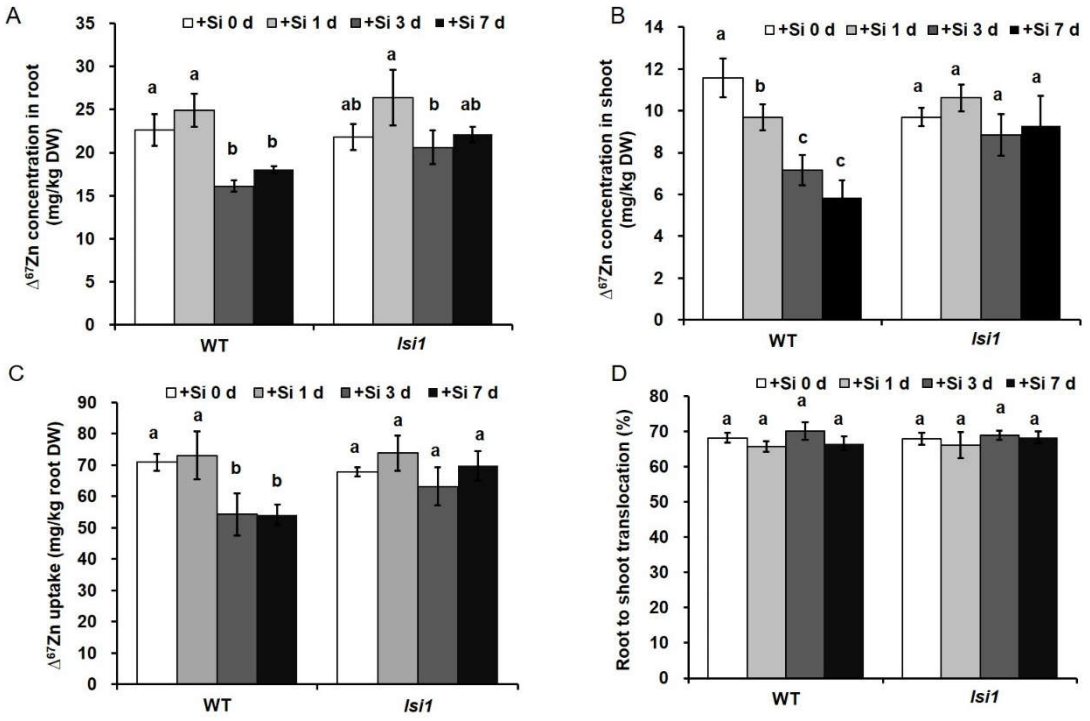

Figure 3.4 Effect of different Si accumulation on Δ^{67}Zn accumulation in wild-type rice and *lsi1* mutant. (A-D) Concentration of Δ^{67}Zn in the roots (A) and shoots (B), uptake (C) and root-to-shoot translocation (D) of Δ^{67}Zn in the wild-type rice (WT) and *lsi1* mutant. Seedlings (21-d-old) of both WT and *lsi1* mutant were pre-cultured with 1 mM Si for 0, 1, 3, and 7 days in a nutrient solution containing 0.4 μM Zn to get the plant with different Si accumulation in the shoots, followed by subjecting to a nutrient solution containing 0.4 μM ^{67}Zn without Si for 24 h. The concentration of ^{67}Zn in the roots and shoots was determined by ICP-MS with isotope mode. The net accumulation (Δ^{67}Zn) was calculated by subtracting natural abundance of ^{67}Zn. Data represent mean ±SD (n=4). Different letters mean significant difference (p<0.01) by Tukey-Kramer's test.

3.4 Effect of Si accumulated in the shoots on Δ^{67}Zn uptake in WT and *lsi1* mutant

Above results suggest that relatively long-term exposure to Si is required for suppressing Zn uptake in the WT (Fig. 3.4). To examine whether Si accumulated in the shoots or Si in the solution exerts this effect, the WT and *lsi1* were precultured with or without 1 mM Si for seven days, followed by exposing to a solution labeled with ^{67}Zn in the presence or absence of 1mM Si for 24 h. Pretreatment with Si significantly decreased $\Delta^{67}Zn$ concentration in both roots and shoots, and uptake (-Si-Si *vs* +Si-Si) in the WT, but not in the *lsi1* mutant (Fig. 3.5A-C). However, co-existence with Si for one day did not affect $\Delta^{67}Zn$ accumulation and uptake in both the WT and mutant (-Si-Si *vs* -Si+Si) (Fig. 3.5A-C). Furthermore, absence of Si in the solution during 24 h did not affect $\Delta^{67}Zn$ concentration and uptake in the WT precultured wit Si (+Si-Si vs +Si+Si) (Fig. 3.5A-C). The root-to-shoot translocation of $\Delta^{67}Zn$ was not altered by Si pretreatment or co-existence in the solution (Fig. 3.5D). These results further indicate that Si accumulated in the shoots, not in the roots and solution decreased Zn uptake.

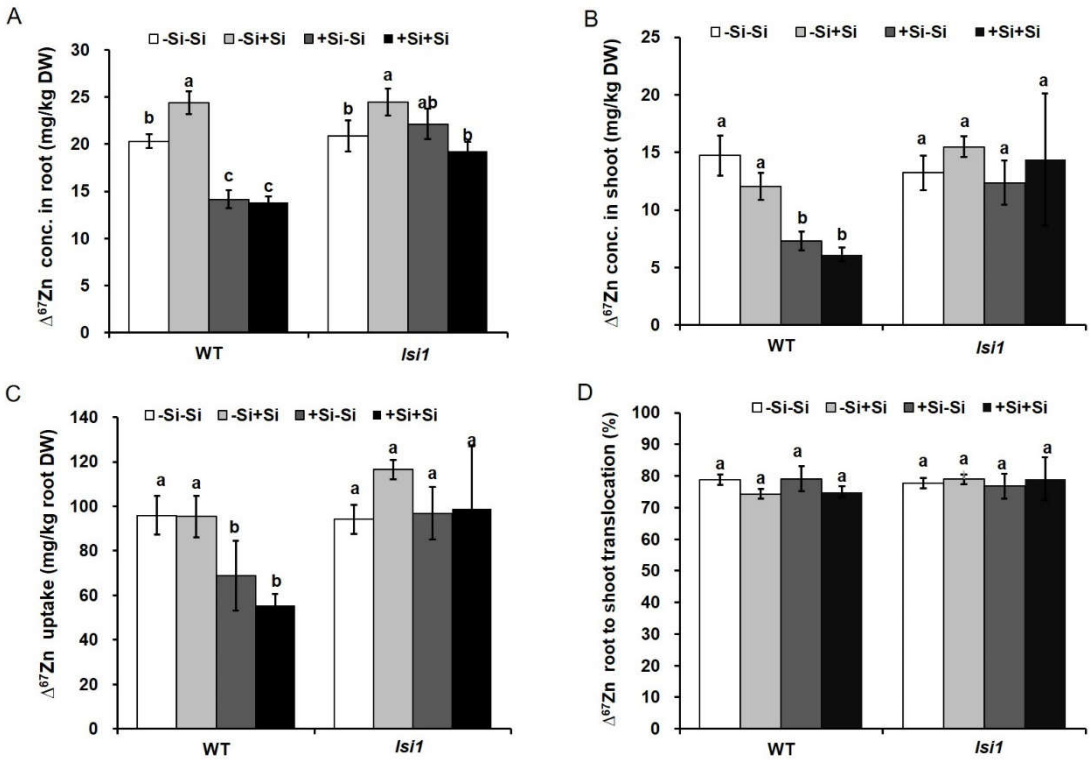

Figure 3.5 Effect of Si accumulated in the shoots on Δ^{67}Zn accumulation in the wild-type rice and *lsi1* mutant. (A-D) Concentration of $\Delta\,^{67}$Zn in the roots (A) and shoots (B), uptake (C) and root-to-shoot translocation (D) of $\Delta\,^{67}$Zn in the wild-type rice (WT) and *lsi1* mutant. Seedlings (21-d-old) of WT and *lsi1* mutant were pre-cultured with or without 1 mM Si for 7 days in a nutrient solution containing 0.4 μM Zn, followed by subjecting to a nutrient solution containing 0.4 μM ^{67}Zn in the presence or absence of 1 mM Si for 24 h. The concentration of ^{67}Zn in the roots and shoots was determined by ICP-MS with isotope mode and the net accumulation ($\Delta\,^{67}$Zn) was calculated by subtracting natural abundance of ^{67}Zn. Data represent the mean ±SD (n=4). Different letters mean significant difference (p<0.01) by Tukey-Kramer's test.

3.5 Effect of Si on Δ^{67}Zn distribution in different organs

The effect of Si on the distribution of Zn in different organs was also investigated. To

do this experiment, both WT and *lsi1* mutant precultured with 1 mM Si for seven days were exposed to a solution labeled with ^{67}Zn. After 24 h, different organs including roots, basal shoot region (0.5 cm above root-to-shoot junction), and individual leaf were separately sampled. The concentration of $\Delta^{67}Zn$ was decreased by Si in all organs of WT, but not of *lsi1* mutant (Fig. 3.6A). $\Delta^{67}Zn$ taken up by the roots was preferentially distributed to the shoot basal region and new leaf (leaf 6) in the shoots of both lines (Fig. 3.6B). However, the distribution ratio of $\Delta^{67}Zn$ to different organs did not differ between plants pretreated with and without Si in both WT and *lsi1* mutant. These results indicate that Si did not affect the distribution of Zn in different organs and that the decreased $\Delta^{67}Zn$ concentration in each organ of WT is the result of Si-decreased Zn uptake.

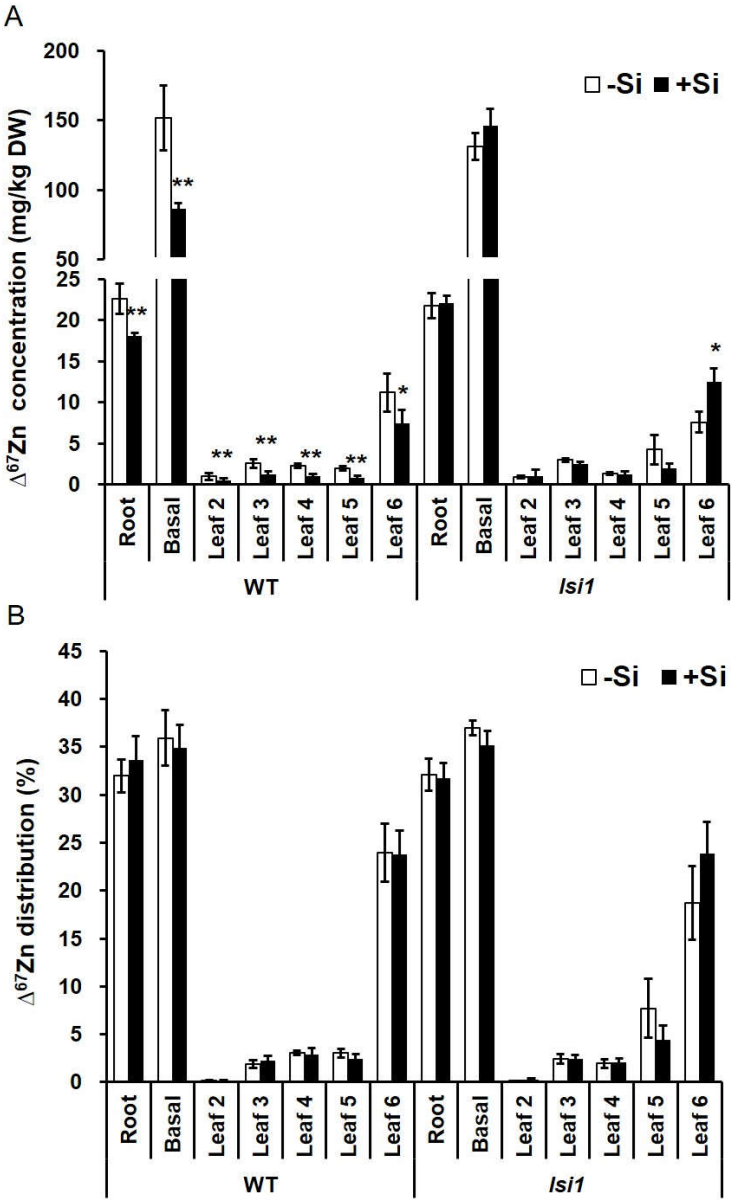

Figure 3.6 Effect of Si on Δ ^{67}Zn distribution in different organs of wild-type rice and *lsi1* mutant. (A, B) Concentration in different organs (A) and distribution ratio (B) of Δ ^{67}Zn in different organs. Seedlings (21-d-old) of wild-type rice (WT) and *lsi1* mutant were precultured with or without 1 mM Si for 7 days, followed by subjecting to a nutrient solution containing 0.4 μM ^{67}Zn. After 24 h, different organs were separately harvested for determination of ^{67}Zn by ICP-MS with isotope mode. The net concentration of ^{67}Zn (Δ ^{67}Zn) in each organ was calculated by subtracting natural

abundance of ^{67}Zn. Distribution ratio is calculated based on Δ^{67}Zn content in each organ/total Δ^{67}Zn content x 100. Data represent the mean ±SD (n=4). Asterisks indicate a significant difference (*p<0.05, **p<0.01) between –Si and +Si by Tukey-Kramer's test.

3.6 Kinetic study of ^{67}Zn uptake

A kinetic study with ^{67}Zn was performed to further examine the Si-altered Zn uptake feature. Both WT and *lsi1* mutants pretreated with or without Si for seven days were exposed to a solution labeled with different concentrations of ^{67}Zn for 30 min at 4℃ and 25℃. The net uptake of ^{67}Zn (uptake difference between 25℃ and 4℃) was significantly decreased by Si in WT, but not in *lsi1* mutant at all ^{67}Zn concentrations tested (Fig. 3.7A, B). In the WT, the K_m value was not altered by Si, but the V_{max} value in Si-plants was decreased to half of non-Si-plants (Fig. 3.7A). By contrast, both K_m and V_{max} values were not altered by Si (Fig. 3.7B).

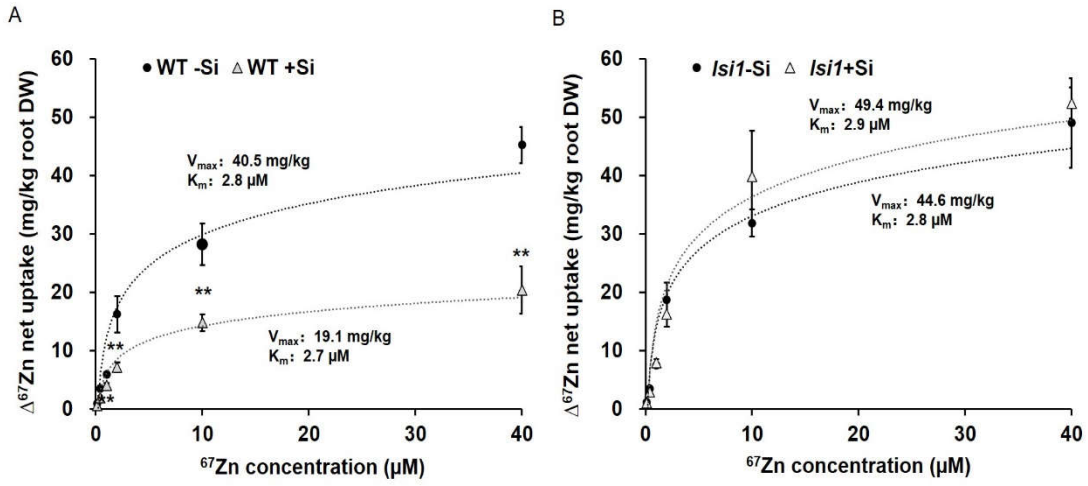

Figure 3.7 Kinetic study of Δ^{67}Zn uptake by the roots of the wild-type (WT) rice (A) and *lsi1* mutant (B). Seedlings (25-d-old) pre-cultured with or without 1 mM Si for 7 days, were exposed to a solution containing different concentrations of ^{67}Zn as indicated in the absence of Si at 25℃ and 4℃ for 30 min. The roots were sampled for determination of ^{67}Zn by ICP-MS with isotope mode. Net uptake of ^{67}Zn (Δ^{67}Zn) was calculated by subtracting the apparent uptake at 4℃ from 25℃. K_m and V_{max} values are shown. Data represent the mean ±SD (n=3). Asterisks indicate a significant difference (**p<0.01) between –Si and +Si by Tukey-Kramer's test.

3.7 Effect of Si on Δ^{67}Zn accumulation in root cell sap and xylem sap

The Δ^{67}Zn concentration in the root cell sap and xylem sap was also compared between the plants pretreated with and without Si. In the WT, plants supplied with Si showed significantly lower Δ^{67}Zn concentration in the root cell sap compared with the plants not supplied with Si (Fig. 3.8A). However, such difference was not found in the mutant (Fig. 3.8A). The Δ^{67}Zn concentration in xylem sap was also decreased by Si in the WT but not in the mutant (Fig. 3.8B).

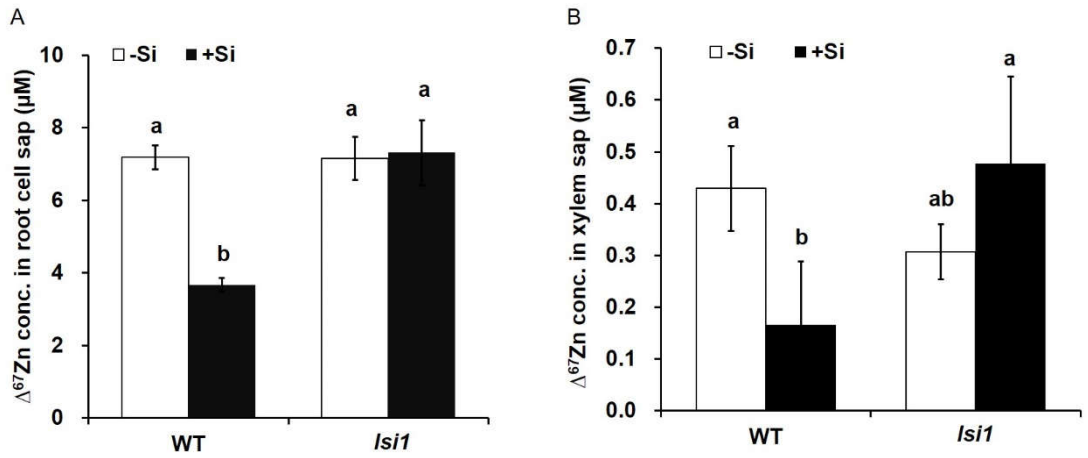

Figure 3.8 Effect of Si on Δ^{67}Zn accumulation in root cell sap (A) and xylem sap (B) of the wild-type rice and *lsi1* mutant. Seedlings (17-d-old) of wild-type rice (WT) and *lsi1* mutant were pre-cultured in a solution with or without 1 mM Si for 7 days, followed by exposing to a solution containing 0.4 μM ^{67}Zn in the absence of Si. After 6 h, the xylem sap and roots for cell sap were collected. Concentration ^{67}Zn in the sap was determined by ICP-MS with isotope mode. Net concentration of ^{67}Zn (Δ^{67}Zn) was calculated by subtracting natural abundance of ^{67}Zn. Data represent the mean ± SD (n=4). Different letters mean significant difference (p<0.01) by Tukey-Kramer's test.

3.8 Effect of Si on Δ^{67}Zn accumulation under different humidity condition

Since Si deposition in the shoots decreases transpiration in rice (Ma and Takahashi, 2002), there is a possibility that Si-decreased Zn uptake is caused by Si-decreased transpiration. To text this possibility, the effect of Si on Δ^{67}Zn accumulation during 12 h was investigated under different humidity condition (high humidity ranging from 70-100% and low humidity ranging from 25-60%). There was about three times difference in the transpiration rate between low humidity and high humidity in both WT and *lsi1* mutant (Fig. 3.9A). At low humidity, similar to previous study (Agarie et al., 1998, Ma and Takahashi, 2002), Si decreased transpiration in the WT, but not in the mutant (Fig. 3.9A). However, Si decreased Δ^{67}Zn concentration in the shoot of WT, irrespectively of humidity (Fig. 3.9B). The shoot Δ^{67}Zn concentration was not affected by Si in the mutant at both humidity (Fig. 3.9B). This result indicates that the Si-decreased Δ^{67}Zn accumulation in the shoots is independent of transpiration.

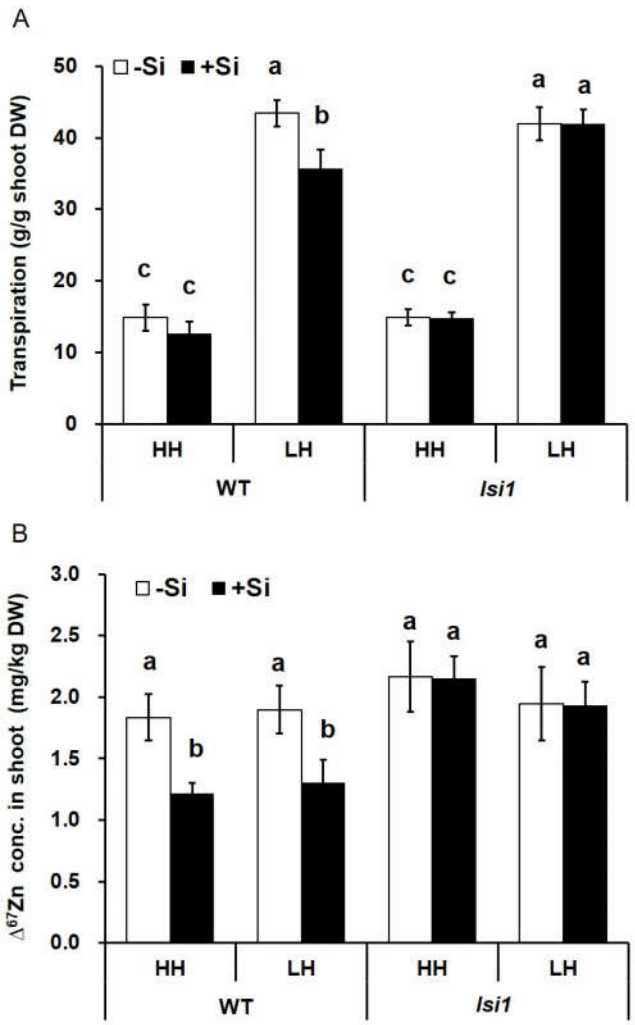

Figure 3.9 Effect of Si on Δ^{67}Zn accumulation under different humidity conditions in wild-type rice and *lsi1* mutant. (A, B) Transpiration (A) and shoot Δ^{67}Zn concentration (B) at different humidity conditions. Seedlings (21-d-old) of wild-type rice (WT) and *lsi1* mutant were pre-cultured with or without 1 mM Si for 7 days. These plants were then exposed to a nutrient solution containing 0.4 μM ^{67}Zn without Si for 12 h at high (70-100%, HH) and low (25-60%, LH) humidity conditions. Transpiration was recorded and the shoot ^{67}Zn concentration was determined by ICP-MS with isotope mode. The net concentration of ^{67}Zn (Δ^{67}Zn) was calculated by subtracting natural abundance of ^{67}Zn. Data represent the mean ±SD (n=4). Different letters mean significant difference (p<0.01) by Tukey-Kramer's test.

3.9 Effect of Si on the expression of ZIP family genes

ZIP family genes have been proposed to be involved in Zn transport in rice (Grotz et al.,1998; Guerinot, 2000). To examine whether Si affects the expression of these genes, the expression of 10 ZIP genes in the roots was compared between WT and *lsi1* mutant with and without Si treatment. Among them, only the expression of *OsZIP1* was significantly decreased by Si supply in the WT (Fig. 3.10). However, the expression of all other ZIP genes was similar between plants treated with and without Si and between WT and *lsi1* mutant (Fig. 3.10).

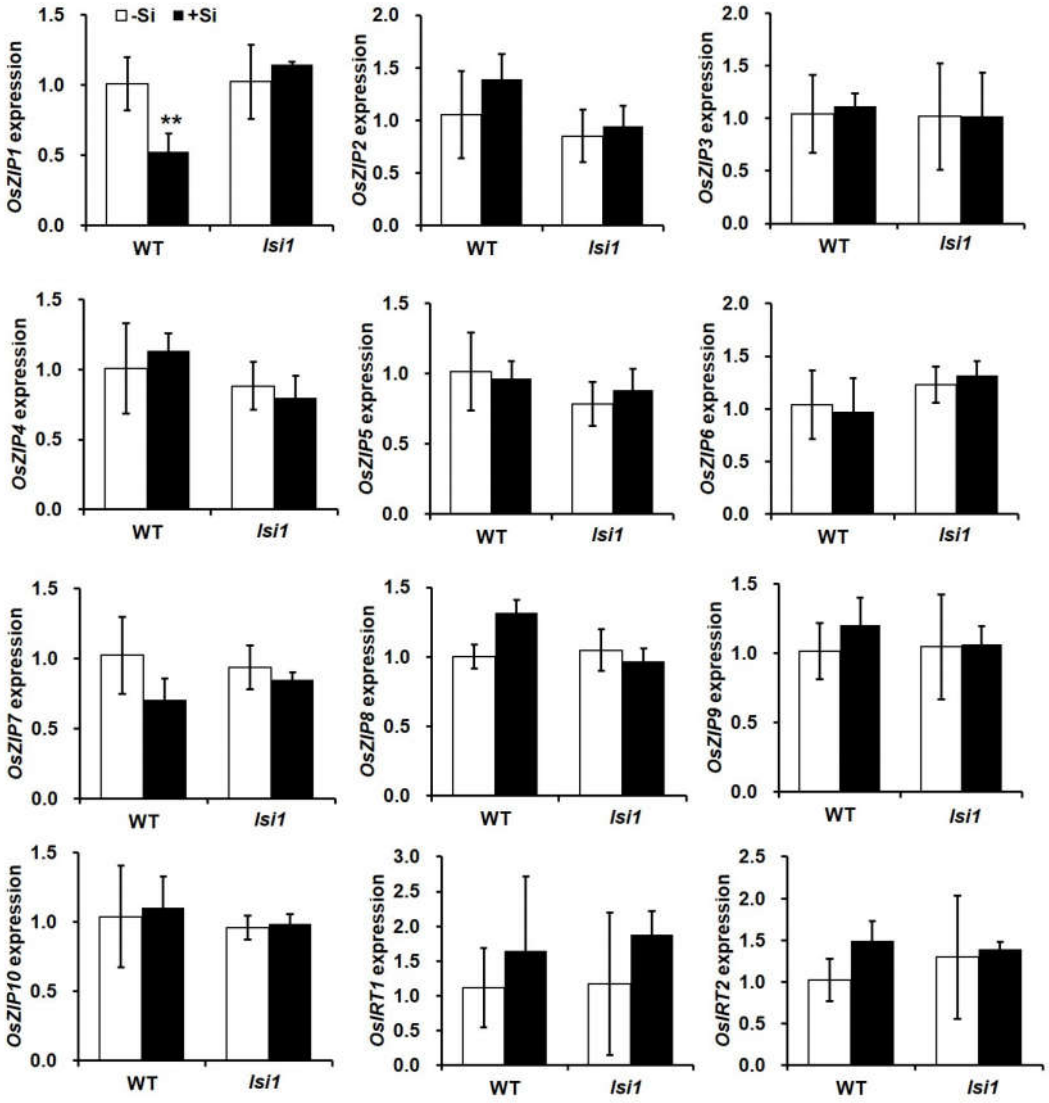

Figure 3.10 Effect of Si on expression of ZIP family genes in the roots. Roots of the

wild-type rice (WT) and *lsi1* were sampled from plants which had been exposed to a solution containing 0 or 1 mM Si for 7 days. The expression of ZIP family genes was determined by quantitative real-time PCR. *Histone H3* was used as the internal standard. Expression relative to (-Si) in WT roots is shown. Data represent the mean ±SD (n=3). Asterisks indicate a significant difference (**p<0.01) between –Si and +Si by Tukey-Kramer's test.

4. Discussion

In the present study, I investigated the effect of Si on Zn accumulation in rice by taking advantage of a rice mutant (*lsi1*), which is defective in Si uptake (Ma et al., 2002). Since *lsi1* mutant accumulates similar Si in the roots, but much less Si in the shoots (Ma et al., 2006), this mutant provides a good material to discriminate the effect of Si in the roots or shoots on Zn accumulation. Through physiological and molecular characterization, I found that Si did not directly alleviate Zn toxicity, but suppressed Zn uptake by down-regulating *OsZIP1* expression in the roots. Furthermore, Si accumulated in the shoots is required for this suppression.

4.1 Si does not alleviate Zn-induced inhibition of root elongation

Several studies reported that Si was able to alleviate high Zn-induced toxicity in rice and other plant species such as maize and cotton based on biomass of both roots and shoots (Kaya et al., 2009; Gu et al., 2011; Song et al., 2011; Anwaar et al., 2015).

However, in the present study, we did not find the alleviative effect of Si on Zn-induced inhibition of root elongation (Fig. 3.1). This discrepancy could be attributed to different Zn concentrations used, duration of treatment and Si sources used. Root elongation during a short-term (e.g. 24 h) is one of the most sensitive parameters for testing metal toxicity, which has been widely used in many studies (Barcelo and Poschenrieder, 2002). In fact, we found that Zn at 200 μM inhibited the root elongation by more than half during 24 h (Fig. 3.1), indicating that this assay method for Zn toxicity is sensitive enough. Since previous studies used high Zn concentrations (e.g. 2 mM) and long treatment time (e.g. 7 d) (Song et al., 2011), some indirect effect of Si is probably observed. Furthermore, different from this study, in which we used silicic acid as a Si source in the treatment solution, most studies used potassium or sodium silicate, which is a highly alkaline solution. Although the pH was adjusted in these studies, some reactions affecting Zn availability may occur in the solution, resulting in different effect of Si on Zn toxicity.

The proposed mechanism for Si-alleviated Zn toxicity is the formation of Zn-Si complex in the solution (Neumann and Zur Nieden, 2001; Hernandez-Apaolaza, 2014). However, this seems unlikely to happen in the solution because Si is present in the form of silicic acid at a pH below 9.0, which has a weak binding capacity to metals such as Zn and Cd (Jones and Handreck, 1967). In fact, addition of 1.8 mM Si to the solution did not affect the activity of free Zn^{2+} based on estimation by Visual MINTEQ program (Gu et al., 2012). Addition of Si also did not alleviate Cd-induced toxicity in rice (Shao et al., 2017). All these findings indicate that Si as silicic acid does not have direct

alleviative effect on Zn toxicity at least in rice.

4.2 Down-regulation of Zn transporter gene is responsible for Si-decreased Zn uptake

Although obvious beneficial effect of Si on plant growth was not observed at Zn ranges used from 0.04 to 10 μM in the present study (Fig. 3.2), Si did decrease Zn accumulation in the roots and shoots of WT at Zn concentrations from 0.4 to 10 μM although similar effect was not observed in the *lsi1* mutant (Fig. 3.3). The short-term labeling experiment with ^{67}Zn revealed that the Si-decreased Zn accumulation results from Si-decreased uptake, rather than the root-to-shoot translocation of Zn and distribution to different organs (Figs. 3.3C, D, 3.6B). Furthermore, Si addition did not alter K_m value of Zn uptake, but decreased V_{max} value in the WT (Fig. 3.7), indicating that the Zn uptake was mediated by similar transporters in both plants with and without Si, but the transporter abundance was decreased by Si in the WT.

Zn uptake in rice roots has been proposed to be mediated by transporters belonging to ZIP family as discussed in Chapter 2 (Grotz et al.,1998; Guerinot, 2000; Huang et al., 2020a). Analysis of expression profile of these ZIP genes showed that only *OsZIP1* was down-regulated by Si in the WT, but not in the mutant (Fig. 3.10). *OsZIP1* is mainly expressed in the roots at high level (Table 2.1). Furthermore, its expression was not induced by Zn-deficiency (Fig. 2.4B). OsZIP1 protein shows transport activity for Zn in yeast (Fig. 2.3; Ramesh et al., 2003) and is expressed in all root cells except the epidermal cells (Fig. 2.5). These results implicate that OsZIP1 is involved in the Zn

uptake. Therefore, it is likely that the Si-decreased Zn uptake results from down-regulation of *OsZIP1*. This is also supported by Si-decreased Zn concentration in the root cell sap and xylem sap (Fig. 3.8).

Recently, it was reported that another ZIP member, OsZIP9 contributes to Zn uptake in rice (Huang et al., 2020b; Tan et al., 2020; Yang et al., 2020). OsZIP9 was localized at the exodermis and endodermis of mature root region and knockout of this gene resulted in significant decrease of Zn uptake under Zn-limited condition (Fig. 2.13; Huang et al., 2020b). However, Si did not affect the expression of this gene (Fig. 3.10), indicating that OsZIP9 is not involved in the Si-decreased Zn uptake. This is consistent with the finding that Si decreased Zn uptake at relatively high Zn concentrations (>0.4 μM Zn) (Fig. 3.3), while *OsZIP9* is greatly induced by Zn-deficiency and only functions at low Zn concentration (<0.4 μM) (Figs. 2.8 and 2.12; Huang et al., 2020b). In addition, the expression of *OsZIP3* involved in Zn distribution was also not affected by Si (Fig. 3.10, Sasaki et al., 2015; Huang et al., 2020a). This is also consistent with the result that Si did not affect the distribution of Zn to different organs (Fig. 3.6B).

4.3 Si accumulated in the shoot is required for suppressing Zn uptake

The results show that Si accumulated in the shoots is required for suppressing Zn uptake through down-regulation of *OsZIP1*. This is supported by several lines of evidence. Firstly, Si-decreased Zn uptake was only observed in the WT, but not in the *lsi1* mutant (Fig. 3.3C). The *lsi1* mutant and WT have similar Si level in the roots, but greatly differ in the shoot Si accumulation (Ma et al., 2002). Secondly, a time-course experiment

showed that the Si-decreased Zn uptake was not observed in WT precultured with Si for one day (Fig. 3.4C), but that was observed in WT precultured with Si for three and longer days (Fig. 3.4C), indicating that sufficient level of Si accumulation in the shoots is required. Thirdly, Si which had been accumulated in the shoots is still effective in suppressing Zn uptake in WT even in the absence of Si in the treatment solution (Fig. 3.5C), whereas co-existance with Si for 1 d did not affect Zn uptake in the WT (Fig. 3.5C). These results consistently support that sufficient accumulation of Si in the shoots is required for suppressing expression of *OsZIP1*, thereby Zn uptake.

In conclusion, the results indicate that Si does not have direct alleviative effect on Zn toxicity in rice, but it suppresses Zn uptake through down-regulation of *OsZIP1* implicated in Zn uptake. Furthermore, Si accumulated in the shoots rather than Si in the roots and solution is required for the down-regulation of *OsZIP1* expression, subsequently for suppression of Zn uptake in rice roots.

Chapter 4 General discussion

Zinc is an essential element for both plants and humans, while Zn-deficiency in soil is a limiting factor of crop production in 30% of arable soil in the world. Furthermore, Zn-deficiency has been considered as “hidden hunger” and one-third population of the world is suffering from Zn-deficiency (WHO, 2002; White and Broadley, 2005, 2009). However, the exact transporter for Zn uptake, the first step for transport of Zn from soil to plant roots, has not been identified. Some members in ZIP family have been implicated in Zn uptake based on the analysis of expression pattern, transport activity and ectopic expression (Grotz et al., 1998), but their exact roles in Zn uptake are poorly understood. In the present study, I revealed that two ZIP family transporter genes; *OsZIP1* and *OsZIP9* are involved in Zn uptake in rice. I also uncovered the mechanism responsible for Si-decreased Zn uptake in rice.

4.1 Transporters for Zn uptake in rice roots

OsZIP1 showed the highest expression in the roots among ZIP genes (Table 2.1), while *OsZIP9* showed the strongest induction by Zn-deficiency. OsZIP1 is implicated in Zn uptake at a wide range of Zn concentrations. This is supported by its high and constitutive expression in the roots (Fig. 2.4). However, the effect of knockout of this gene on Zn uptake and its contribution to total Zn uptake remain to be investigated in future. On the other hand, through detailed analysis, OsZIP9 was demonstrated to be responsible for Zn uptake under Zn-deficiency condition in rice. This is supported by

the finding that knockout of *OsZIP9* resulted in the decreased Zn uptake only under Zn-limited condition but not Zn-sufficient conditions (Fig. 2.12).

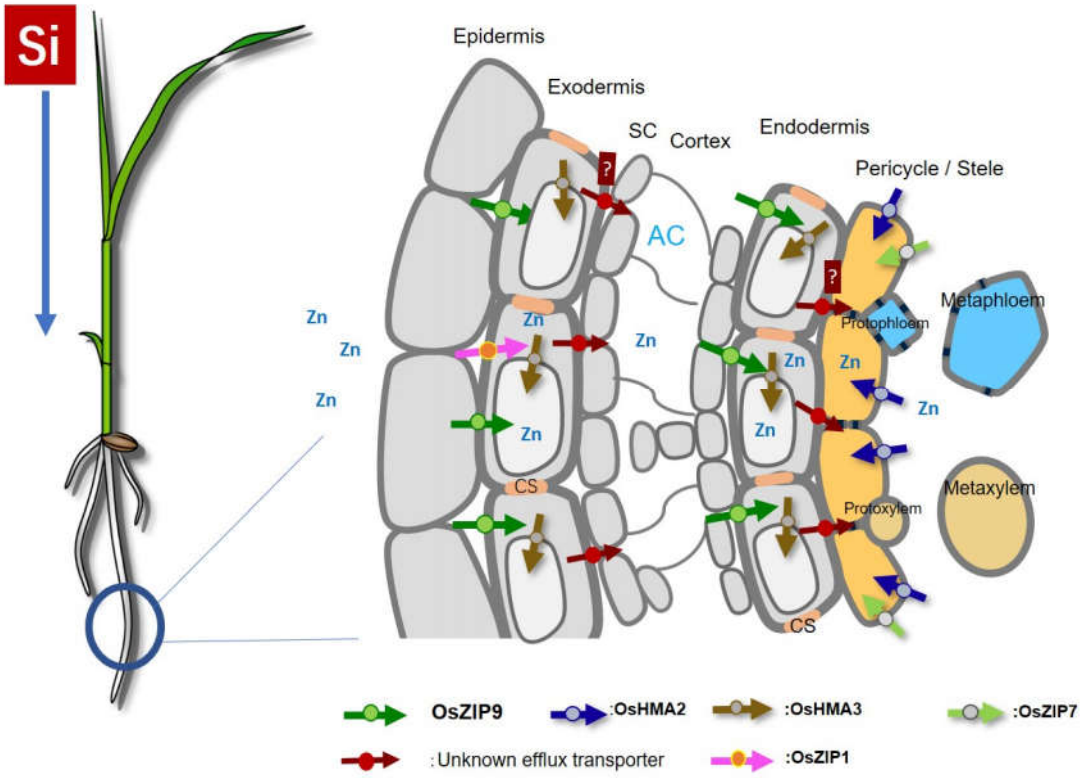

Figure 4.1 Schematic diagram of Zn transport and Si-mediated regulation in rice roots. SC, schelanchyma cell; CS, Casparian strip; AC, aerenchyma.

Identification of OsZIP1 and OsZIP9 in the present study provides further understanding of the Zn transport system in rice. Zn in soil is first taken up by OsZIP9 localized at the exodermis and endodermis of the roots or OsZIP1 localized at all root cell layers except epidermis and other uncharacterized transporters (Figs. 2.5 and 2.110). A portion of Zn taken up is sequestered by OsHMA3 localized at the tonoplast in root cells (Cai et al., 2019) and the remaining Zn is translocated to the shoot by OsHMA2 localized at the pericycle cells (Yamaji et al., 2013). OsZIP7 was also implicated in Zn

xylem loading although its exact role remains to be examined (Tan et al., 2019). At the node, Zn is preferentially delivered to developing organs such as new leaves and grains by OsZIP3 and OsHMA2. OsZIP3 is localized to xylem transfer cells in enlarged vascular bundles (EVBs) of the nodes and responsible for unloading of Zn from the xylem of EVB (Sasaki et al. 2015), whereas OsHMA2 is localized at the phloem region of both EVBs and diffuse vascular bundles (DVBs) and is responsible for loading Zn to the phloem of DVBs and EVBs (Yamaji et al. 2013). However, some missing transporters, such as Zn efflux transporter(s) in root and node, remain to be identified in future to gain a holistic understanding of the Zn transport system in rice. This will contribute to breeding rice cultivars with high tolerance to Zn deficiency and/or with high Zn accumulation in the grain.

Recently, transcription factors; OsbZIP48 and OsbZIP50 are potentially involved in the regulation of Zn accumulation by regulating the expression of ZIP transporters (Lilay et al., 2020). Overexpressing the *OsbZIP48* and *OsbZIP50* in Arabidopsis *bzip19bzip23* double mutant can complement the zinc deficiency-hypersensitive phenotype of *bzip19bzip23* double mutant. Furthermore, over-expression of *OsbZIP48* and *OsbZIP50* significantly increased Zn concentration in both roots and shoots and also increased the expression of ZIP family genes such as *AtZIP1*, *AtZIP4* and *AtZIP5* compared with *bzip19bzip23* double mutant under Zn-limited condition. (Assunção et al., 2010; Lilay et al., 2020). However, the exact role of these transcription factors in rice is unknown and further investigation on mechanisms regulating ZIP genes in rice is required in future.

4.2 Effect of Si on Zn uptake

Si has multiple beneficial effects on plant growth, especially in rice, which is a typical Si accumulating species. One of them is to mitigate nutrient imbalance (Ma, 2004). Recently, it was reported that Si is able to decrease the Mn and P accumulation in rice (Che et al., 2016; Hu et al., 2017). In the present study, I found that Si significantly decreased the Zn uptake in rice (Fig. 3.3). Furthermore, high Si accumulated in the shoots, but not in the roots and solution is required for this decrease (Fig. 3.4). The expression of Zn transporter gene *OsZIP1* in the roots was down-regulated by Si (Fig. 3.10). From previous and present studies, *OsZIP1* is implicated in the Zn uptake by the roots. Therefore, the Si-decreased Zn uptake results from down-regulation of *OsZIP1*expression in the roots.

Recently, it was reported that Si accumulated in the shoots also down-regulated the expression of *OsNramp5* and *OsPT6*, which are involved in the uptake of Mn and P, respectively, in rice (Che et al., 2016; Hu et al., 2017). Si was also reported to modulate jasmonic acid (JA) biosynthesis by down-regulating the expression of JA biosynthesis genes including *OsLOX, OsAOS1, OsAOS2, OsOPR1, OsOPR3*, and *OsAOC*, under wounding stress in rice (Kim et al., 2014). Although the exact mechanism for Si-suppressed gene expression remains to be investigated in future, Si accumulated in the shoots seems to produce some signals such as hormone, which is transferred to the roots for suppressing the gene expression including *OsZIP1*.

Summary

Zinc (Zn) is an essential micronutrient for plant growth and development. It plays structural and catalytic roles in large number of proteins. However, the exact transporters involved in Zn uptake have not been identified. In the present study, I functionally characterized two rice genes; *OsZIP1* and *OsZIP9*, which belong to the Zn-regulated transporter, iron-regulated transporter-like proteins (ZIP; ZRT-IRT-related protein). I further investigated the effect of silicon (Si) on Zn uptake in rice.

1. Identification of transporter genes involved in Zn uptake in rice

RNA-seq analysis showed that *OsZIP1* shows the highest expression among ZIP genes in rice roots, while *OsZIP9* shows the strongest induction by Zn-deficiency. *OsZIP1* is mainly expressed in the roots through the whole growth period and its expression is not induced by Zn-deficiency. Furthermore, the expression of *OsZIP1* is higher in the mature root region than the root tip. Analysis on tissue-specificity of *OsZIP1* expression using transgenic line carrying *OsZIP1* promoter fused with *GFP* showed that it is expressed in all root cells except epidermal cells. The protein encoded by *OsZIP1* is able to transport Zn in the yeast.

On the other hand, *OsZIP9* is also mainly expressed in the roots throughout all growth stages, but the expression level is much lower than *OsZIP1* in the presence of Zn. However, unlike *OsZIP1*, the expression of *OsZIP9* is greatly up-regulated by Zn-deficiency. Furthermore, the expression of *OsZIP9* is also higher in the root mature

region than in the root tip. However, different from *OsZIP1*, *OsZIP9* is specifically expressed in the exodermis and endodermis of the roots. OsZIP9 showed transport activity of Zn when expressed in yeast system, but not Fe and Cu. Transient assay with rice protoplast and onion as well as the immunostaining with OsZIP9 antibody showed that OsZIP9 was mainly localized to the plasma membrane. Knockout of *OsZIP9* significantly reduced plant growth, which was accompanied by decreased Zn concentrations in both the root and shoot when grown at low Zn concentrations. However, the plant growth and Zn accumulation did not differ between knockout lines and wild-type rice under Zn-sufficient conditions. When grown in soil, Zn concentrations in the shoots and grains of knockout lines were decreased to half of wild-type rice, whereas the concentrations of other mineral nutrients were not altered. A short-term kinetic experiment with stable isotope ^{67}Zn showed that ^{67}Zn uptake in knockout lines was much lower than that in wild-type rice. These results indicate that OsZIP1 is implicate in Zn uptake at wide range of Zn although its role in rice remains to be further investigated, while OsZIP9 contributes to Zn uptake only under Zn-limited conditions in rice.

2. Effect of Si on Zn uptake in rice

Si was reported to affect Zn uptake in rice and other plant species, but the mechanism underlying this effect is unknown. I investigated the mechanism responsible for Si-induced effect on Zn uptake in rice by using a mutant (*lsi1*) defective in Si uptake and its wild-type rice. High Zn inhibited the root elongation of both wild-type rice and *lsi1*

mutant, but Si did not alleviate this inhibition in both lines. By contrast, Si supply decreased Zn concentration in both the roots and shoots of the wild-type rice, but not in the *lsi1* mutant. A short-term (24 h) labeling experiment with stable isotope ^{67}Zn showed that Si decreased ^{67}Zn uptake, but did not affect the root-to-shoot translocation and distribution ratio to different organs of ^{67}Zn in the WT. Furthermore, Si accumulated in the shoots, rather than Si in the external solution is required for suppressing Zn uptake, but this was not caused by Si-decreased transpiration. A kinetic study showed that Si did not affect K_m value of root Zn uptake, but decreased V_{max} value in the wild-type rice. Analysis of genes related with Zn transport showed that among ZIP family genes, the expression of only *OsZIP1* implicated in Zn uptake, was down-regulated by Si in the wild-type rice, but not in the *lsi1* mutant. These results indicate that Si does not have direct alleviative effect on Zn toxicity, but that the Si accumulated in the shoots suppresses the Zn uptake through down-regulating transporter gene involved in Zn uptake in rice.

Reference

Adriano DC, Paulson GM, Murphy LS (1971) P-Fe and P-Zn relationship in corn seedlings as affected by mineral nutrition. Agron J 63: 36–39

Agarie S, Uchida H, Agata W, Kubota F, Kaufman PB (1998) Effects of silicon on transpiration and leaf conductance in rice plants (O*ryza sativa* L.). Plant Prod Sci 1: 89–95

Agarwala SC, Mehrotra SC, Bisht SS, Sharma CP (1979) Mineral nutrient element composition of three varieties of chickpea grown at normal and deficient levels of iron. J Indian Bot Soc 8: 153–162

Akhtar MS, Oki Y, Adachi T (2010) Growth behavior, nitrogen-form effects on phosphorus acquisition, and phosphorus–zinc interactions in brassica cultivars under phosphorus-stress environment. Commun Soil Sci Plant Anal 41: 2022–2045

Alloway BJ (2008) Micronutrients and crop production. In Micronutrient Deficiencies in Global Crop Production. Springer Science Business Media BV, pp 1–39

Alloway BJ (2004) Zinc in soils and crop nutrition. Areas of the World with Zinc Deficiency Problems. International Zinc Association. Brussels, Belgium. pp 1–16

Alloway BJ (2009) Soil factors associated with zinc deficiency in crops and humans. Environ Geochem Health 31: 537–548

Andreini C, Bertini I, Rosato A (2009) Metalloproteomes: a bioinformatic approach. Accounts Chem Res 42: 1471–1479

Anwaar SA, Ali S, Ali S, Ishaque W, Farid M, Farooq MA, Najeeb U, Abbas F, Sharif

M (2015) Silicon (Si) alleviates cotton (*Gossypium hirsutum* L.) from zinc (Zn) toxicity stress by limiting Zn uptake and oxidative damage. Environ Sci Pollut Res 22: 3441–3450

Arnon DI, Stout PR (1939) The essentiality of certain elements in minute quantity for plants with special reference to copper. Plant Physiol 14: 371–375

Assunção AGL, Herrero E, Lin YF, Huettel B, Talukdar S, Smaczniak C, Immink RGH, van Eldik M, Fiers M, Schat H, Aarts MG (2010) *Arabidopsis thaliana* transcription factors bZIP19 and bZIP23 regulate the adaptation to zinc deficiency. Proc Natl Acad Sci USA 107: 10296–10301

Astudillo C, Fernandez AC, Blair MW, Cichy KA (2013) The *Phaseolus vulgaris* ZIP gene family: identification, characterization, mapping, and gene expression. Front Plant Sci 4: 286.

Auld DS (2009) The ins and outs of biological zinc sites. Biometals 22: 141–148

Auld DS and Bergman T (2008) The role of zinc for alcohol dehydrogenase structure and function. Cell Mol Life Sci 65: 3961–3970

Badger MR and Price GD (1994) The role of carbonic anhydrase in photosynthesis. Annu Rev Plant Biol 45: 369–392

Barcelo J, Poschenrieder C (2002) Fast root growth responses, root exudates, and internal detoxification as clues to the mechanisms of aluminum toxicity and resistance: a review. Environ Exp Bot 48: 75–92

Barker AV, Pilbeam DJ (2015) Zinc. *In* Handbook of Plant Nutrition. CRC press, pp 537–564

Bernal M, Cases R, Picorel R, Yruela I (2007) Foliar and root Cu supply affect differently Fe-and Zn-uptake and photosynthetic activity in soybean plants. Environ Exp Bot 60: 145–150

Bityutskii N, Pavlovic J, Yakkonen K, Maksimović V, Nikolic M (2014) Contrasting effect of silicon on iron, zinc and manganese status and accumulation of metal-mobilizing compounds in micronutrient-deficient cucumber. Plant Physiol Biochem 74: 205–211

Boardman R, McGuire DO (1990) The role of zinc in forestry. I. Zinc in forest environments, ecosystems and tree nutrition. For Ecol Manage 37: 167–205

Bokor B, Vaculík M, Slováková Ľ, Masarovič D, Lux A (2013) Silicon does not always mitigate zinc toxicity in maize. Acta Physiol Plant 36: 733–743

Bolger AM, Lohse M, Usadel B (2014) Trimmomatic: a flexible trimmer for Illumina sequence data. Bioinformatics 30: 2114–2120

Bosnić D, Nikolić D, Timotijević G, Pavlović J, Vaculík M, Samardžić J, Nikolić M (2019) Silicon alleviates copper (Cu) toxicity in cucumber by increased Cu-binding capacity. Plant Soil 441: 629–641

Broadley M, Brown P, Cakmak I, Rengel Z, Zhao, F (2011) Function of nutrients: micronutrients. In Marschner's Mineral Nutrition of Higher Plants (Marschner, P., ed). San Diego: Academic Press, pp 212–223

Broadley MR, White PJ, Hammond JP, Zelko I, Lux A (2007) Zinc in plants. New Phytol 173: 677–702

Bughio N, Yamaguchi H, Nishizawa NK, Nakanishi H, Mori S (2002) Cloning an iron-

regulated metal transporter from rice. J Exp Bot 53:1677–1682

Cakmak I (2000) Role of zinc in protecting plant cells from reactive oxygen species. New Phytol 146: 185–205

Cakmak, I, Marschner, H (1986) Mechanism of phosphorus-induced zinc deficiency in cotton. I. Zinc deficiency-enhanced uptake rate of phosphorus. Physiol Plant 68, 483–490

Cakmak I, Marschner H (1987) Mechanism of phosphorus-induced zinc deficiency in cotton. II. Changes in physiological availability of zinc in plants. Physiol Plant 70: 13–20.

Çakmak İ, Marschner H (1988a) Enhanced superoxide radical production in roots of zinc-deficient plants. J Exp Bot 39: 1449–1460

Çakmak İ, Marschner H (1988b) Zinc-dependent changes in ESR signals, NADPH oxidase and plasma membrane permeability in cotton roots. Physiol Plant 73: 182–186

Cakmak I, Marschner H (1988c). Increase in membrane permeability and exudation of roots of zinc deficient plants. J Plant Physiol 132: 356–361

Cakmak I, Ozturk L, Eker S, Torun Kalfa HI, Yilmaz A (1997) Concentration of zinc and activity of copper/zinc superoxide dismutase in leaves of rye and wheat cultivars differing in sensitivity to zinc deficiency. J Plant Physiol 151: 91–95

Cakmak I, Sari N, Marschner H, Ekiz H, Kalayci M, Yilmaz A, Braun HJ (1996) Phytosiderophore release in bread and durum wheat genotypes differing in zinc efficiency. Plant Soil 180: 183–189

Cai H, Huang S, Che J, Yamaji N, Ma JF (2019) The tonoplast–localized transporter

OsHMA3 plays an important role in maintaining Zn homeostasis in rice. J Exp Bot 70:2717–2725

Clemens S (2001) Molecular mechanisms of plant metal tolerance and homeostasis. Planta 212: 475–486

Che J, Yamaji N, Ma JF (2018) Efficient and flexible uptake system for mineral elements in plants. New Phytol 219: 513–517

Che J, Yamaji N, Shao JF, Ma JF Shen RF (2016) Silicon decreases both uptake and root-to-shoot translocation of manganese in rice. J Exp Bot 67: 1535–1544

Chen S, Tao L, Zeng L, Vega-Sanchez ME, Umemura K, Wang GL (2006) A highly efficient transient protoplast system for analyzing defence gene expression and protein-protein interactions in rice. Mol Plant Pathol 7: 417–427

Chen WR, Feng Y, Chao YE (2008) Genomic analysis and expression pattern of *OsZIP1*, *OsZIP3*, and *OsZIP4* in two rice (*Oryza sativa* L.) genotypes with different zinc efficiency. Russ J Plant Physiol 55: 400–409

Choo Y, Klug A (1994) Selection of DNA binding sites for zinc fingers using rationally randomized DNA reveals coded interactions. Proc Natl Acad Sci USA 91: 11168–11172

Coleman JE (1992) Zinc proteins: enzymes, storage proteins, transcription factors, and replication proteins. Annu Rev Biochem 61: 897–946

Connolly EL, Fett JP, Guerinot ML (2002) Expression of the IRT1 metal transporter is controlled by metals at the levels of transcript and protein accumulation. Plant Cell 14: 1347–1357

Coskun D, Deshmukh R, Sonah H, Menzies JG, Reynolds O, Ma JF, Herbert J.

Kronzucker, HJ, Bélanger RR (2019) The controversies of silicon's role in plant biology. New Phytol 221: 67–85

Currie HA, Perry CC (2007) Silica in plants: biological, biochemical and chemical studies. Ann Bot 100: 1383–1389

Dai X, Schonbaum C, Degenstein L, Bai W, Mahowald A, Fuchs E (1998) The *ovo* gene required for cuticle formation and oogenesis in flies is involved in hair formation and spermatogenesis in mice. Genes Dev 12: 3452–3463

Eide D, Broderius M, Fett J, Guerinot ML (1996) A novel iron-regulated metal transporter from plants identified by functional expression in yeast. Proc Natl Acad Sci USA 93: 5624–5628

Enstone DE, Peterson CA, Ma F (2002) Root endodermis and exodermis: structure, function, and responses to the environment. J Plant Growth Regul 21: 335–351

Evens NP, Buchner P, Williams LE, Hawkesford MJ (2017) The role of ZIP transporters and group F bZIP transcription factors in the Zn-deficiency response of wheat (*Triticum aestivum*). Plant J 92: 291–304

Gaitán-Solís E, Taylor NJ, Siritunga D, Stevens W, Schachtman DP (2015) Overexpression of the transporters AtZIP1 and AtMTP1 in cassava changes zinc accumulation and partitioning. Front Plant Sci 6: 492

Garty J, Karary Y, Harel J (1992) Effect of low pH, heavy metals and anions on chlorophyll degradation in the lichen *Ramalina duriaei* (De Not) Bagl, Environ Exp Bot 32: 229–241

GBD. (2016) Mortality and causes of death collaborators. Global, regional, and national

life expectancy, all-cause mortality, and cause-specific mortality for 249 causes of death, 1980-2015: a systematic analysis for the Global Burden of Disease Study 2015. Lancet 388: 1459–1544

Giordano M, Noggle JC, Mortvedt JJ (1974) Zinc uptake by rice, as affected by metabolic inhibitors and competing cat ions. Plant Soil 41: 637–646

Gong HJ, Randall DP, Flowers TJ (2006) Silicon deposition in the root reduces sodium uptake in rice (*Oryza sativa* L.) seedlings by reducing bypass flow. Plant Cell Environ 29: 1970–1979

Gonzalez DH (2015) Plant transcription factors: evolutionary, structural and functional aspects. Academic Press

Graham RD, Knez M, Welch RM (2012) How much nutritional iron deficiency in humans globally is due to an underlying zinc deficiency? In *Advances in Agronomy*. Academic Press, pp 1–40

Gregory PJ, Wahbi A, Adu-Gyamfi J, Heiling M, Gruber R, Joy EJ, Broadley MR (2017) Approaches to reduce zinc and iron deficits in food systems. Glob Food Secur 15: 1–10

Grewal HS, Graham RD, Stangoulis J (1998) Zinc-boron interaction effects in oilseed rape. J Plant Nutr 21: 2231–2243

Grotz N, Fox T, Connolly E, Park W, Guerinot ML, Eide D (1998) Identification of a family of zinc transporter genes from Arabidopsis that respond to zinc deficiency. Proc Natl Acad Sci USA 95: 7220–7224

Guerinot ML (2000) The ZIP family of metal transporters. Biochim Biophys

Acta 1465:190–198

Gu, HH, Zhan SS, Wang SZ, Tang YT, Chaney RL, Fang XH, Cai XD, Qiu RL (2011) Silicon-mediated amelioration of zinc toxicity in rice (*Oryza sativa* L.) seedlings. Plant Soil 350: 193–204

Hafeez B, Khanif YM, Saleem M (2013) Role of zinc in plant nutrition-a review. Aust J Exp Agric 21: 374–391

Haydon MJ, Cobbett CS (2007) A novel major facilitator superfamily protein at the tonoplast influences zinc tolerance and accumulation in Arabidopsis. Plant Physiol 143: 1705–1719

Hernandez-Apaolaza L (2014) Can silicon partially alleviate micronutrient deficiency in plants? A review. Planta 240, 447–458

Hiei Y, Ohta S, Komari T, Kumashiro T (1994) Efficient transformation of rice (*Oryza sativa* L.) mediated by *Agrobacterium* and sequence analysis of the boundaries of the T-DNA. Plant J 6: 271–282

Hossain MA, Barrow JJ, Shen Y, Haq MI, Bungert J (2015) Artificial zinc finger DNA binding domains: versatile tools for genome engineering and modulation of gene expression. J Cell Biochem 116: 2435–2444

Hosseini SM, Maftoun M, Karimian N, Ronaghi A, Emam Y (2007) Effect of zinc× boron interaction on plant growth and tissue nutrient concentration of corn. J Plant Nutr 30: 773–781

Huang S, Wang P, Yamaji N, Ma JF (2020a) Plant nutrition for human nutrition: hints from rice research and future perspectives. Mol Plant 13: 825–835

Huang S, Sasaki A, Yamaji N, Okada H, Mitani-Ueno N, Ma, JF (2020b) The ZIP transporter family member OsZIP9 contributes to root Zn uptake in rice under Zn-limited conditions. Plant Physiol 183: 1224–1234

Hu AY, Che J, Shao JF, Yokosho K, Zhao XQ, Shen RF, Ma JF (2017) Silicon accumulated in the shoots results in down-regulation of phosphorus transporter gene expression and decrease of phosphorus uptake in rice. Plant Soil 423: 317–325

Inaba S, Kurata R, Kobayashi M, Yamagishi Y, Mori I, Ogata Y, Fukao Y (2015) Identification of putative target genes of bZIP19, a transcription factor essential for Arabidopsis adaptation to Zn deficiency in roots. Plant J 84: 323–334

Ishimaru Y, Masuda H, Suzuki M, Bashir K, Takahashi M, Nakanishi H, Mori S, Nishizawa NK (2007) Overexpression of the OsZIP4 zinc transporter confers disarrangement of zinc distribution in rice plants. J Exp Bot 58: 2909–2915

Ishimaru Y, Suzuki M, Kobayashi T, Takahashi M, Nakanishi H, Mori S, Nishizawa NK (2005) OsZIP4, a novel zinc-regulated zinc transporter in rice. J Exp Bot 56: 3207–3214

Ishimaru Y, Bashir K, Nishizawa NK (2011) Zn uptake and translocation in rice plants. Rice 4: 21–27

Ishimaru Y, Suzuki M, Tsukamoto T, Suzuki K, Nakazono M, Kobayashi T, Wada Y, Watanabe S, Matsuhashi S, Takahashi M, Nakanishi H, Mori S, Nishizawa NK (2006) Rice plants take up iron as an Fe^{3+}-phytosiderophore and as Fe^{2+}. Plant J 45: 335–346

Jones LHP, Handreck KA (1967) Silica in soils, plants and animals. Adv Agron 19: 107–149

Kabata-Pendias A, Pendias, H (2001) Trace elements in soils and plants–CRC Press. Boca Raton p 403

Kavitha PG, Kuruvilla S, Mathew MK (2015) Functional characterization of a transition metal ion transporter, OsZIP6 from rice (*Oryza sativa* L.). Plant Physiol Biochem 97:165–174

Kaya C, Tuna AL, Sonmez O, Ince F, Higgs D (2009) Mitigation effects of silicon on maize plants grown at high zinc. J Plant Nutr 32: 1788–1798

Kim D, Pertea G, Trapnell C, Pimentel H, Kelley R, Salzberg SL (2013) TopHat2: accurate alignment of transcriptomes in the presence of insertions, deletions and gene fusions. Genome Biol 14: R36

Kim YH, Khan AL, Waqas M, Jeong HJ, Kim DH, Shin JS, Kim JG, Yeon MH, Lee IJ (2014) Regulation of jasmonic acid biosynthesis by silicon application during physical injury to *Oryza sativa* L. J Plant Res 127: 525–532

Kochian LV (1991) Mechanisms of micronutrient uptake and translocation in plants. In JJ Mortvedt, ed, Micronutrients in Agriculture. Soil Science Society of America, Madison, WI, pp 251–270

Korshunova YO, Eide D, Clark WG, Guerinot ML, Pakrasi HB (1999) The IRT1 protein from Arabidopsis thaliana is a metal transporter with a broad substrate range. Plant Mol Biol 40: 37–44

Krishna TA, Maharajan T, Roch GV, Ignacimuthu S, Ceasar SA (2020) Structure, function, regulation and phylogenetic relationship of ZIP family transporters of plants. Front Plant Sci doi: 10.3389/fpls.2020.00662

Lasat MM, Kochian LV (2000) Physiology of Zn hyperaccumulation in *Thlaspi caerulescens* . In: Terry N, Bañuelos G, eds. Phytoremediation of contaminated soil and water. Boca Raton, FL, USA: CRC Press LLC, pp 59–169

Lee S, Jeong HJ, Kim SA, Lee J, Guerinot ML, An G (2010a) OsZIP5 is a plasma membrane zinc transporter in rice. Plant Mol Biol 73: 507–517

Lee S, Kim SA, Lee J, Guerinot ML, An G (2010b) Zinc deficiency-inducible *OsZIP8* encodes a plasma membrane-localized zinc transporter in rice. Mol Cells 29: 551–558

Liang Y, Sun W, Zhu YG, Christie P (2007) Mechanisms of silicon-mediated alleviation of abiotic stresses in higher plants: a review. Environ Pollut 147: 422–428

Lilay GH, Castro PH, Guedes JG, Almeida DM, Campilho A, Azevedo H, Aarts MG, Saibo NJ, Assunção AG (2020) Rice F-bZIP transcription factors regulate the zinc deficiency response. J Exp Bot https://doi.org/10.1093/jxb/eraa115

Li P, Song A, Li Z, Fan F, Liang Y (2012) Silicon ameliorates manganese toxicity by regulating manganese transport and antioxidant reactions in rice (*Oryza sativa* L.). Plant Soil 354: 407–419

Lin YF, Liang HM, Yang SY, Boch A, Clemens S, Chen CC, Wu JF, Huang JL, Yeh KC (2009) Arabidopsis IRT3 is a zinc-regulated and plasma membrane localized zinc/iron transporter. New Phytol 182: 392–404

Li S, Zhou X, Huang Y, Zhu L, Zhang S, Zhao Y, Guo J, Chen J, Chen R (2013) Identification and characterization of the zinc-regulated transporters, iron-regulated transporter-like protein (ZIP) gene family in maize. BMC Plant Biol 13: 1–4

Loneragan JF, Grove TS, Robson AD, Snowball K (1979). Phosphorus toxicity as a

factor in zinc-phosphorus interactions in plants. Soil Sci Soc Am J 43: 966–972

Ma JF (2004) Role of silicon in enhancing the resistance of plants to biotic and abiotic stresses. Soil Sci Plant Nutr 50: 11–18

Ma JF, Miyake Y, Takahashi E (2001) Silicon as a beneficial element for crop plants. In L Datonoff, G, Korndorfer, G Snyder, eds, Silicon in Agriculture. Elsevier Science Publishing, New York, pp 17–39

Ma JF, Takahashi E (1990) Effect of silicon on the growth and phosphorus uptake of rice. Plant Soil 126: 115–119

Ma JF, Takahashi E (2002) Soil, Fertilizer, and Plant Silicon Research in Japan. Dordrecht, The Netherlands: Elsevier

Ma JF, Tamai K, Ichii M, Wu GF (2002) A rice mutant defective in Si uptake. Plant Physiol 130: 2111-2117

Ma JF, Tamai K, Yamaji N, Mitani N, Konishi S, Katsuhara M, Ishiguro M, Murata Y, Yano M (2006) A silicon transporter in rice. Nature 440: 688–691

Ma JF, Yamaji N (2006) Silicon uptake and accumulation in higher plants. Trends Plant Sci 11: 392–397

Ma JF, Yamaji N (2015) A cooperative system of silicon transport in plants. Trends Plant Sci 20: 435–442

Ma JF, Yamaji N, Mitani N, Tamai K, Konishi S, Fujiwara T, Katsuhara M, Yano M (2007) An efflux transporter of silicon in rice. Nature 448: 209–212

Miki D, Shimamoto K (2004) Simple RNAi vectors for stable and transient suppression of gene function in rice. Plant Cell Physiol 45: 490–495

Marschner H, Oberle H, Cakmak I, Römheld V (1990) Growth enhancement by silicon in cucumber (*Cucumis sativus*) plants depends on imbalance in phosphorus and zinc supply. Plant Soil 124: 211–219

Marschner P (2012) Zinc. *In* Marschner's Mineral Nutrition of Higher Plants. Academic Press, pp 212–223

Masarovič D, Slováková Ľ, Bokor B, Bujdoš M, Lux A (2012) Effect of silicon application on Sorghum bicolor exposed to toxic concentration of zinc. Biologia 67: 706–712

Mehrabanjoubani P, Abdolzadeh A, Sadeghipour HR, Aghdasi M (2015) Impacts of silicon nutrition on growth and nutrient status of rice plants grown under varying zinc regimes. Theor Exp Plant Physiol 27: 19–29

Mikkelsen DS, Kuo S (1977) Zinc fertilization and behavior in flooded soil. Commonw Bur Soils, Spec Publ 5Milner MJ, Seamon J, Craft E, Kochian LV (2013) Transport properties of members of the ZIP family in plants and their role in Zn and Mn homeostasis. J Exp Bot 64: 369–381

Miller J, Mclachlan AD, Klug A (1985) Repetitive zinc binding domains in the protein transcription factor IIIA from *Xenopus oocytes*. EMBO J 4: 1609–1614

Mitani-Ueno N, Yamaji N, Ma JF (2018) Transport system of mineral elements in rice. *In* T Sasaki, M Ashikari, eds, Rice Genomics, Genetics and Breeding. Springer, Singapore, pp.223–240

Mondal TK, Ganie SA, Rana MK, Sharma TR (2013) Genome-wide analysis of zinc transporter genes of maize (*Zea mays*). Plant Mol Biol Rep 32: 605–616

Nakandalage N, Seneweera S (2018) Micronutrients use efficiency of crop-plants under changing climate. In *Plant Micronutrient Use Efficiency.* Academic Press, pp 209–224

Neumann D, Zur Nieden U (2001) Silicon and heavy metal tolerance of higher plants. Phytochemistry 56: 685–692

Nikolic DB, Nesic S, Bosnic D, Kostic L, Nikolic M, Samardzic JT (2019) Silicon alleviates iron deficiency in barley by enhancing expression of Strategy II genes and metal redistribution. Front Plant Sci 10: 416

Okuda A, Takahashi E (1962) Studies on the physiological role of silicon in crop plants Part 5 Effect of silicon supply on the injuries of barley and rice plant due to excessive amount of Fe^{II}, Mn^{II}, Cu^{II}, As^{II}, Al^{III}, Co^{II}. J Sci Soil Manure 33: 1–8

Olsen LI, Palmgren MG (2014) Many rivers to cross: the journey of zinc from soil to seed. Front Plant Sci 5:30

Påhlsson AM (1989) Toxicity of heavy metals (Zn, Cu, Cd, Pb) to vascular plants. Water Air Soil Pollut 47: 287–319

Palmer CM, Guerinot ML (2009) Facing the challenges of Cu, Fe and Zn homeostasis in plants. Nat Chem Biol 5: 333–340

Pascual MB, Echevarria V, Gonzalo MJ, Hernández-Apaolaza L (2016) Silicon addition to soybean (*Glycine max* L.) plants alleviate zinc deficiency. Plant Physiol Biochem 108: 132–138

Peleg Z, Saranga Y, Fahima T, Aharoni A, Elbaum R (2010) Genetic control over silica deposition in wheat awns. Physiol Plant 140: 10–20

Pontigo S, Ribera A, Gianfreda L, de la Luz MoraM, Nikolic M, Cartes P (2015) Silicon

in vascular plants: uptake, transport and its influence on mineral stress under acidic conditions. Planta 242: 23–37

Ramesh SA, Shin R, Eide DJ, Schachtman DP (2003) Differential metal selectivity and gene expression of two zinc transporters from rice. Plant Physiol 133: 126–134

Romheld V, Marschner H, Kramer D (1982) Response to Fe deficiency in roots of "Fe efficient" plant. J Plant Nutr Soil Sci 5: 489–498

Ruano A, Barceló J, Poschenrieder C (1987) Zinc toxicityinduced variation of mineral element composition in hydroponically grown bush bean plants. J Plant Nutr 10: 373–384

Ryan MH, McInerney JK, Record IR, Angus JF (2008) Zinc bioavailability in wheat grain in relation to phosphorus fertilizer, crop sequence and mycorrhizal fungi. J Sci Food Agric 88: 1208–1216

Saeed M, Fox RL (1977) Relation between suspension pH and Zn solubility in acid and calcareous soils. Soil Sci 124: 199–204

Sagardoy R, Morales F, López-Millán AF, Abadía A, Abadía J (2009) Effects of zinc toxicity on sugar beet (*Beta vulgaris* L.) plants grown in hydroponics. Plant Biol 11: 339–350

Sandmann G, Böger P (1983) The enzymatological function of heavy metals and their role in electron transfer processes of plants. In *Encyclopedia of Plant Physiology, New Series* (A. Läuchli and R. L. Bieleski, eds) Springer-Verlag, Berlinand New York, pp 563–593

Sasaki A, Yamaji N, Ma JF (2016) Transporters involved in mineral nutrient uptake in

rice. J Exp Bot 67: 3645–3653

Sasaki A, Yamaji N, Mitani-Ueno N, Kashino M, Ma, JF (2015) A node-localized transporter OsZIP3 is responsible for the preferential distribution of Zn to developing tissues in rice. Plant J 84: 374–384

Sasaki A, Yamaji N, Yokosho K, Ma JF (2012) Nramp5 is a major transporter responsible for manganese and cadmium uptake in rice. Plant Cell 24: 2155–2167

Sasaki H, Hirose T, Watanabe Y, Ohsugi Y (1998) Carbonic anhydrase activity and CO_2-transfer resistance in Zn-deficient rice leaves. Plant Physiol 118: 929–934

Sattelmacher B (2001) The apoplast and its significance for plant mineral nutrition. New Phytol 149: 167–192

Shao FJ, Che J, Yamaji N, Shen RF, Ma JF (2017) Silicon reduces cadmium accumulation by suppressing expression of transporter genes involved in cadmium uptake and translocation in rice. J Exp Bot 68: 5641–5651

Sillanpää M (1990) Micronutrients assessment at the country level: An international study. FAO Soils Bulletin 63. Food and Agriculture Organisation of the United Nations, Rome

Sinclair SA, Krämer U (2012) The zinc homeostasis network of land plants. Biochim Biophys Acta 1823: 1553–1567

Song A, Li P, Li Z, Fan F, Nikolic M, Liang Y (2011) The alleviation of zinc toxicity by silicon is related to zinc transport and antioxidative reactions in rice. Plant Soil 344: 319–333

Song A, Li P, Fan F, Li Z, Liang Y (2014) The effect of silicon on photosynthesis and

expression of its relevant genes in rice (*Oryza sativa* L.) under high-zinc stress. PLoS One 9, e113782

Sousa SF, Lopes AB, Fernandes, PA, Ramos MJ (2009) The zinc proteome: a tale of stability and functionality. Dalton Trans 7946–7956

Sillanpaa M (1990) Micronutrient assessment at the country level an international study. FAO, Rome, 63: 208

Takahashi R, Ishimaru Y, Shimo H, Ogo Y, Senoura T, Nishizawa NK, Nakanishi H (2012) The OsHMA2 transporter is involved in root-to-shoot translocation of Zn and Cd in rice. Plant Cell Environ 35: 1948–1957

Tamai K, Ma JF (2008) Reexamination of silicon effects on rice growth and production under field conditions using a low silicon mutant. Plant Soil 307: 21–27

Tamura K, Stecher G, Peterson D, Filipski A, Kumar S (2013) MEGA6: molecular evolutionary genetics analysis version 6.0. Mol Biol Evol 30: 2725–2729

Tan L, Qu M, Zhu Y, Peng C, Wang J, Gao D, Chen C (2020) ZINC TRANSPORTER5 and ZINC TRANSPORTER9 function synergistically in zinc/cadmium uptake. Plant Physiol 183: 1235–1249

Tan L, Zhu Y, Fan T, Peng C, Wang J, Sun L, Chen C (2019) OsZIP7 functions in xylem loading in roots and inter-vascular transfer in nodes to deliver Zn/Cd to grain in rice. Biochem Biophy Res Commu 23: 112–118

Tiong J, McDonald GK, Genc Y, Pedas P, Hayes JE, Toubia J, Langridge P, Huang CY (2014) HvZIP7 mediates zinc accumulation in barley (*Hordeum vulgare*) at moderately high zinc supply. New Phytol 201: 131–143

Tiong J, McDonald G, Genc Y, Shirley N, Langridge P, Huang CY (2015) Increased expression of six ZIP family genes by zinc (Zn) deficiency is associated with enhanced uptake and root-to-shoot translocation of Zn in barley (*Hordeum vulgare*). New Phytol 207: 1097–109

Trapnell C, Williams BA, Pertea G, Mortazavi A, Kwan G, Van Baren MJ, Salzberg SL, Wold BJ, Pachter L (2010) Transcript assembly and quantification by RNA-Seq reveals unannotated transcripts and isoform switching during cell differentiation. Nature Biotechnol 28: 511–515

Trehan, SP, Sekhon, GS (1977) Effect of clay, organic matter and CaCO3 content of zinc adsorption by soils. Plant Soil 46: 329–336

Ueno D, Sasaki A, Yamaji N, Miyaji T, Fujii Y, Takemoto Y, Moriyama S, Che J, Moriyama Y, Iwasaki K, Ma JF (2015) A polarly localized transporter for efficient manganese uptake in rice. Nat Plants 1: 15170

Vallee BL, Falchuk KH (1993) The biochemical basis of zinc physiology. Physiol Rev 73: 79–118

Vert G, Briat JF, Curie C (2001) Arabidopsis *IRT2* gene encodes a root-periphery iron transporter. Plant J 26: 181–189

Vert G, Grotz N, Dédaldéchamp F, Gaymard F, Guerinot ML, Briat JF, Curie C (2002) IRT1, an Arabidopsis transporter essential for iron uptake from the soil and for plant growth. Plant Cell 14: 1223–1233

Von Grebmer K, Saltzman A, Birol E, Wiesman D, Prasai N, Yin S, Yohannes Y, Menon P, Thompson J, Sonntag A (2014) Synopsis: 2014 Global Hunger Index: The Challenge

of Hidden Hunger. Intl. Food Policy Res. Inst

Wang P, Yamaji N, Inoue K, Mochida K, Ma JF (2019) Plastic transport systems of rice for mineral elements in response to diverse soil environmental changes. New Phytol 226: 156–169

Welch RM (2002) The impact of mineral nutrients in food crops on global human health. Plant and Soil 247: 83–90

Waters BM, Sankaran RP (2011) Moving micronutrients from the soil to the seeds: genes and physiological processes from a biofortification perspective. Plant Sci 180: 562–574

Welch RM, Webb MJ, Loneragan JF (1982) Zinc in membrane function and its role in phosphorus toxicity. In: Scaife A (ed) Proceedings of the Ninth Plant Nutrition Colloquium. Warwick, UK. Wallingford, UK: CAB International, pp 710–715

White, PJ (2001) The pathways of calcium movement to the xylem. J Exp Bot 52: 891–899

White PJ, Whiting SN, Baker AJM, Broadley MR (2002) Does zinc move apoplastically to the xylem in roots of *Thlaspi caerulescens*? New Phytol 153: 201–207

White PJ, Broadley MR (2009) Biofortification of crops with seven mineral elements often lacking in human diets-iron, zinc, copper, calcium, magnesium, selenium and iodine. New Phytol 182: 49–84

WHO (2002) The world health report 2002-reducing risks, promoting healthy life. World Health Organization (WHO), Geneva, Switzerland

Woolhouse HW (1983) Toxicity and tolerance in the responses of plants to metals. In:

Lange OL, Nobel PS, Osmond CB, Ziegler H, eds. Encyclopedia of Plant Physiology, New series, Vol. 12C. Berlin: Springer-Verlag, 245–300

Yamaji N, Ma JF (2014) The node, a hub for mineral nutrient distribution in graminaceous plants. Trends Plant Sci 19: 556–563

Yamaji N, Ma JF (2007) Spatial distribution and temporal variation of the rice silicon transporter Lsi1. Plant Physiol 143: 1306–1313

Yamaji N, Ma JF (2017) Node-controlled allocation of mineral elements in Poaceae. Curr Opin Plant Biol 39: 18–24

Yamaji N, Xia J, Mitani–Ueno N, Yokosho K, Ma JF (2013) Preferential delivery of zinc to developing tissues in rice is mediated by P-type heavy metal ATPase OsHMA2. Plant Physiol 162: 927–939

Yang M, Li Y, Liu Z, Tian J, Liang L, Qiu Y, Wang G, Du Q, Cheng D, Cai H, Shi L (2020) A high activity zinc transporter OsZIP9 mediates zinc uptake in rice. Plant J doi: 10.1111/tpj.14855

Yang X, Huang J, Jiang Y, Zhang HS (2009) Cloning and functional identification of two members of the *ZIP* (Zrt, Irt-like protein) gene family in rice (*Oryza sativa* L.). Mol Biol Rep 36: 281–287

Yokosho K, Yamaji N, Mitani-Ueno N, Shen RF, Ma JF (2016) An aluminum-inducible IREG gene is required for internal detoxification of aluminum in buckwheat. Plant Cell Physiol 57: 1169–1178

Zhang F, Romheld V, Marschner H (1991) Diurnal rhythm release of phytosiderophore and uptake rate of zinc in Fe-efficient wheat. Soil Sci Plant Nutr 37: 671–678

Zhao H, Eide D (1996) The yeast *ZRT1* gene encodes the zinc transporter protein of a high-affinity uptake system induced by zinc limitation. Proc Natl Acad Sci USA 93: 2454–2458

Zhu YG, Smith SE, Smith FA (2001) Zinc (Zn)-phosphorus (P) interactions in two cultivars of spring wheat (*Triticum aestivum* L.) differing in P uptake efficiency. Ann Bot 88: 941–945

Acknowledgements

My deepest gratitude goes first and foremost to my supervisor, Professor Jian Feng Ma. I am really grateful to him for giving me the opportunity to study in his laboratory. I do appreciate his patient, valuable and professional instructions and advice in my experiments. And I also sincerely appreciate his great help on my daily life.

Secondly, I would like to express my sincere thanks to Dr. Naoki Yamaji for his valuable suggestions and technical help especially on immunostaining. I want to express my deep thanks to Dr. Akimasa Sasaki for providing a good experiment basis especially for preparing the transgenic plants and performing the transport activity in yeast. I also want to give my sincere thanks to Drs. Namiki Mitani-Ueno and Kengo Yokosho for their kind help during my experiments and Prof. Maki Katsuhara for the instruction on my research. Many thanks to all of my lab members for their warm-hearted help and encouragement.

Thirdly, many thanks to my family who has been assisting, supporting and caring me all the time.

Finally, I would like to thank China Scholarship Council (CSC) for the financial support during my study in Japan.